TECHNICAL SERVICE CENTER
Denver, Colorado

Technical Memorandum No. D8330-2004-04

2003 Status Report-Paradox Valley Seismic Network
Paradox Valley Project
Southwestern Colorado

U.S. Department of the Interior
Bureau of Reclamation

April 2004

U.S. Department of the Interior
Mission Statement

The mission of the Department of the Interior is to protect and provide access to our Nations's natural and cultural heritage and honor our trust responsibilities to Indian tribes and our commitments to island communities.

Bureau of Reclamation
Mission Statement

The mission of the Bureau of Reclamation is to manage, develop, and protect water and related resources in an environmentally and economically sound manner in the interest of the American public.

TECHNICAL SERVICE CENTER
Denver, Colorado

Technical Memorandum No. D8330-2004-04

2003 Status Report-Paradox Valley Seismic Network
Paradox Valley Project
Southwestern Colorado

Prepared by

Kenneth Mahrer
Jon Ake
Daniel O'Connell
Lisa Block

U.S. Department of the Interior
Bureau of Reclamation

April 2004

Bureau of Reclamation
Technical Service Center
Seismotectonics and Geophysics Group

Technical Memorandum No. D8330-2004-04

2003 Status Report-Paradox Valley Seismic Network
Paradox Valley Unit
Southwestern Colorado

Prepared By

Kenneth Mahrer
Geophysicist

4/5/04
Date

Jon Ake
Seismologist

4/7/04
Date

Daniel O'Connell
Seismologist

4/5/2004
Date

for Lisa Block
Geophysicist

4-5-04
Date

Peer Review

Jerry Wright
Geophysicist

4-5-04
Date

Table of Contents

1.0 Executive Summary 2
- **1.1 Background 2**
- **1.2 Cumulative Findings 4**
- **1.3 Acknowledgements 6**

2.0 New in 2003 7
- **2.1 New PVU Operations Nomenclature 7**
  - *2.1.1 Phase I - (22-May 1996 through 26-July 1999) 8*
  - *2.1.2 Phase II - (27-July 1999 through 22-June 2000) 8*
  - *2.1.3 Phase III - (23-June 2000 through 7-January 2002) 9*
  - *2.1.4 Phase IV - (8-January 2002 through the Present) 9*
- **2.2 Excess Energy Model 9**
  - *2.2.1 Background - Energy 9*
  - *2.2.2 Background - Hydraulic Fracturing 10*
  - *2.2.3 The Excess Energy Model 11*
  - *2.2.4 Findings 14*
- **2.3 Swarm Analysis 19**
- **2.4 Mohr Circle Analysis 21**
  - *2.4.1 General 21*
  - *2.4.2 Paradox Injection and Mohr Circle 25*
- **2.5 Total Seismic Event Production at PVU 26**
- **2.6 A Fractal Model to Accommodate Injectate Volume 28**
  - *2.6.1 Background 28*
  - *2.6.2 Mathematical Foundation 28*
  - *2.6.3 Calculations 30*
  - *2.6.4 Fractal Model Implications 32*
- **2.7 Remote (Northern) Seismic Swarms 33**
- **2.8 Second Well Considerations 34**
- **2.9 (Hickman) Breakout Analysis 34**
- **2.10 Reference: Pressure and Pressure-Gradient Plot 35**

3.0 Local Setting 37
- **3.1 PVU Salinity Control Well No. 1 ..... 40**
- **3.2 Wray Mesa Fault and Fracture System 41**

4.0 PVSN instrumentation 43
- **4.1 Telemetry and Software 46**
- **4.2 PVSN Operational Efficiency 47**

5.0 Well Operations 49
- **5.1 Operational Adjustments to Reduce Seismicity 50**
  - *5.1.1 Bi-Annual Shutdowns 50*
  - *5.1.2 Reduced Injection Rate 50*
- **5.2 Injectate: 70/30 PVB/Fresh Versus 100% PVB 51**

6.0 Seismic Analysis 53

6.1 Local Seismic Magnitude Scale 53
6.2 Preliminary Event Location Method 53
6.3 Advanced Event Location - Seismic Modeling 55
7.0 Observations 59
7.1 Local, Pre-Injection Seismicity 59
7.2 Seismic Events and Well Testing (1991-1995) 59
7.3 Seismic Events and Continuous Injection (1996-Present) 61
7.4 Event Magnitudes 66
7.5 Felt Events 66
7.6 2003 Event Locations 67
7.7 1991-2002 Near Wellbore Event Locations 72
7.8 Earthquake Recurrence 72
7.9 Focal Mechanisms - Preliminary Analysis 77
7.10 Focal Mechanisms - Advanced 78
7.10.1 Strike-Slip Focal Mechanisms 82
7.10.2 Oblique Focal Mechanisms 84
7.11 Earthquake Slip Mode 84
7.12 Seismic Magnitude versus Location 88
8.0 Modeling Rock Properties 91
8.1 Injection Data and Fracture Modeling 91
8.2 Seismicity, Fault Properties, and Injectate Volume 91
8.3 Seismicity and Effective Porosity 93
9.0 Conclusions 95
9.1 Specific to 2003 95
9.2 Since Inception of Continuous Pumping 95
10.0 Miscellaneous 98
10.1 Appendices List 98
10.2 Accompanying CD File List 98
11.0 References 100
12.0 APPENDIX A - 2ND WELL ACTIVITIES IN 2003 104
12.1 Memo Submitted October, 2003 104
12.2 Figures Used During Tele-Conferences on 2nd Well Considerations 115
13.0 APPENDIX B - 39TH ANNUAL ROCK SYMPOSIUM 119
14.0 APPENDIX C - INJECTION CONFERENCE 120

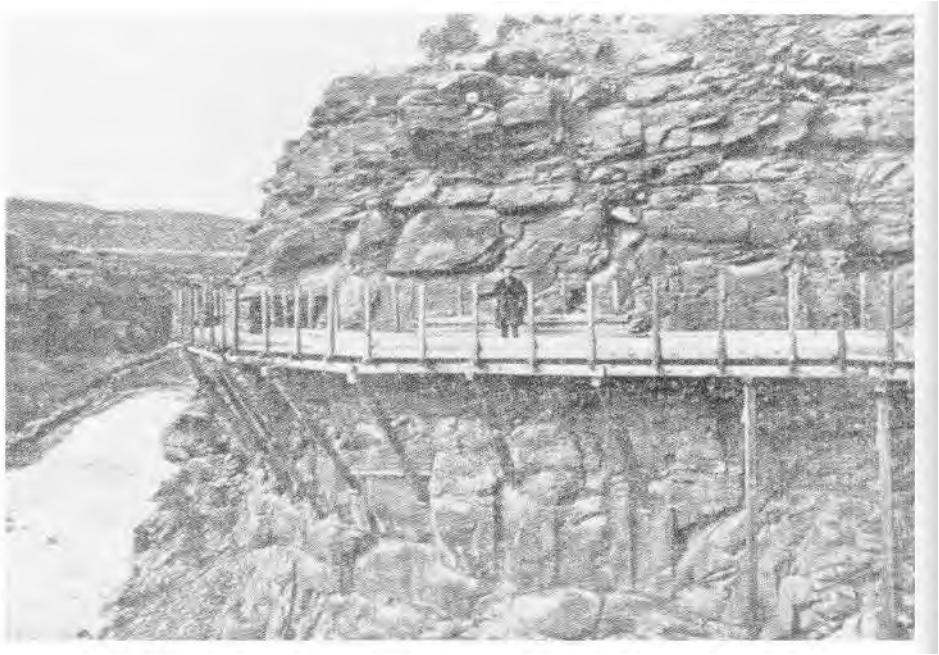

Dolores River, Northeast of Paradox Valley and Hanging Flume - 1890 (Parker, 1992)

Dolores River and Hanging Flume - Today (Parker, 1992)

1.0 EXECUTIVE SUMMARY

Based on other deep-well injection projects, including the Denver Arsenal, CO in the 1960's and in Rangley, CO in later 1960's and early 1970's, the U. S. Bureau of Reclamation (Reclamation) recognized and planned for small earthquakes induced by the Paradox Valley Unit (PVU) injection. In 1985, six years before the onset of injection at PVU, Reclamation began monitoring seismicity with its surface-based Paradox Valley Seismic Network (PVSN) in the Paradox Valley region. Recording, analyzing, and interpreting these data was, and still is, the mandate of PVSN. Specifically, PVSN operations (1) gathers continuous ground motion data originating in and around Paradox Valley and the surrounding region; (2) electronically collates and telemeters these data to the Denver Federal Center (DFC) in Lakewood, CO; (3) isolates, evaluates, and catalogs local, injection-induced seismic events within the data; (4) locates the sources of these events; (5) determines cumulative and individual characteristics (e.g., source mechanics or focal mechanisms) of the events when feasible; (6) identifies and evaluates relationships between seismicity, geology, tectonics, subsurface brine and connate water/pressure movements and locations, and injection parameters; (7) maintains a database of both event and injection parameters; (8) and reports its findings both internally and to the scientific community.

1.1 Background

This report summarizes the calendar year 2003 seismic data, observations, and related work for PVSN and its support staff. Since 1985, Reclamation has operated PVSN, its local, surface-based, 15-station seismometer network, as part of the Paradox Valley Unit (PVU) of its Colorado River Basin Salinity Control Project. PVU collects and disposes Paradox Valley brine (PVB) prior to it contaminating the Dolores River, a tributary of the Colorado River. From 1991 through the end of 2003, the Paradox Valley Unit (PVU) has operated the world's deepest US-EPA Class V disposal well, the PVU Salinity Control Well No. 1, to dispose ~4 billion liters of PVB-rich injectate (~600 million+ kg of salts) ~4.3 km below the Earth's surface into the Mississippian-aged Leadville Limestone and surrounding formations. Between 1991 and 1995 injection was a punctuated sequence of 7 injection tests and an acid stimulation aimed at acquiring a Class V EPA permit for deep disposal. Since 1996 the injection has been round-the-clock with the exception of as-needed maintenance shut downs and, since 2000, a scheduled, 20-day shut down every 6 months.

Throughout most of its operating history, the (downhole) injection pressure at PVU has been in the range of 80±2 MPa (~12,000 psi) with surface pressure ranging between 30 and 34 MPa (4,400 and 4,950 psi). The injection pressure has induced, probably, over 2 million microseisms (i.e., seismic events with magnitudes equal to or greater than **M**-3.0 up to the maximum induced event, a **M**4.3). By the end of December 2003 and being a surfaced-based network, PVSN recorded over 4,000 of the largest of these events, those with magnitudes ~**M**0.0 or greater. The recorded events occur in two, disconnected seismic event zones: the principal, asymmetric, E-W elongated zone that surrounds the injection well and contains more than 3,800 events and a secondary zone that is also asymmetric and lies ~8 km northwest of the injection well. From the injection well, the secondary region lies along the local major fault trend of the Leadville and its underlying and overlaying formations, the Wray Mesa Fault system.

Within both seismogenic regions, the PVSN-recorded seismic events are not tensile events created by the injectate or connate fluid wedging open the local rock mass. The tensile events, which include new tensile fracture and the widening of existing tensile openings, are too small to radiate sufficient energy to be recorded by PVSN. Instead the recorded events are shear failures. The shear sources are not uniformly or randomly distributed, but are patterned. These patterns form well-defined groups that delineate secondary networks of fractures and faults of the Wray Mesa system. The shear planes of slip (i.e., fault-planes of the induced seismicity, also called focal mechanisms or moment tensors) align with the strikes of these fractures and faults or with their anticipated principal shear stress directions. The mapped fractures and faults show that substantial pressure perturbations (either injectate or connate) have migrated along through the Wray Mesa network of faults and fractures at least the 8 km from the injection well to the second seismogenic region.

The estimated maximum volume of the injectate held by the seismically-identified fractures and faults is nominally only a few percent of the total injectate volume; the remaining injectate has diffused into the local porosity: either into new microfractures created by the injections or the poorly-developed system of pre-existing pores and microfractures. Since the injection pressure exceeds the fracture pressure, the injectate creates new or widens existing pores, fractures, and joints.

Over its history, PVU has instituted strategies to mitigate the risk of inducing larger seismic events while maintaining the economic viability of injection. These strategies have included reducing injection rate and biannual 20-day shut downs. The reduced injection rate allows the injectate to more easily diffuse into the target formations. Similarly, the shut downs allow the formation stresses to relax as the injectate leaks off from main fractures into the pore and small fractures of the reservoir rock matrix. Since mid-2002, these changes have substantially reduced seismic event production and seem to have reduced the proclivity to produce larger, felt events.

1.2 Cumulative Findings

Throughout the continuous pumping, beginning in 1996, the nominal injection pressure at PVU exceeds fracture pressure of the injection reservoir.

The initial induced seismicity was probably due to injectate or connate fluids reducing the friction across faults, liberating pre-existing, *in situ* tectonic stress across the faults. However, some fraction of the later seismicity may also result from inflation by the injectate and displaced connate fluids changing the *in situ* stresses.

The induced seismicity at Paradox illuminates an extensive, non-symmetric connected network of fractures, faults, joints, etc. and does not demonstrate the traditional hydraulic fracture picture of two, vertical, symmetric fractures emanating from opposite sides of the injection well.

Surface-recorded seismic events are radiated from shear slippage on pre-existing faults, joints, planes of weakness, not tensile or "new-fracture" openings.

Injection has induced two distinct seismic event zones: a primary zone, asymmetrically surrounding the well to a maximum radial distance of ~3+ km and a secondary zone, centered~8 km to the northwest of the injection well along the trend of the local fault system, the Wray Mesa system. The primary zone covers a reservoir of between 20 and 30 cubic kilometers

Based on extrapolation of the PVSN data and comparison with data from injection sites that were monitored with *in situ* instruments, our best estimate indicates PVU has induced ~2 million events with magnitudes between **M**-3.0 and **M**4.3. The small events probably

include both shear slippage and tensile (i.e., crack-opening) events. Being a surface array with its closest instrument ~4 km from the downhole injection interval, PVSN's sensitivity limit is approximately **M**0.0. Thus, PVSN records ~0.1% of the events PVU induces.

More than 99.9% of the over 4,000 surface-recorded events induced at the Paradox Valley injection since 1991 have magnitudes less than **M**2.0. (Human detection threshold ~ **M**2.6.): ~15 events have been felt.

The largest seismic event, an **M**4.3 in May 2000, occurred after ~4 years of continuous injecting.

The first seismic event induced by continues pumping occurred 111 days after pumping began.

The rate of seismicity is not uniform; there are single, multi-day, and multi-week quiet periods and multi-hour to multi-week active periods.

Spatially, the seismicity occurs as isolated events and occasional swarms; swarms can occur over hours to days in a single location. We have identified one swarm region that has been active since 1996.

The seismic swarms at Paradox are like typical earthquake swarms that culminate in one, large event, some smaller foreshocks and a few smaller aftershocks or one large event followed by 5 to 15 aftershocks.

One seismic zone/swarm region has shown correlation with large-scale pressure changes and is possibly triggered only after pressure exceeds a threshold.

The seismicity occurs within the interior and on the border of the existing seismic zones; since about mid-1999, the extent of the zones shows negligible, if any expansion.

By the end of 2003, PVU injected ~0.004 cubic kilometers of injectate. Since the injectate invasion, increases the connate fluid pressure, the volumetric extent of the injectate is probably less than the volumetric extent defined by the seismicity.

Seismic event depths are vertically contained between ~3.5 km and ~6 km below the wellhead.

The epicenters group into lineaments that illustrate the secondary fracture and fault network of the Wray Mesa. The alignment of the epicenter lineaments imply the locations of the major, through-going faults of the Wray Mesa system.

The major faults of the Wray Mesa fault system align with the principal stress direction, show-

ing only minor, if any, surface-recordable seismicity. However, these faults align with the predicted hydraulic gradient of the region and, most likely, act as fluid conduits. The location and activation of the secondary seismic zone confirms the fluid-conduit model of these faults.

The fault-planes defined by focal mechanism solutions (i.e., moment tensors) align with the predicted (principle) shear planes and with the secondary faults and fractures of the Wray Mesa.

Economically reasonable, 20-day shut downs relax the *in situ* stress state, resulting in a reduced proclivity for large events.

Since 2002, the increase in percentage of Paradox Valley Brine in the injectate has not directly affected seismicity. It has increased the bottom-hole pressure, slightly, due to change in specific gravity of injectate, which can alter the seismicity.

The storage of injectate must be facilitated by existing pore space and by the injection pressure creating new volume, since injection can hydraulically fracture the rock matrix; the identified primary and secondary faults and fractures of the Wray Mesa system can only accommodate a few percent of the injectate volume.

The *b*-value, a parameter relating the number of seismic events and the size of events has been altered by the changes in injection phases.

1.3 Acknowledgements

This study and the continuous operation of the Paradox Valley Seismic Network are made possible through the continued and generous support of Andy Nicholas, Project Manager at the Paradox Valley Unit, Colorado. We are greatly appreciative. In addition, Dee Overturf and Tom Bice (US Geological Survey, Denver) provided outstanding field support throughout the history of this project. Rick Martin, US Bureau of Reclamation, Denver (Reclamation), developed and installed PVSN and recognized many of the potential issues during early stages of the project. Chris Wood (Reclamation) developed software and provided helpful discussions. Ute Vetter (formerly with Reclamation) provide technical support and a scrutinous copy editor's eye. We also benefitted from stimulating discussions with Roger Denlinger, Evelyn Roeloffs, Steve Hickman, Art McGarr (all at the US Geological Survey), Jim Bundy (Subsurface Technology, Inc.) and Ivan Wong (URS Corporation). Mike Sullivan (Reclamation) helped with maps.

2.0 NEW IN 2003

[***Note to Reader***: *This report is the 2003 annual report on the operations of the Paradox Valley Seismic Network (PVSN). Much of the information are updates from previous years. In order to highlight the new work and findings of 2003 we created this separate section,* **NEW IN 2003**. *If you are new to PVSN operations, we recommend skimming this section and reading the subsequent sections to gain insight into the fundamentals and background of this project. After that, we recommend returning to this section.*]

2.1 New PVU Operations Nomenclature

Since continuous injection began in May 1996, PVU has instituted and maintained three major injection changes. Each change was invoked to mitigate the potential for seismicity or improve injection economics. Each change was maintained for a sufficient period to be considered an injection phase, not a test. Consistent with these changes, we have chosen the nomenclature, "Phase", for each sustained injection period. We made this choice to distinguish operational parameters and resulting reservoir response(s), including induced seismicity. Described below are

the four injection phases at PVU. **Table 2-1** gives a summary of the injection phases.

Table 2-1 Phases of Continuous Pumping

Phases	Approx. Duration	Avg. Wellhead Pressure	Avg. Pressure @ 4,300 m* depth	Avg. Inj. Rate	Injectate: %PVB:% H_2O	Biannual 20-day Shutdown	Approx. No. Seismic Events
	days	(MPa)	(MPa)	(l/min)		y/n	
I	1100	33.8	80.7	1290	70:30	No	2446
II	332	33.8	80.7	1290	70:30	Yes	496
III	566	30.3	77.2	855	70:30	Yes	140
IV	724+**	30.3	79.3	855	100:0	Yes	277

*Depth = Top of the casing perforation interval, i.e., the top of the injection target horizon, the Leadville Limestone, which well testing indicates has the greatest injectivity
**Number includes days through 12/31/03
MPa = megapascals, 1 MPa = 145 psi

2.1.1 Phase I - (22-May 1996 through 26-July 1999)

Following inception and a few months of building up injection pressure, PVU injected at maximum: ~1290 l/min (~345 gpm) at ~33 MPa (~4,900+ psi) surface pressure which corresponded to ~80 MPa (~11,600 psi) downhole pressure at 4.3 km (14,080 ft). The injectate during *Phase I* was 70% Paradox Valley Brine (PVB), 30% fresh water. Throughout *Phase I*, PVU injected continuously with the exception of unscheduled maintenance or pressure diffusion shut downs. [*Note*: A pressure diffusion shut down is a stoppage of injection because the wellhead pressure approached a pre-determined limit. By shutting down injection, the wellhead pressure reduced due to fluid diffusion in the reservoir (i.e., from the fractures and faults into the rock matrix.)] During *Phase I*, shut downs ran for minutes, hours, a few days or a few weeks up to a maximum of 71 days in mid 1997 to replace the injection pumps.

2.1.2 Phase II - (27-July 1999 through 22-June 2000)

Following the June-1999, **M**3.5-event and the July-1999 **M**3.6 event, PVU augmented injection to include the same injection pressure and rate as *Phase I* plus a 20-day shutdown (i.e., "shut-in") every six months (one in December-January and one in May). These scheduled shut downs were included so that the injectate from the pressurized fractures and faults could diffuse into the formation rock matrix (i.e., *in situ* stress relaxation). As detailed below (e.g., **Figure 7-4**), the shut downs reduced the seismicity, but did not sufficiently reduce the proclivity to produce large seismic events.

2.1.3 Phase III - (23-June 2000 through 7-January 2002)

Following the May 2000, **M**4.3 earthquake, PVU reduced the injection rate ~33% to ~870 l/min (~230 gpm) while maintaining the 70:30 ratio of brine to fresh water. The lower injection rate reduced surface pressure about 10%. Together, the bi-annual, 20-day shutdowns and lower injection rate reduced earthquake production. From 1998 through the **M**4.3 event, PVSN recorded an average ~81 earthquakes/month; following the reduced injection in late June 2000 through the end of 2001, that average dropped to ~13 earthquakes/month.

2.1.4 Phase IV - (8-January 2002 through the Present)

In January 2002, PVU began injecting 100% brine at the *Phase III* injection rate. This is the present injection schedule: 100% PVB @ ~870 l/min (~230 gpm) and a 20-day shutdown every six months. Since the specific gravity of PVB is ~5% greater than the 70:30 mixture, surface pressures initially decreased while maintaining the same downhole pressure. [Note: At the beginning of *Phase IV*, the surface pressure was ~30 MPa (~4,400 psi), and downhole pressure was ~79 MPa (~11,500 psi). By December 2003, these pressures had increased by ~2 MPa (~290 psi).]

2.2 Excess Energy Model

2.2.1 Background - Energy

Until this year, we viewed the injection and resulting seismicity at PVU in terms of single param-

eters, either rate or pressure. During 2003 we began examining the injection from a perspective of energy: input energy; preexisting energy, and output energy.

The input energy is the energy recoverable from the injectate at the injection interval depth. This includes the energy from the velocity of the injectate, the energy from the compression of the injectate, and energy from temperature. Based on our calculations, the velocity of the injectate is comparable to a small fire hose and is not a particularly important factor in this model. We do not include it in this model. The thermal energy from the injectate (i.e., a cold fluid contacting a hot formations) maybe a factor in creating microfractures, but is also not an important factor in this injection-seismicity model. We do not include it. The main source of energy into the formation is the compression of the injectate. The compressive energy contained in the injectate manifests as its volume decrease in response to confining pressure. At the perforation depth, the confining pressure is sum of the pressure from the pumps at the surface and the hydrostatic head (i.e., the weight of fluid column in the wellbore). This will be discussed more thoroughly below.

As its name implies, the preexisting energy is the available energy independent of PVU. It is the energy in the local geology. We call this available energy because it is the strain energy in the rock that can be liberated as seismicity and aseismic sliding across preexisting planes of weakness (e.g., faults, joints, bedding planes, veins, etc.). Since this model is designed to study seismicity, we limit the strain to that created by the tectonics, both local and regional, and liberates as earthquakes. We recognize that the injectate creates additional strain by opening new and old surfaces (i.e., faults, fractures, joints, veins, etc.), but we consider this energy to be a manifestation of some of the injectate compression noted above.

The output energy or energy released includes creating new fractures (i.e., hydraulic fracturing), the opening or moving apart of new and old surfaces and the slipping or shear movement across surfaces (i.e., seismic events). There are other energy release mechanisms including thermal and chemical, but these are not considered in this model.

2.2.2 Background - Hydraulic Fracturing

Hydraulic fracturing is used to nucleate and grow fractures *in situ* by forcing fluids into a forma-

tion at sufficient pressure to fracture and separate new surfaces. A mini-hydraulic fracture is a hydraulic fracture that uses a small volume of fluid, typically a few hundreds of liters (1 gallon = 3.8 liters), to determine the minimum pressure needed to fracture the formation. The injection pressure is slowly increased to determine the threshold pressure sufficient to separate facing rock surfaces; this value is the least principal stress of the formation. Envirocorp (1995) states that the Leadville Limestone, PVU's primary injection target, showed fracture initiation (i.e., least principal stress threshold) at a depth of ~4.3 km (~14,080 ft) at about 28 MPa (4,000 psi) surface pressure using fresh water injectate. Neglecting wellbore friction, which is quite small, this corresponds to a least principal stress of ~70 MPa (4,000 psi at the surface + 6100 psi for the hydrostatic column of the well).

2.2.3 The Excess Energy Model

The hypothesis of Excess Energy Model (EE Model) is that some of the input (i.e., injectate compressive) energy in excess of the minimum (i.e., threshold) energy needed to fracture and separate rock surfaces (i.e., hydraulic fracture energy) will manifest as surface-measurable (output) energy. We investigated if one (output) energy mechanism is seismic and, if it is seismic, whether or not we can use the EE Model (a) to understand the recorded seismicity and (b) to predict seismic behavior for future injection parameters.

To begin the development of the EE Model we first determine the volumetric change of water as a function of compression. For later reference, the volume change is a function of the energy stored in the injectate. We begin with the definition of compressibility, *k*:

$$k = (\Delta V / V) / (\Delta P) \qquad (1)$$

where $\Delta V / V$ is the percentage change to the initial volume V due to the application of a pressure ΔP. Based on the compressibility data for water in the American Institute of Physics (AIP) Handbook (1972), we developed **Figure 2-1**, the volumetric compression of water as a function of confining pressure. The figure shows our fitted curve to the AIP data and its mathematical formula. Note, because the pressure at PVU is measured in psi, the data and formula in **Figure 2-1** are in

psi. For consistency with the units in this report, to convert psi to MPa multiply psi by 0.00689.

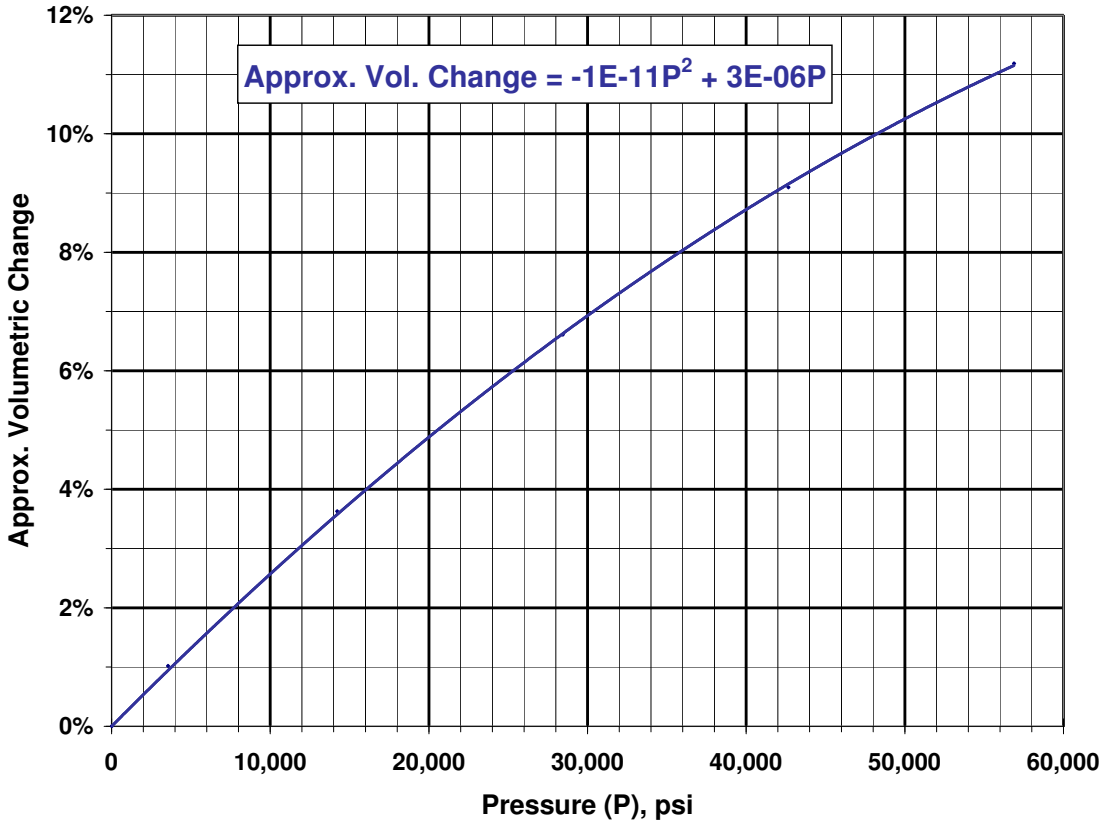

Figure 2-1 Volumetric Compression (i.e.,% decrease in volume) of Water as a Function of Confining (hydrostatic) Pressure

Next we develop an expression for the energy stored in a compressed unit volume. Consider **Figure 2-2**.The figure shows the application of hydrostatic pressure, P, to all faces on a unit-volume (shaded) cube and the resulting compressed (solid-colored) cube whose volume is $(1-\Delta x)^3$, where Δx is the length change of the cube in each of the 3 Cartesian directions shown in the figure. Since the volumetric change ΔV for the unit cube equals $1 - (1-\Delta x)^3$, the numerical change in length of each side of the cube, $\Delta x = \Delta V/3$, where Δx is small compared to the original cube edge length, 1.

Next we calculate E, the energy stored in the unit cube by the application of the pressure, *P*. The energy, E, is the work done against 3 faces of the cube and, as shown in **Figure 2-2**, is the product

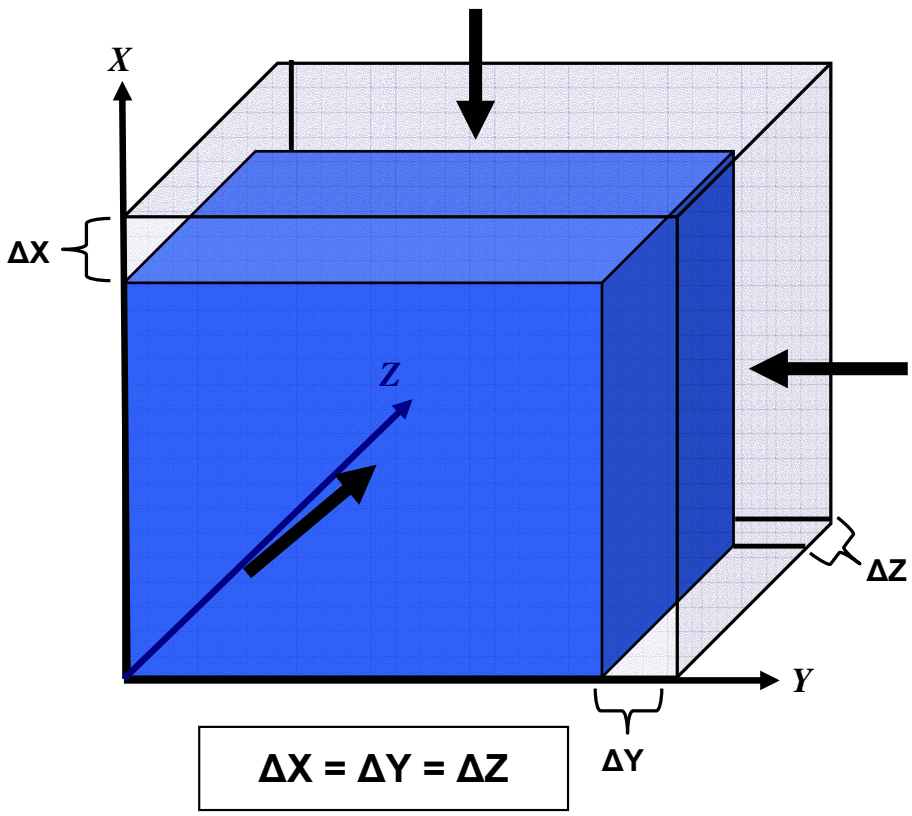

Figure 2-2 Schematic of cubic volume being compressed by the equivalent or hydrostatic pressure applied to each face (arrows). For graphic simplicity, pressure arrows have been drawn to only 3 of the 6 faces.

of force on a face (pressure times unit area) times distance the face moves (Δx) times 3 faces or

$$Energy = Force \times Distance = (P \times (UnitArea)) \times (\Delta V/3) \times 3 \qquad (2)$$

This expression simplifies to equation (3)

$$E = P\Delta V = PV\Delta V(\%) \qquad (3)$$

where P is the pressure in psi, V is the average, uncompressed injected volume in gallons [or V is the average, uncompressed injection rate, if one wishes to calculate energy rate], and $\Delta V(\%)$ is the percentage volume change, as shown in **Figure 2-1**. The final expression for the energy in Megajoules or Mjoules [or Mjoules/day, if V is a rate] at pressure P is given by equation (4)

$$E(P,V) = PV(-1\times10^{-11}P^2 + 3\times10^{-6}P) \times 231 \times 1.13\times10^{-7} \qquad (4)$$

where 231 is the conversion factor for gallons to cubic inches and 1.13×10^{-7} is the conversion from pound-inches to Mjoules. Typically, the reported data from PVU is in gallons/day at a daily-averaged, surface pressure. From this we calculate the bottomhole pressure, ignoring wellbore friction (<0.3 MPa), at 4.3 km (14,080 ft) by adding 42 MPa (6096 psi) for fresh water, 47 MPa (6822 psi) for 70:30 ratio of Paradox Valley Brine (PVB) to fresh water, or 49.2 MPa (7133 psi) for 100% PVB. With these data, E, in equation (4) is either average injected energy in Mjoules, if V is a volume, or E is the daily-average injected energy rate, if V is a volume rate.

Using equation (4), we define the excess energy (EE) to be the pressure in excess of the threshold pressure needed to hydraulically fracture the target formation. Using Envirocorp's data (1995), threshold hydraulic fracturing at 4.3 km (14,080 ft) occurred at 27.6 MPa (4,000 psi) surface pressure and 69.6 MPa (10,100 psi) downhole pressure. Hence, using equation (4), we define EE as

$$\mathrm{EE} = E(P,V) - E(69.6, V) \qquad (5)$$

where P is the daily-averaged downhole injectate pressure and V is either the average injected volume or the average injectate rate.

2.2.4 Findings

Using equation (5) we tried a number of approaches to correlate EE and seismic energy, where seismic energy per event as a function of event magnitude is given by the standard Gutenberg-Richter magnitude-energy relationship

$$SeismicEnergy = 10^{1.5\mathbf{M} + 11.8} \qquad (6)$$

where **M** is magnitude. Note, the units of energy in equation (6) are ergs (1 kjoule = 10^{10} ergs). Using equation (6) we show in **Figure 2-3** that comparing the observed events at PVU, **M**0.5 - **M**4.3, with the (projected) small events at PVU (**M** -3.0 - **M** 0.0), the energy from observed data (i.e., the larger events) dominates the results. In **Figure 2-3,** we calculated the number of small events by fitting a trend line to the number of observed events versus magnitude between **M**0.5 - **M**4.3 (**Table 7-5**, **Figure 7-5**), which resulted in the equation shown in **Figure 2-3**. Using this

equation, we calculated the cumulative seismic energy for the projected (small magnitude) events using equation (6). Note that the energy in these small events is insignificant and can be ignored. For reference, the extrapolation described above resulted in over 600,000 events of **M**-3.0.

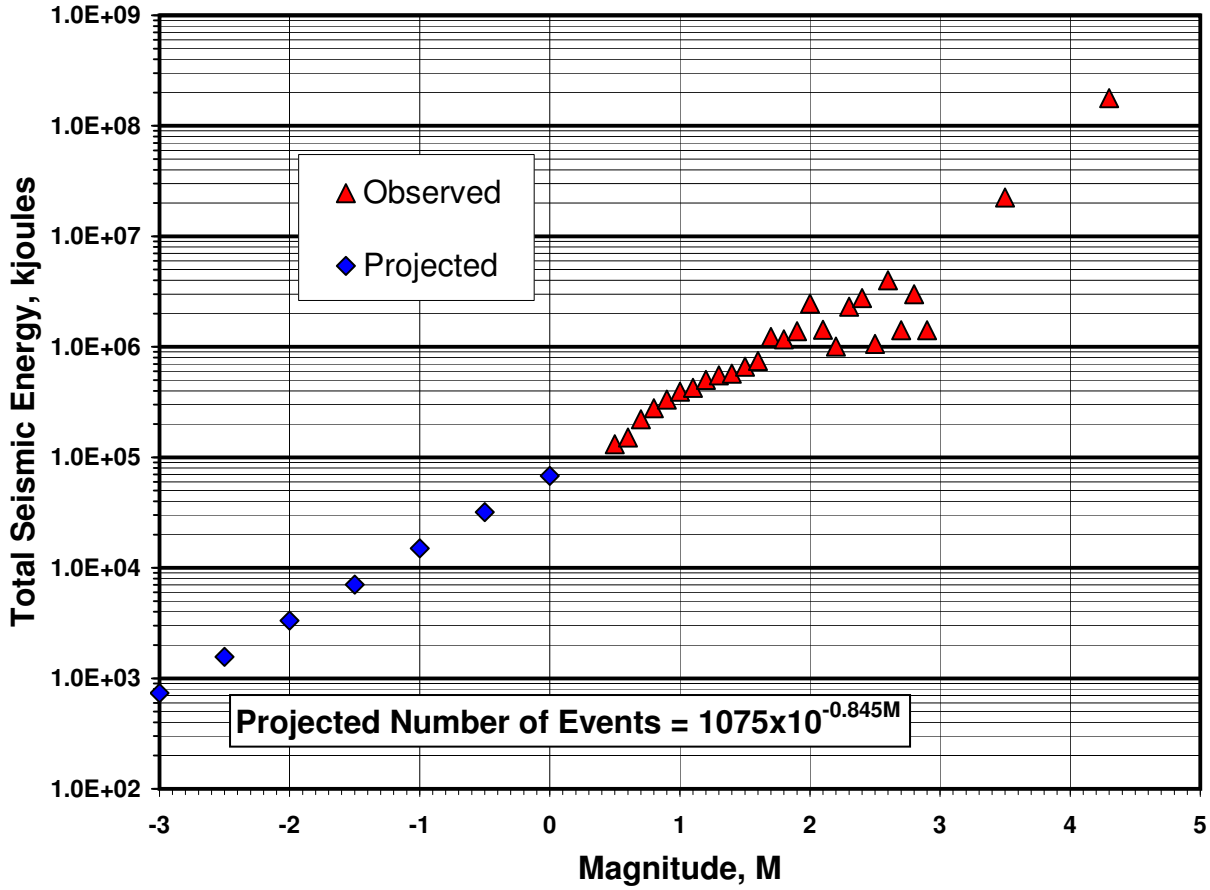

Figure 2-3 Total Seismic Energy by Event Magnitude. Red Triangles are events recorded or observed by PVSN; blue diamonds are linear extrapolations from the observed data shown. Note the insignificant amount of energy in the small magnitudes

Using only the observed data, we separate larger events from smaller events and compared the cumulative seismic energy over time and the cumulative EE over time. Our intent was to determine if there was a correlation with the input energy, speciality the EE, and the output energy of the seismicity. After some trial-and-error we found a good correlation between EE during the continuous pumping period (1996-present) and the cumulative seismic energy for events **M**1.7 and smaller. This correlation is shown in **Figure 2-4**. Note in the figure, the injectate energy (i.e., EE)

is in Mjoules and the seismic energy is in kjoules. Hence the vertical placement or amplitude of the individual curves and the fact that they appear to touch at one spot is either not significant or a function of the efficiency (i.e. ratio of output to input energy) of these energy mechanisms. This is still being studied.

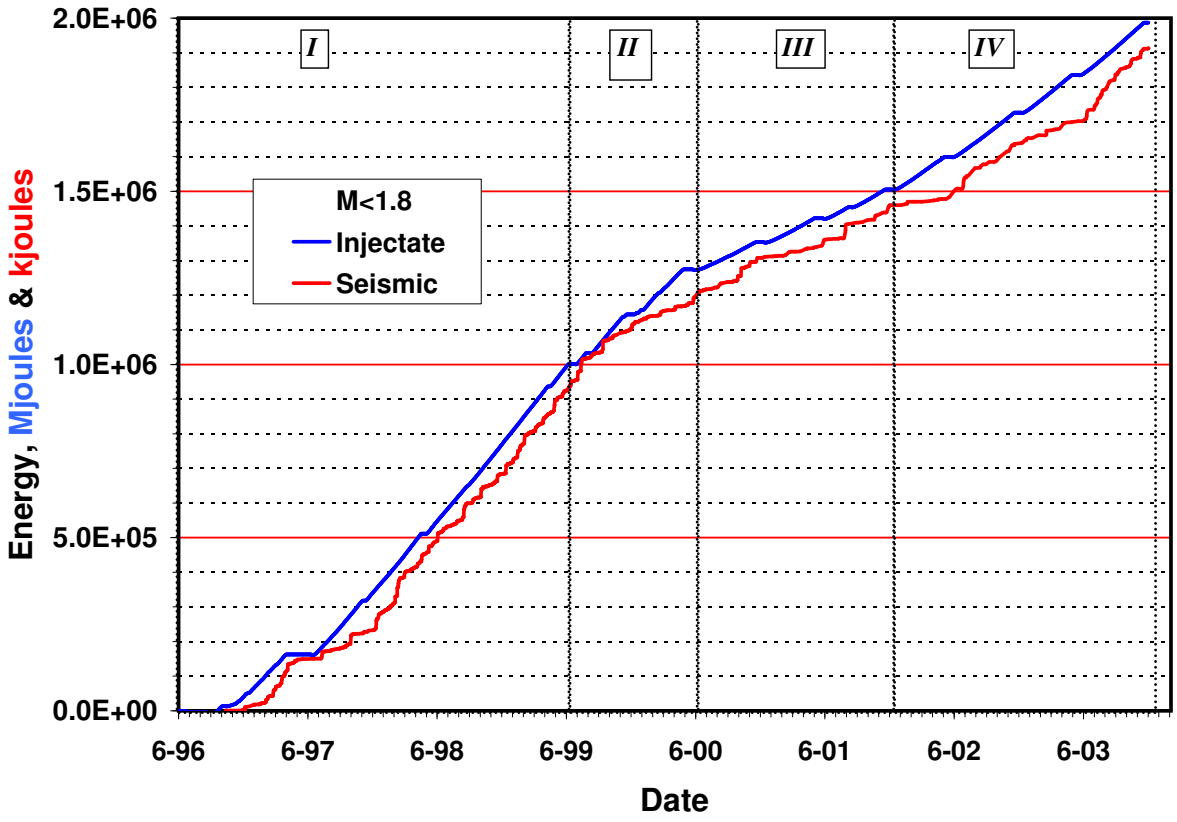

Figure 2-4 Comparison of Seismic Energy for Events of Magnitude M1.7 and Smaller to the Excess Energy ("Injectate") during the Four Injection Phases Covering 1996 through the end of 2003. Note the injectate excess energy (blue) is in Mjoules and the seismic energy (red) is in kjoules.

Ignoring the amplitudes, **Figure 2-4** shows a very good correlation in shapes between the seismic energy released and EE for the noted magnitude range. If we include events **M**1.8 and larger, the correlation between seismic energy and EE breaks down. This may mean that the energy liberated in the **M**0.0 - **M**1.7 range are more strongly controlled by or derived from the injectate energy. While the seismic energy liberated from the larger events may include a strong component of stored (preexisting) tectonic energy. We are still considering the ramifications of **Figure 2-4** and

the possible explanations.

In addition to trying to understand seismicity based on energy balance at PVU, we used EE to predict future injection, especially pressure, based on past EE and possible future seismicity rates. Consider **Figure 2-5**. The figure shows EE per day since 1996 and the corresponding number of

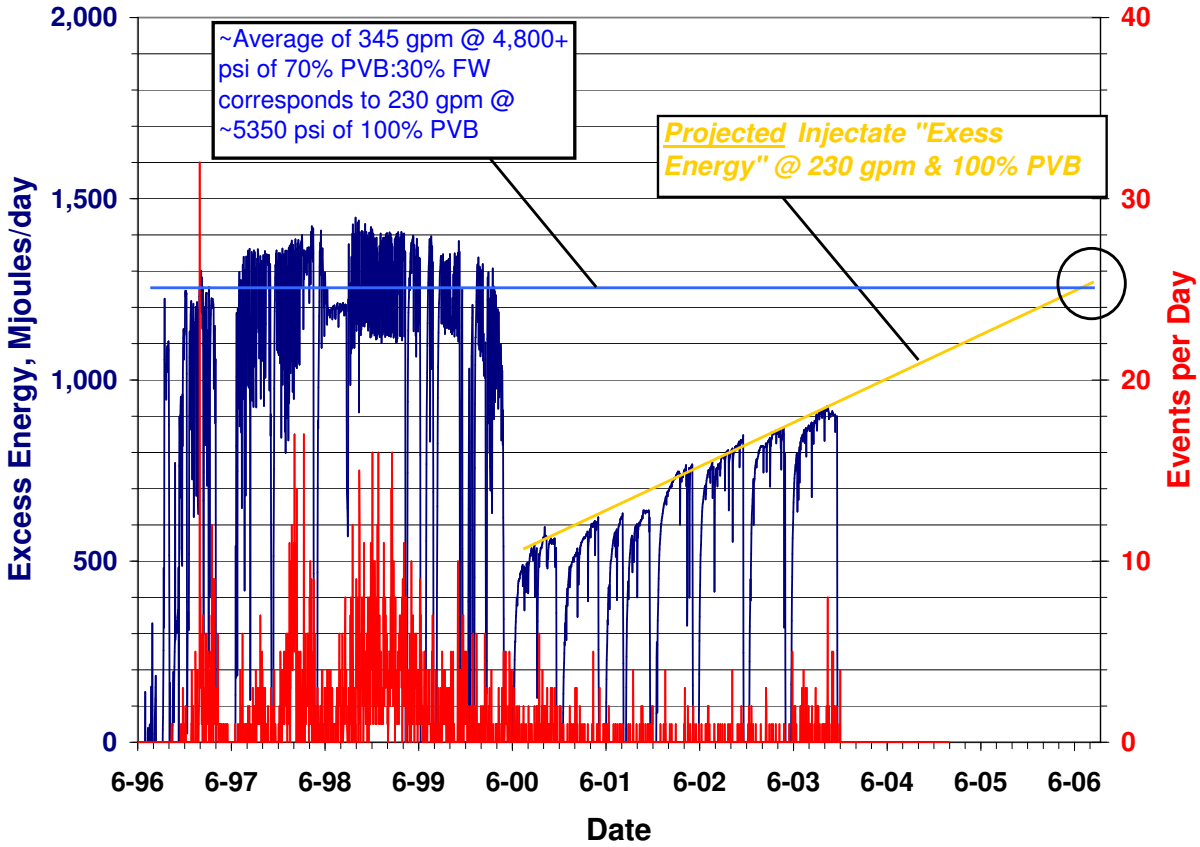

Figure 2-5 Excess Energy (Rate) and Number of Seismic Events as a Function of Time for 1996 through end of 2003. Circle shows projected time when presently increasing excess energy rate will match average, pre-2000 excess energy rate.

seismic events per day for the same period. Note how the number of events tends to track EE. We stress the inexactness of the term "tends to track," realizing that the correlation in **Figure 2-5** is not mathematical but visual. Note also, the increase in events in the later half of 2003 compared to later 2000 and all of 2001, 2002 and the first half of 2003. This increase seems to follow the increase in EE, which by the end of 2003 was at its highest since PVU reduced from ~345 gpm to ~230 gpm in mid 2000. Also shown in the figure are gold and horizontal (light) blue lines. The

gold line is a projection of the *Phase IV* EE, the current pumping schedule, and the horizontal blue line is a projection of average *Phase I* EE, PVU's most aggressive pumping. The circle at the right shows where the gold and horizontal (light) blue lines intersect showing the projected time when the excess energy for *Phase IV* matches that for *Phase I*. As noted in the graph, EE for *Phase I* injection (1306 lpm (345 gpm) @ 33.1+ MPa (4,800+ psi) surface pressure and 70:30 PVB to fresh water) corresponds to an EE for *Phase IV* injection at 870 lpm (230 gpm) @ ~36.9 MPa (~5350 psi) of 100% PVB. At wellhead pressure above ~36.9 MPa at 100% PVB, PVU will be injecting at a level for which we have no (previous) data with which to compare.

We can use the EE model to examine daily seismic event production and possible ramifications. Consider **Figure 2-6**, the average number of seismic events per day as a function of the average excess energy per day. In the figure the large data points are for all events with **M** > 0, while the small data points are the subgroup 0 < **M** < 1.8. In addition two lines have been added, one, a horizontal (blue) line through the small event per day data points and a second, diagonal line (red) through the large event per day data. The lines were eye-balled and have been added to distinguish what appears to be two states in the inducement of seismicity. One state is a lower excess energy; the other is at higher excess energy. These states seem to segment at a threshold designated by the large grey circle (i.e., the intersection of the two lines). In support of the concept of two states, consider the large grey circle. It is located at ~750 Mjoules/day (i.e, ~0.75 Gjoules/day) EE. Now consider **Figure 2-5**. The *Phase IV* (i.e., 2002 and 2003) excess energy in the figure is increasing with time and the event per day data in **Figure 2-5** shows an increase in the last half of 2003. If one draws a 750 Mjoule/day (horizontal) line across the figure it intersects the 2003 data at about the onset of the increased seismic activity. **Figure 2-6** predicts a change (i.e., an increase) in seismic activity at roughly about 750 Mjoule/day. At that same level, roughly 750 Mjoule/day, **Figure 2-5** shows the onset of an increase in seismic active in the second half of 2003. We believe this feature in **Figure 2-5** supports the prediction of a change in seismicity at roughly 750 Mjoules/day.

We've considered this two-state model for induced seismicity and have a couple of working hypotheses. One hypothesis states that at low excess energy, injection overcomes both the least principal stress and the injectate leak off and is sufficient to induce events by liberating only

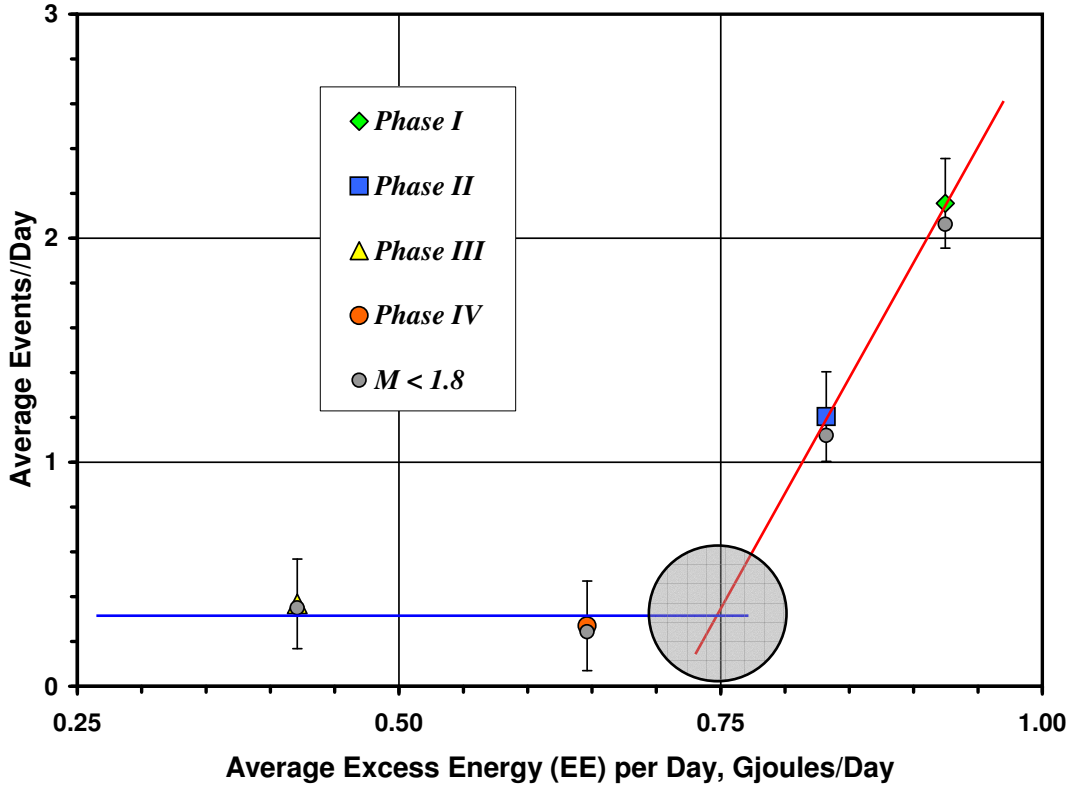

*Figure 2-6 Average Number of Seismic Events per Day versus Average Excess Energy per Day for events with **M** > 0. Data are listed by injection phase. Small gray circle data points are the subgroup 0 < **M** < 1.8 for the same phases.*

events in or near the maximum resolved shear stress direction. This holds until the excess energy reaches the threshold zone. In and beyond this zone, the excess energy is sufficient to liberate events along the maximum shear direction. Once maximum shear has been reached the number of events should increase dramatically. The second hypothesis agrees with the low excess energy explanation of the first hypothesis. However, at and above the threshold, the second hypothesis sees the increased liberation of events as a function of the increased energy overcoming the asperities or roughness of the locked faults, joints, planes of weakness, etc. We are presently delving deeper into the data to determine if either of these or another hypothesis is correct.

2.3 Swarm Analysis

For some years we have noted that some regions within the seismic zone surrounding the injection well seem to become active and then inactive. During 2003 we isolated a region that seems very responsive to changes in injection. We have defined the region as a square region running from -0.2 km south of the well to 0.5 km north of the well and west from the well to -0.7 km (i.e., area = ~0.5 km^2); in map view, the region is shown in **Figure 2-7**. **Figure 2-8** shows a close up of the swarm zone and a break down of events into 1996-2003, pre-November 2003, and November and December of 2003. Since 1996, this region has generated ~680 or ~18% of the near-well-

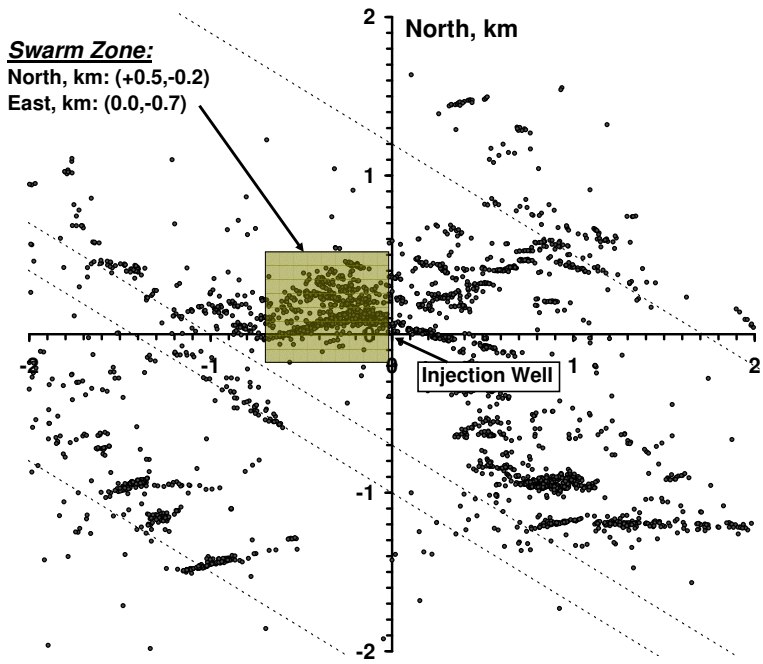

Figure 2-7 Square Region Identified as an Injection-Sensitive Active Swarm Zone.

bore events. By comparison, it covers less than 5% of the near-well zone.

We have found that within the region designated in **Figure 2-7** and **Figure 2-8**, the seismicity is very responsive to wellbore injection. **Figure 2-9** shows the downhole pressure (since 1996) and the occurrence times of events (yellow diamonds) within the swarm regions in **Figure 2-7** and **Figure 2-8**. To prevent confusion, the y-axis location of the occurrence data is arbitrary. The importance of the occurrence data is time. Note how closely the gaps in the occurrence data follow the gaps (i.e., shut downs) in the pressure data. When the injection is shut down, the swarm region very quickly stops being seismically active. Normally, the delay between seismic response

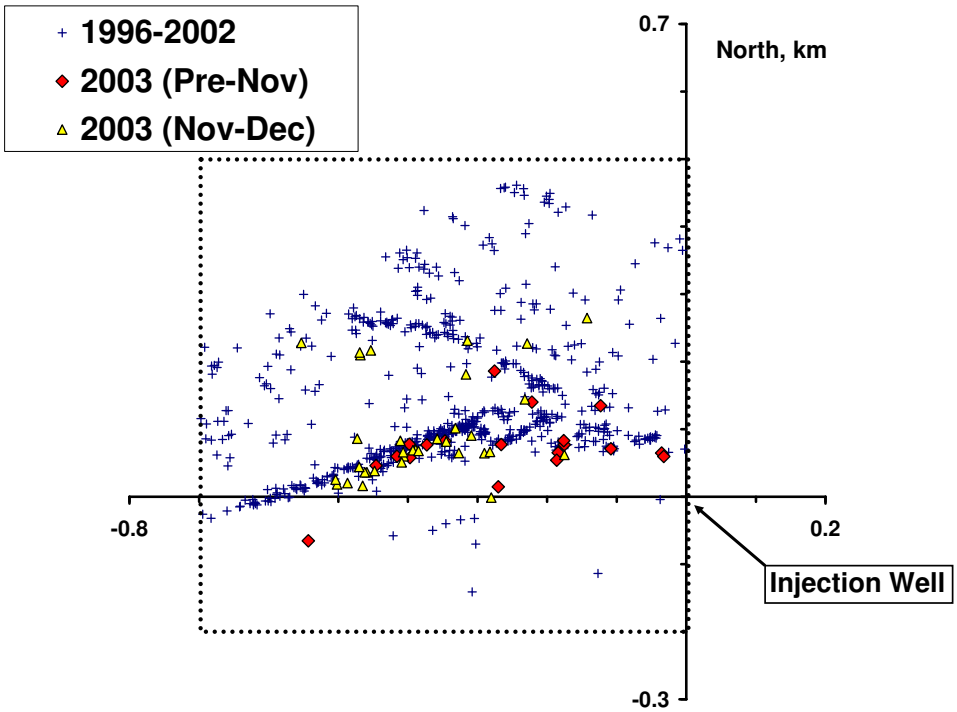

Figure 2-8 Close-up of the Active Swarm Region Designated in Figure 2-6. Events are shown by pre-2003, pre-Nov. 2003 and Nov. and Dec. of 2003.

and injection cessation is much longer, weeks to months. In this swarm zone, this time delay is hours to a few days. Note also in **Figure 2-9**, when the downhole (injection) pressure is below a threshold of about 11,000 psi (~76 MPa), the region is inactive even though PVU is still injecting. To examine this threshold more closely, consider **Figure 2-10** and **Figure 2-11**, the excess energy and event occurrence in the swarm region and the excess energy and event occurrence in the swarm region for only *Phase IV*. For both figures we used an 11-day moving-window average to smooth the excess energy. Note that in these figures, the *Phase IV* excess energy seems to show a swarm-initiation threshold of ~825 Mjoules/day. This analysis is in its preliminary stages and will be further examined in the coming year.

2.4 Mohr Circle Analysis

2.4.1 General

[*Note*: We give a short tutorial of the Mohr circle analysis based on Cosgrove (1995).] The Mohr

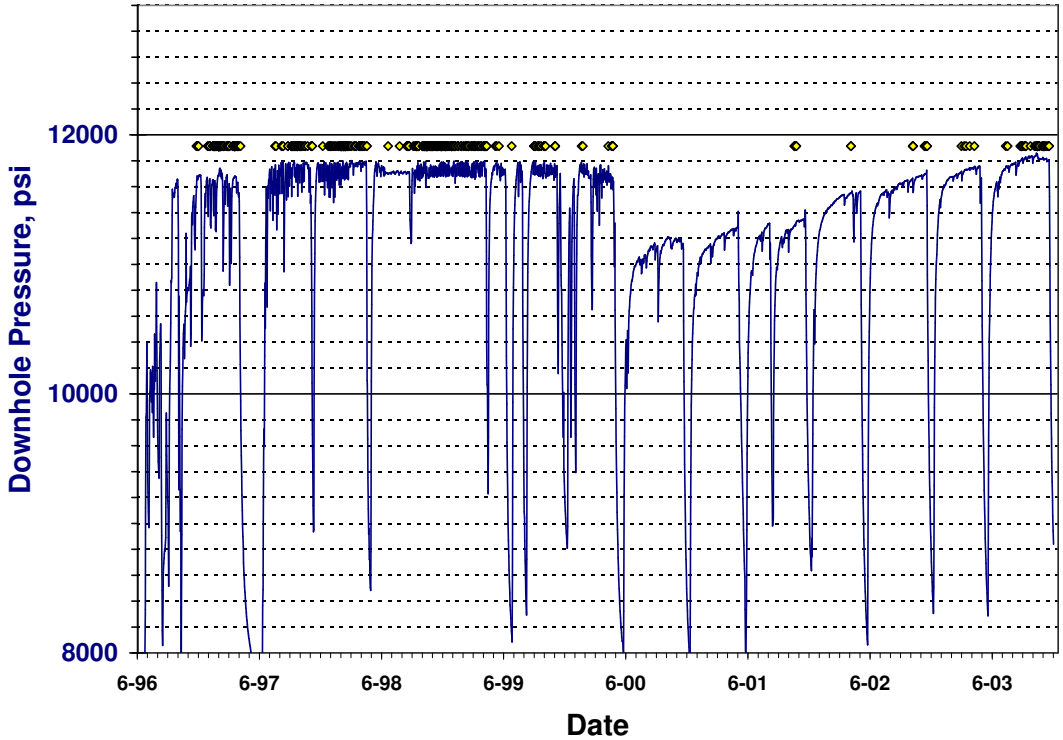

Figure 2-9 Downhole Pressure (@4.3 km, 14080 ft) versus Date and Occurrence Time of Events in the Swarm Region Shown in Figure 2-7 and Figure 2-8.

circle is a graphical method for resolving the shear and normal stresses and the potential for shear and tensile failure based on the maximum and minimum principal stresses of a system in compression. The equations that give shear and normal stresses from the maximum and minimum principal stresses result in a circle, the Mohr circle, when the principal stress are plotted on the x-axis and the shear stress on the y-axis of a graph (**Figure 2-12**).

To determine shear and tensile failure, respectively, we add the Navier-Coulomb criteria and the Griffith criteria, respectively, to the graph, as shown in **Figure 2-12**. The Navier-Coulomb criteria, which plots as a straight line, is given by the expression

$$\tau = C + \mu \cdot \sigma_n \qquad (7)$$

where τ is the peak shear stress of the eventual slip plane, C is the cohesive strength of the plane (C=0, no cohesive strength, preexisting fracture), μ is the coefficient of friction and is frequently written as tan(ϕ) where is ϕ is called the friction angle (see **Figure 2-12**), and σ_n is the normal stress across the failure plane. The Griffith criteria, which plots as a curved surface on the left side

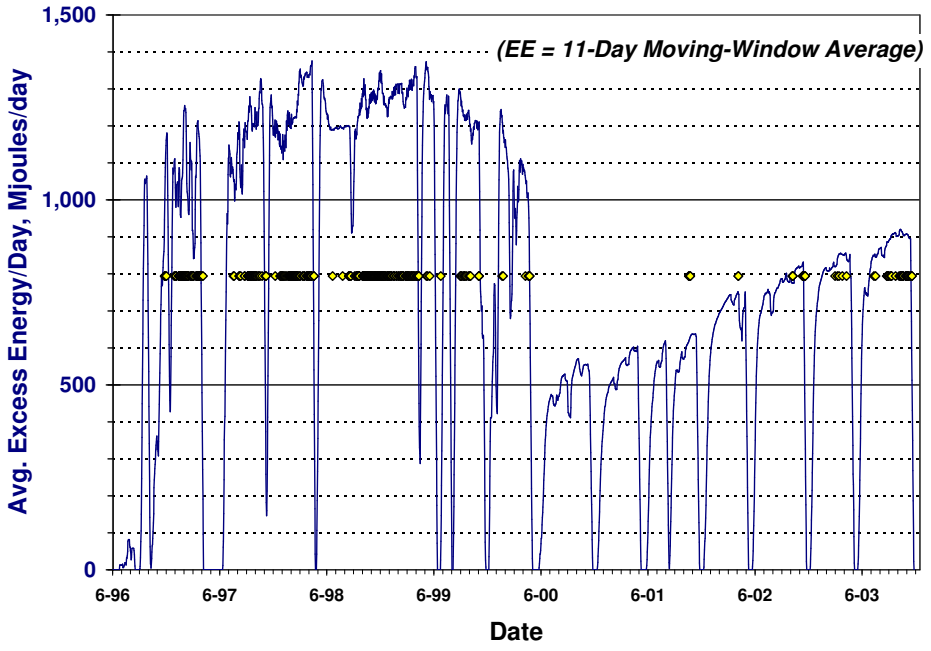

Figure 2-10 Average Excess Energy and Event Occurrence for Swarm Region Defined in Figure 2-7 and Figure 2-8.

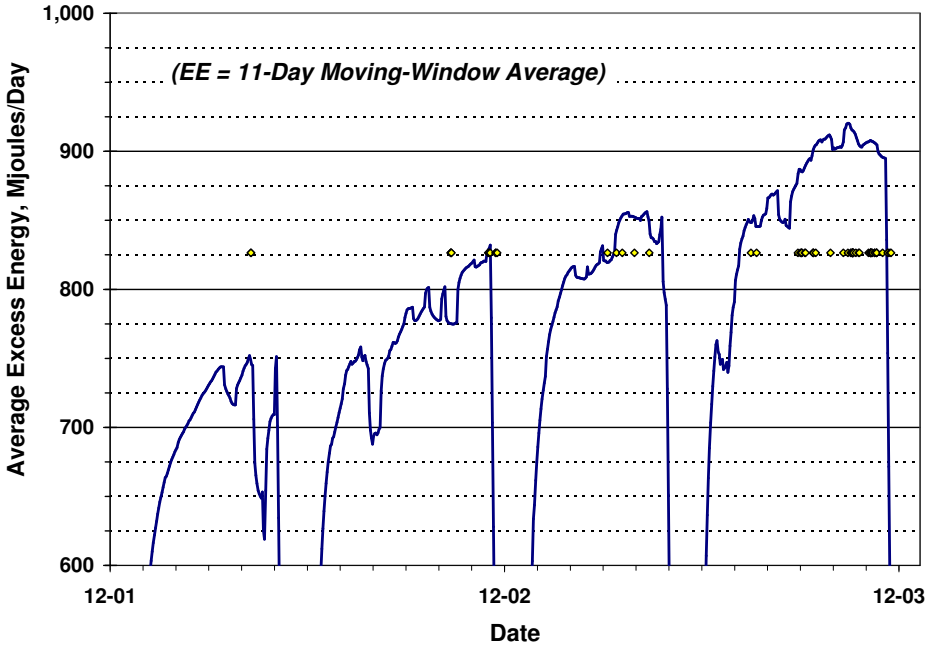

Figure 2-11 Close Up of Average Excess Energy and Event Occurrence for Swarm Region (Figure 2-7 and Figure 2-8) with Time Window Limited to Phase IV Injection Only.

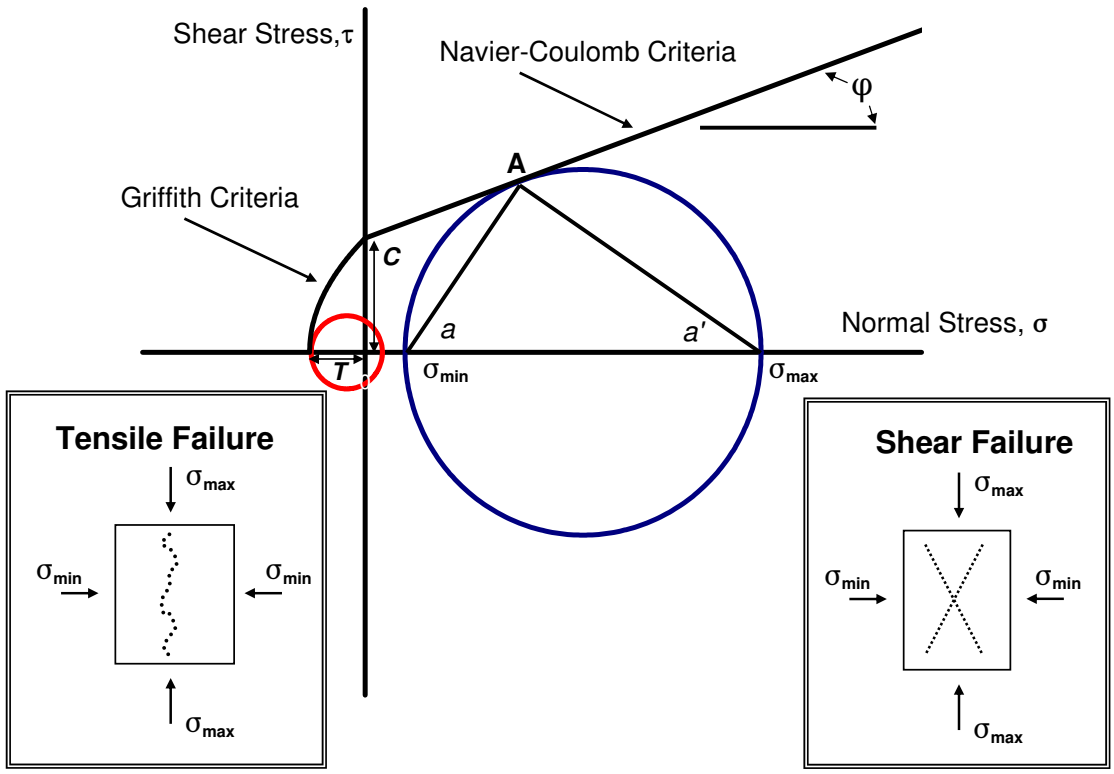

Figure 2-12 Tutorial Plot of Mohr Circles, Failure Criteria, Key Parameters.

of the graph and which equals the Navier-Coulomb value at the y-axis, is given by the expression

$$\tau^2 + 4T\sigma_n - 4T^2 = 0 \qquad (8)$$

where T is the tensile strength of the rock and is typically given as C=2T. As noted in **Figure 2-12**, the positive x-axis or right side of the figure corresponds to shear failure and the negative x-axis or left side corresponds to tensile failure. If the Mohr circle that describes a physical system is to the right of the Navier-Coulomb line (blue circle in **Figure 2-12**), then all fracture planes are locked by their own friction and cohesive strength. If one introduces fluid in the system through pore pressure then the Mohr circle is shifted to the left. The shift is by the amount of the pore pressure. If the shift results in the Mohr circle becoming tangent to the Navier-Coulomb line (point A in **Figure 2-12**), then a plane at a preferred angle to the maximum and minimum stress can slip in shear, as shown in the right side insert in the figure. From **Figure 2-12**, the angles **a** and **a'** give the angles of the shear failure plane with respect to the minimum and maximum principal stress, respectively: **a** = 45° - $\phi/2$ and **a'** = 45° + $\phi/2$. In order for tensile failure to occur, the Mohr cir-

cle must touch the Griffith criteria at the point $\tau = 0$, $\sigma_{min} = T$. As noted in the insert to the left, in **Figure 2-12**, the failure plane will be in the direction perpendicular to the minimum principal stress. As one can see in the figure, the diameter of the Mohr circle is the maximum principal stress - minimum principal stress. For tensile failure to occur, this diameter, must be small compared to the T, the shear strength of the rock.

2.4.2 Paradox Injection and Mohr Circle

Figure 2-13 shows three Mohr circles for Paradox injection at 4.3 km (14080 ft) depth. and two

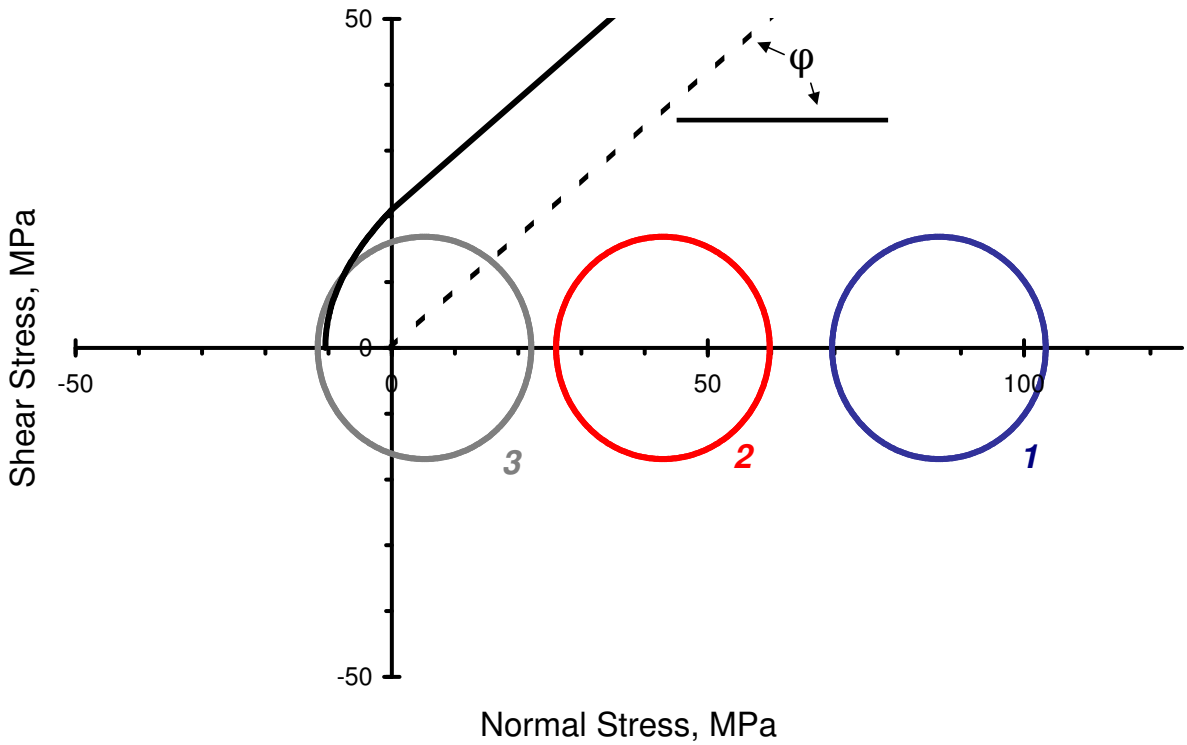

Figure 2-13 Mohr Circle Plots for Three Different States (numbered circles, see text), Navier-Coulomb Criterion (straight lines) and Griffith Criterion (solid curve) for Average Limestone.

Navier-Coulomb failure criteria and one Griffith criteria. The solid line in the figure is the criteria for average parameters for competent (i.e., unfractured), intact limestone, as given by Hendron (1968, p. 33) and Goodman (1980, p. 78). These are friction angle of 40° and cohesive strength of ~21 MPa. (~3050 psi). The dash failure criteria assumes the same friction angle, but with no shear strength.

Circle number 1 in **Figure 2-13** is the state of stress inferred from the well logs of mechanic properties and the inferred hydraulic fracture pressure (Envirocorp, 1995) with no fluid pressure included. The well logs were used to estimate an assumed lithostatic or maximum principal stress, which is vertical and found to be ~103 MPa (15,000 psi or 1.07 psi/ft); the hydraulic fracture pressure gives a least principal stress, which is horizontal, and found to be ~69.6 MPa (10,100 psi or 0.72 psi/ft). Circle 1 is totally to the right of the failure criteria and therefore, in the absence of fluid pressure, there would be no slippage across any planes. Circle 2 is the same as circle 1 but with the addition of fluid pressure. The pressure here is the Leadville Limestone (native) aquifer pressure at 4.3 km, ~43.6 MPa (6330 psi or 0.45 psi/ft). The addition of the native aquifer fluid pressure is not sufficient to cause failure. Circle 3 is the circle 2 with the addition of PVU downhole injection pressure at the end of 2003, 81.4 MPa (11,800 psi); note that portions of it are to the left of the solid and dashed lines. Simply put, circle 3 shows that the injection pressure as PVU is sufficient to induce both shear and tensile failure.

2.5 Total Seismic Event Production at PVU

One question that has been asked since the beginning of injection is how many microevents (i.e., events of magnitude -2.0 or -3.0 and greater) are generated by the injection. The observed PVSN data cannot answer this question, since its cutoff (i.e., smallest recorded events) ranges between **M** 0.0 and **M** -0.5, and the numbers recorded in this range are incomplete. We extrapolated the recurrence curve for the PVSN data at **M**0.5 and greater (discussed in section 7.8) assuming that the Gutenberg-Richter relation for number of events versus magnitude remains valid for microevents.In an earlier discussion we extrapolated the 1996-2003 PVSN data and predicted roughly 600,000 total events of **M** -3.0 and greater for this period. However, we used a second method and we apply this method to all the PVSN data, 1991-2003, with **M**0.7 or greater. We used **M**0.7 as the cutoff because we feel more confident in having a complete data set above this cutoff.

The new method is based on *in situ* seismic monitoring of hydraulic fractures. Unlike PVSN monitoring in which the seismometers are stationed at the surface, *in situ* monitoring has seismometers in wells neighboring the injection well at or near the depth of injection. These neighboring wells can be less than 100 m from the injection well. Because of the proximity of the *in situ* seis-

mometers to the injection, much smaller events can be recorded than can be recorded at the surface. Data from a series of 6 *in situ* monitoring was published by Phillips et al. (2002) and is shown in **Figure 2-14**.

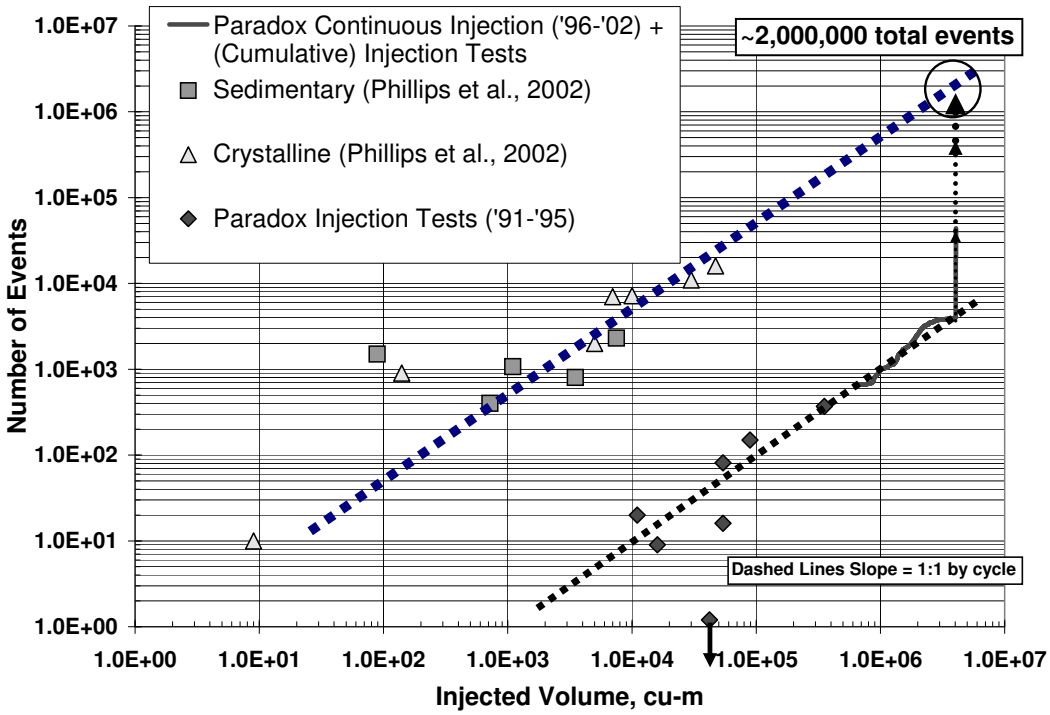

Figure 2-14 Cumulative Number of Seismic Events Produced vs. Injected Volume

Figure 2-14 shows number of seismic events produced as a function of injected volume from Phillips et al. (2002) and for Paradox. The Phillips data is divided into target zone rock type, crystalline and sedimentary, and the Paradox data is divided into the injection test data and the cumulative data, including test data plus the continuous injection data (solid red line). The dark blue dash line through the Phillips et al. data is a linear trend line. We projected a same-slope line as the Phillips et al. line through the Paradox data and found that it fit these data quite well. From the end of the (Paradox) red line we projected a vertical line (dashed-line arrows in the figure) to the Phillips line. The intersection point of the Phillips et al. line and our projected line, indicated by the circle, is an estimate of the total number of events at Paradox if we had an *in situ* array. This number is ~2,000,000 events. We then looked for the 2,000,000-events point on the back-projected recurrence curve for all the Paradox data (1991-2003), not the 1996-2003 data discussed

above, and found this corresponded approximately to magnitude **M** -2.3. As a means to gage an **M**-2.3 event, we calculated an approximate area (equation (12) below; **Figure 7-25**) and found its diameter (assuming a round or penny-shaped flip area) to be on the order of a few meters.

2.6 A Fractal Model to Accommodate Injectate Volume

2.6.1 Background

Since inception in 1991, PVU has injected ~4.1×10^6 m^3 of fluid. For a first-order approximation consider a 2 km tall fracture uniformly open 2 mm, to accommodate this volume would require ~1,000 km of fracture length. Looking at a map of the seismicity at Paradox, we find between 10 and 20 km of seismically-illuminated fault and fracture length and maybe 20 to 30 km of implied fault length (i.e., making robust assumptions about the main and non-seismically activated faults of the Wray Mesa system). These faults and fractures are not 2 km tall, but if we error on the side of conservatism and put an upper bound on faults of 2 km, we find, at most, only a few percent of the total injected volume can be accommodated by the known and implied fractures, faults, joints, etc. This then begs the question of where the remaining ~95+% injectate resides. Typically injectate leaks from the main and illuminated fractures, faults, etc. into the native porosity. However, the native porosity (i.e., pre-injection small fractures and pores) for the target formations at PVU is very small. Since the injection pressure at PVU is in excess of that necessary to nucleate and grow hydraulic fractures in the target rocks, we surmise that the PVU injection is fracturing the target horizons, creating new fractures (i.e., creating new volume space that accepts most of the injectate). Similar to the creation of new fracture volume at PVU, Turcotte (1997) discusses fragmentation/fracturing processes and shows that fracturing typically results a fractal distribution of fracture sizes. Following Turcotte, we developed a fractal model of fracture sizes for PVU.

2.6.2 Mathematical Foundation

The concept of fractals were first developed when it was recognized that special figures or shapes could be created that did not change in appearance under increasing magnification. This figures

exhibited fractal behavior. This concept is captured in the following equation

$$N = cr^{-D} \tag{9}$$

where N is the number of entities being considered (we will consider small fractures), c is a proportionality constant, r is a size associated with the entities (we will use r = radius of fracture), and D is the fractal dimension. D is an elusive parameter to define. Physically it describes how a distribution or group of entity fills space. For example, geometric figures like circles or squares have a fractal dimension of 2, since they are 2-dimensional bodies and fill a space as 2-dimensional bodies. Similarly, spheres or cubes have fractal dimensions of 3, since they are 3-dimensional bodies. A fractal distribution of fractures typically has a fractal dimension of between 2 and 3, meaning it fills a space more completely than a 2-dimensional body and less completely then a 3-dimensional body. Mathematically, for a fractal distribution, as developed here, D determines the increase in number of entities in the distribution as one increments to the next smaller size (i.e., increases the magnification) of the distribution.

For the model we developed, we incremented (i.e., step through magnifications) the fracture radii in decadal increments (i.e., powers of 10). At two adjacent levels of magnification we have the equation

$$N_{i+1}/N_i = (c(r_{i+1})^{-D})/(c(r_i)^{-D}) \tag{10}$$

which simplifies to

$$N_{i+1} = N_i \cdot (r_{i+1}/r_i)^{-D} \quad \text{where } (r_{i+1}/r_i) = 10 \tag{11}$$

To complete equation (11), we determined an initial value, N_o, for the fracture distribution. As is common for this type of modeling we will assume a thin, circular fracture or penny-shaped fracture. Based on the seismicity, we assume an initial fracture radius of 100 m. Using an equation

from Wells and Coppersmith (1994) that relates the magnitude **M** of an earthquake and the area of slip with radius *r*

$$\mathbf{M} = 4.07 + 0.98 \times Log_{10}(\pi r^2) \tag{12}$$

we find that for radius of 100 m, M = ~2.6. From our seismic data we have ~20 events with M = ~2.6. Hence, we fixed N_o at 20.

2.6.3 Calculations

Normally we'd begin the calculations with 20, r = 100 m penny-shaped fractures (i.e., N_o) and use equation (8) to determine N_1, the number of 10-m fractures. Then from N_1 we would calculate N_2 for 1-m fractures etc. We would calculate down to a radius of 0.01 mm. To do this calculation we need the fractal dimension *D*, which we have not computed, yet. To determine *D*, we used another fixed (i.e., boundary) condition of this model, the injected volume. We solved for *D* by calculating the volume of the fractures and comparing it to the injectate volume. We then adjusted *D* until the fracture volume approached the injectate volume as closely as possible limiting *D* to two decimal accuracy. To determine the volume of the fractures we assumed penny-shaped fractures with the aforementioned decadal increment in radius and fixed fracture openings. We separately calculated models with 1, 2, and 3 mm openings for all fractures with 10 mm or larger radii and 0.1*r* openings for all smaller fractures. To make each model more realistic we included 3 10-km long by 1 km high, Wray-Mesa style faults. During the calculations, each of these faults had the same aperture as the fractally distributed faults. The results of the calculations found *D* equal to 2.76, 2.66, and 2.60 for apertures of 1 mm, 2 mm, and 3 mm, respectively. **Table 2-2** gives the results of the calculation noting the event magnitude (Wells and Coppersmith, 1994; equation (12)) for each size fracture, if one slipped; the cumulative percent volume of injectate in the cumulative volume for each fracture size; and the number of fractures of that size, all for each of the 1-mm, 2-mm, and 3-mm models. **Figure 2-15** shows additional results of the model. In that figure, the Paradox data with magnitudes less than 0.0 are linearly projected from the data with magnitudes greater than 0.0.

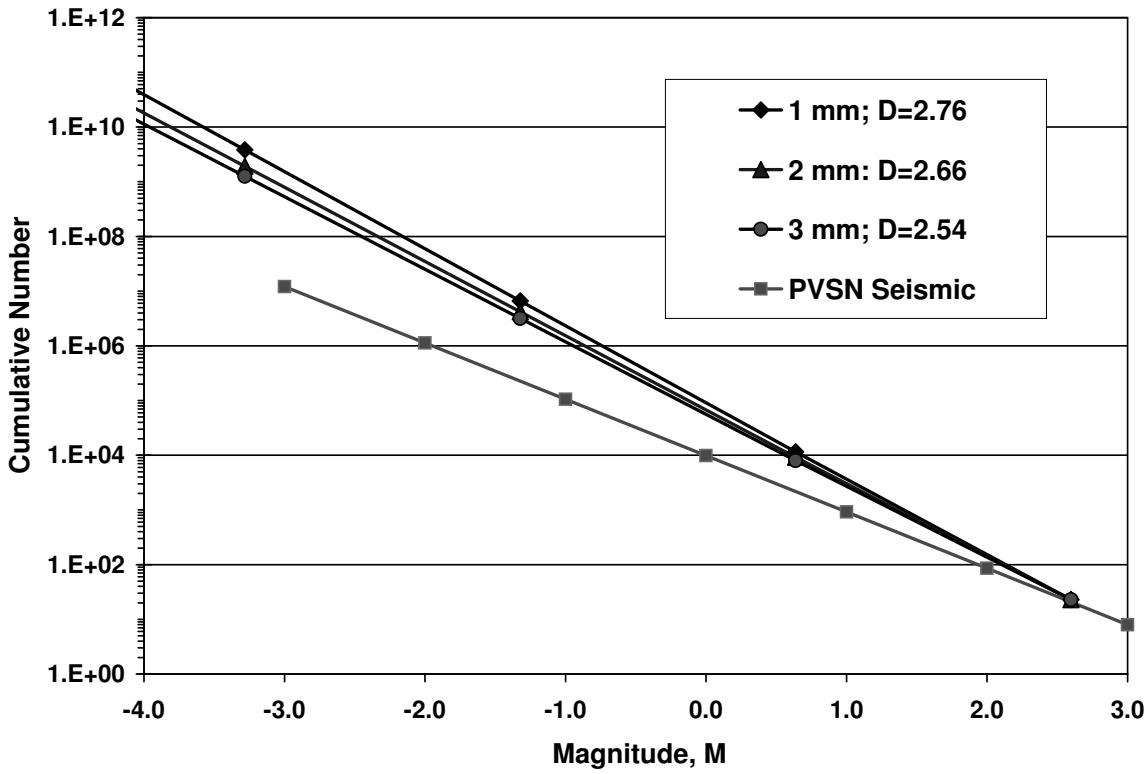

Figure 2-15 Comparison of Cumulative Number of Fractures for Various Fractal Model and PVSN Seismic Data, all versus Event Size. For the Fractal Model Magnitude is Calculated Assuming Each became Seismically Active

Table 2-2 Fractal Model Results

		Fracture Opening Models					
Radius	**W&C[a]**	**1-mm**		**2-mm**		**3-mm**	
mm	**M**	**Cum.% Volume[b]**	**No. Fracs.**	**Cum.% Volume[b]**	**No. Fracs.**	**Cum.% Volume[b]**	**No. Fracs.**
1.0e+5	2.6	0.02%	20	0.04%	20	0.06%	20
1.0e+4	0.6	0.11%	1.1e4	0.18%	9.1e3	0.23%	8.0e3
1.0e+3	-1.3	0.65%	6.6e6	0.82%	4.2e6	0.93%	3.2e6
1.0e+2	-3.3	3.7%	3.8e9	3.8%	1.9e9	3.7%	1.3e9

[a]Wells and Coppersmith (1994) fault area-magnitude relation, equation (12)
[b]Percentage of injectate total volume; cumulative total given at bottom of column

Table 2-2 Fractal Model Results

		Fracture Opening Models					
Radius	**W&C[a]**	**1-mm**		**2-mm**		**3-mm**	
mm	**M**	**Cum.% Volume[b]**	**No. Fracs.**	**Cum.% Volume[b]**	**No. Fracs.**	**Cum.% Volume[b]**	**No. Fracs.**
1.0e+1	-5.2	21.5%	2.2e12	17.1%	8.7e11	14.8%	5.0e11
1.0	-7.2	12.4%	1.3e15	15.7%	4.0e14	17.7%	2.0e14
1.0e-1	-9.2	7.1%	7.3e17	7.2%	1.8e17	7.0%	8e16
1.0e-2	-11.1	4.1%	4.2e20	3.3%	8.3e19	2.8%	3.2e19
		99.5%		96.1%		94.5%	

[a]Wells and Coppersmith (1994) fault area-magnitude relation, equation (12)
[b]Percentage of injectate total volume; cumulative total given at bottom of column

2.6.4 Fractal Model Implications

We recognize that the results in **Table 2-2** are based on very speculative premises, but it is very interesting to note that for all the fracture opening models, ~90% of the injectate is emplaced in fractures of 1 mm in radius or greater. If this is true, it is quite significant. It shows that at Paradox, the small to interstitial sized porosity, which is negligible, is fortunately not a factor in the operations and life of this reservoir. What is important, is maintaining the injectate pressure above the fracture pressure and creating new fracture volume in which to emplace the injectate.

Another interesting result of this model is that the fractal dimension *D* is a dynamic parameter. As more injectate invades the reservoir, *D* must increase. Fortunately, the results given in **Table 2-2** are very sensitive to fractal dimension. A very small increase in D gives a substantial increase in fracture volume. Despite making this statement, further analysis is warranted. Consider the calculated number of fractures of 10, 1 and 0.1 mm. Roughly, they correspond to 10^{12}, 10^{15}, and 10^{17}, respectively. In a volume of 20 km^3, this corresponds to an average fracture density of one 10-mm fracture per $2x10^4$ cm^3, one 1-mm fracture per 20 cm^3, and five 0.1-mm fractures per cm^3, respectively. Even at 10 times the current cumulative volume (~80+ years of injecting), this model

says there is still plenty of room in the reservoir to accommodate the necessary fractures (i.e., future injectate volume).

The results shown in **Figure 2-15** imply that many more fractures are created than are seismically activated. Recall that the projected number of seismic events in **Figure 2-15** is based on the number of events, specifically shear failures, that are recorded at the surface. The difference between the number of projected seismic events and the number of modeled fractures is consistent with our understanding of fracturing. Fractures most easily open against the smallest or least principal stress. The direction of fracture opening is itself a principal stress direction, meaning it has not shear stress across it faces and no tendency to slip dynamically radiating seismic energy. However, once a fracture has been created, the local stress field may change with shear stress developing across the fracture face. If the shear stress becomes large enough to overcome the friction across the fracture, then the fracture can slip and radiate seismic energy. We are presently considering a model in which stress readjust due to inflation from the injectate.

2.7 Remote (Northern) Seismic Swarms

PVSN is a local seismic network, but is not limited to only events near the injection well. **Figure 2-16** shows events located between 10 and 20 km north of the injection well. During 2003 this region saw active swarms. One was in January and consisted of 7 events spread over about 21 days. All the events were **M**1.8 or smaller, well below human detection. This swarm is centered ~11 km north and 3 to 4 km west of the injection well. The second swarm occurred in August and consisted of 16 events spanning 6 days and all of magnitude **M**1.5 or smaller. In the figure it is a very tight swarm located ~10.5 km north and ~1 km east of the injection well. At this time, we believe these events are not induced by the PVU injection. Harr and Bremkamp (1988) and the established seismicity induced by injection do not strongly support fluid or pressure migration to the north of the well. The shape and time histories of the induced seismic regions support pressure migration to the northwest. However, neither Harr and Bremkamp nor the induced seismicity can preclude migration to the north. It must also be noted that in this area only one event was recorded during the 5 years prior to injection that PVSU monitored the regional seismicity. Presently, we are evaluating this area.

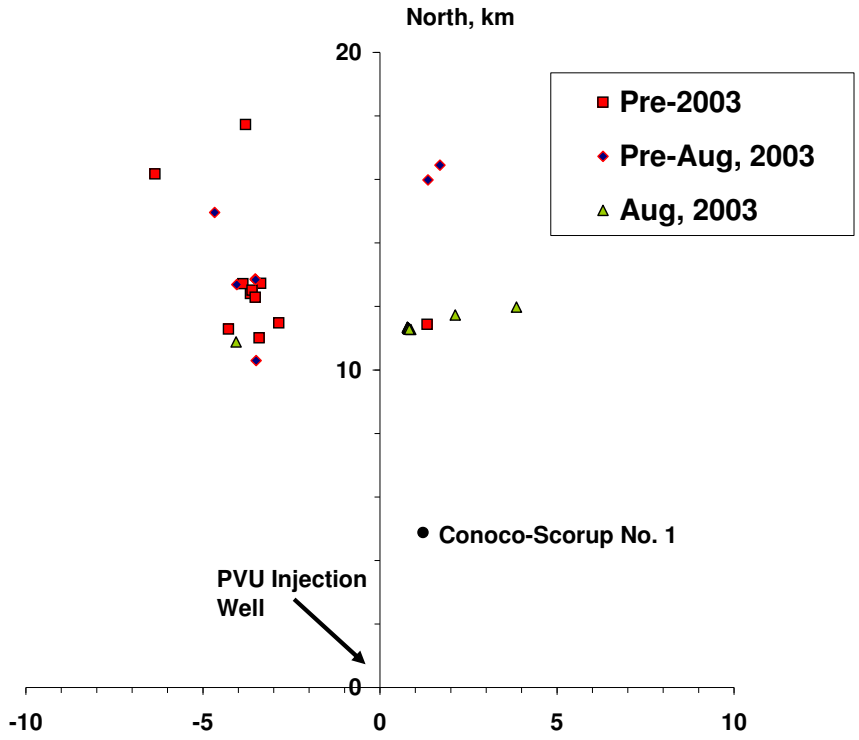

Figure 2-16 Seismically Active Swarms North of PVU Injection well

2.8 Second Well Considerations

During 2003 Reclamation had a number of discussion and prepared documents with regard to developing a second injection well at PVU. Most of our work for the development of a second injection well is slated for 2004. Appendix A at end of this report does show the final transmitted memo in 2003 regarding the proposed second injection site. The appendix also contains figures used during tele-conferences.

2.9 (Hickman) Breakout Analysis

During 2003 Drs. Stephen Hickman and Robert Summers of the US Geological Survey in Menlo Park, CA analyzed borehole breakouts from the original (1987) injection well televiewer logs. Appendix D gives their results for *in situ* stress which is consistent with our seismic analysis.

2.10 Reference: Pressure and Pressure-Gradient Plot

Saturated brine (100% PVB) at 20°C (68°F) contains 26.4% NaCl. It's specific gravity (s.g.) is 1.2. Using the pressure gradient of 0.433 psi/ft for fresh water (s.g. = 1.0), 70% (saturated) and 30% fresh water has a pressure gradient of 0.494 psi/ft, and 100% brine has a pressure gradient of 0.520 psi/ft. For PVB the commonly assumed specific gravity is 1.17 which gives a pressure gradient of 0.506 psi/ft for 100% PVB and 0.484 psi/ft for the 70:30 mixture.

Downhole pressure and pressure gradient frequently come up in discussion. We offer **Figure 2-17**, a plot of downhole pressure at 4.3 km (14,080 ft) and pressure gradient for 70:30 ratio of PVB to fresh water (s.g. = 1.119) and for 100% PVB (s.g. = 1.17). Because it is insignificant at this scale, these plots ignore borehole friction.

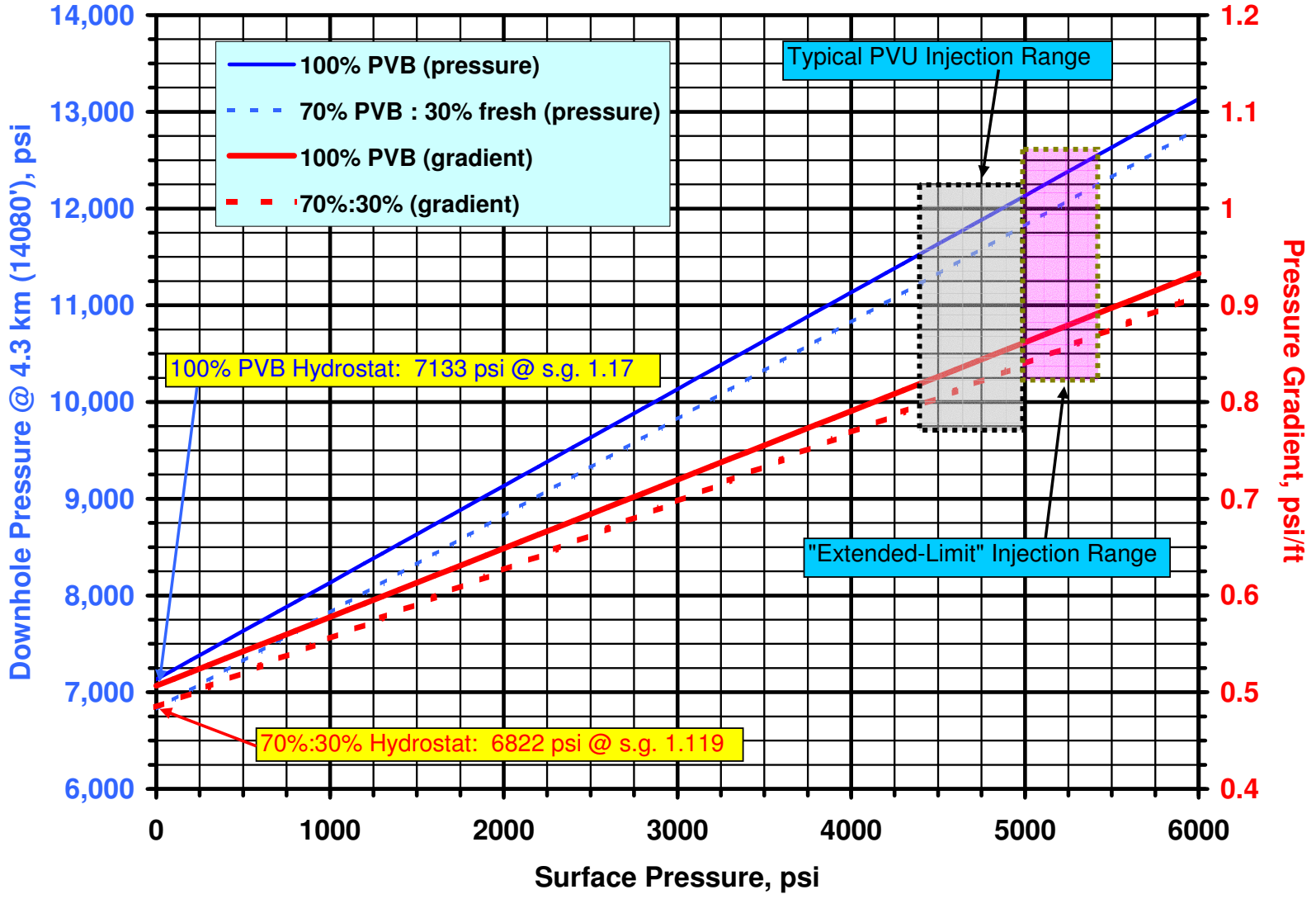

Figure 2-17 Downhole Pressure (blue) and Pressure Gradients (red) for 100% PVB and 70:30 PVB to Fresh Water. Graph ignore borehole friction. Pressure is calculated @ 4.3 km (14,080 ft).

3.0 LOCAL SETTING

The Paradox Valley Unit is located in western Montrose County approximately 90 km southwest of Grand Junction, CO and 16 km east of the Colorado-Utah border. Paradox Valley is about 40 km long on a N55^{o}W axis and from 5 to 10 km wide (**Figure 3-1**, **Figure 3-2** & **Figure 3-3**). The most prominent local feature is the LaSal Mountains in the Manti-LaSal National Forest, which rise to an elevation of about 3.7 km above msl and border Paradox Valley on the northwest. Paradox Valley has a relatively flat floor enclosed by steep walls of sandstone. Elevations vary from about 1.5 km above mean sea level (msl) in the valley to about 2.0 km above msl along the valley rim.

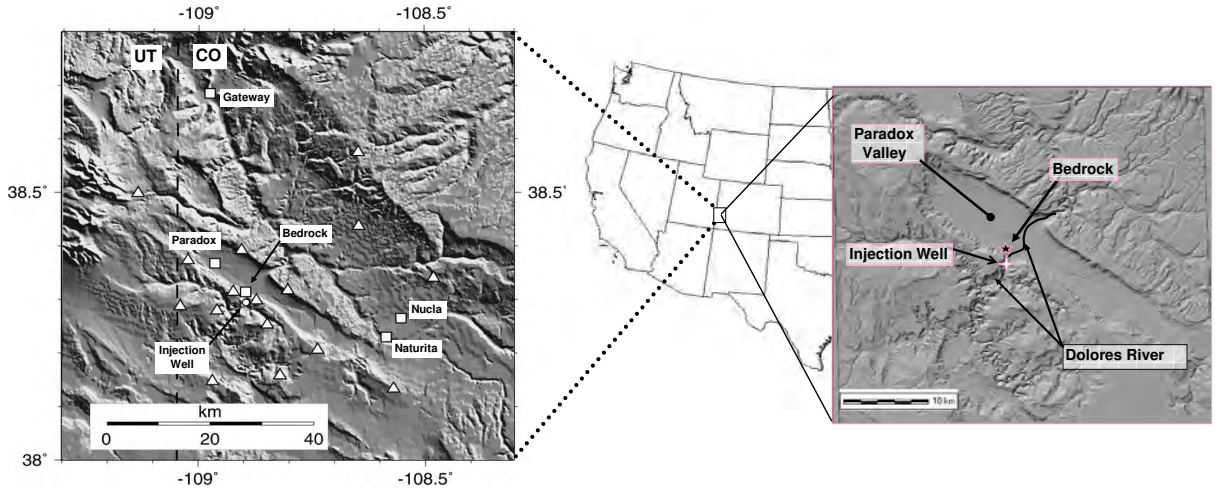

Figure 3-1 Location of Paradox Valley Unit and Regional Topography

Paradox Valley is one of five northwest-striking, collapsed diapiric salt anticlines in southwestern Colorado and southeastern Utah. The formation of these anticlines began about 250 mya when the emergence of mountainous uplifts placed intensive lateral stresses on the intervening sedimentary formations, causing faulting and fracturing along weak axial zones. Subsequently the stresses relaxed and combined with the weight of overlaying strata forced a deeply buried, salt-rich layer to flow upward into the faulted area creating the anticline. As pressures eased, the crest of the

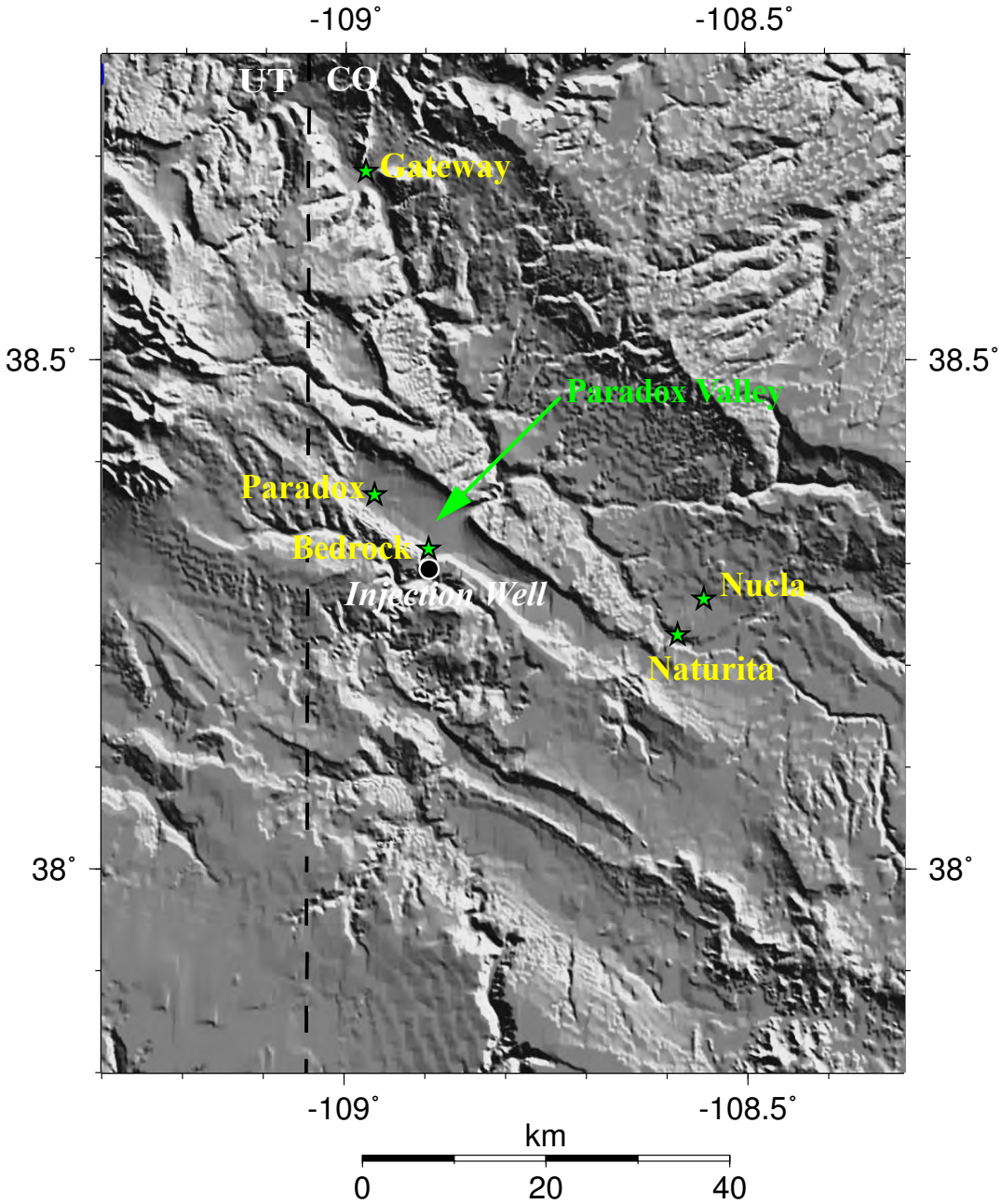

Figure 3-2 Regional topographic setting of PVU injection well, Paradox Valley, and local municipalities.

anticline gradually dropped downward into fault blocks. That and subsequent erosion created Paradox Valley. Currently, the Dolores River flows normal to the strike of the valley.

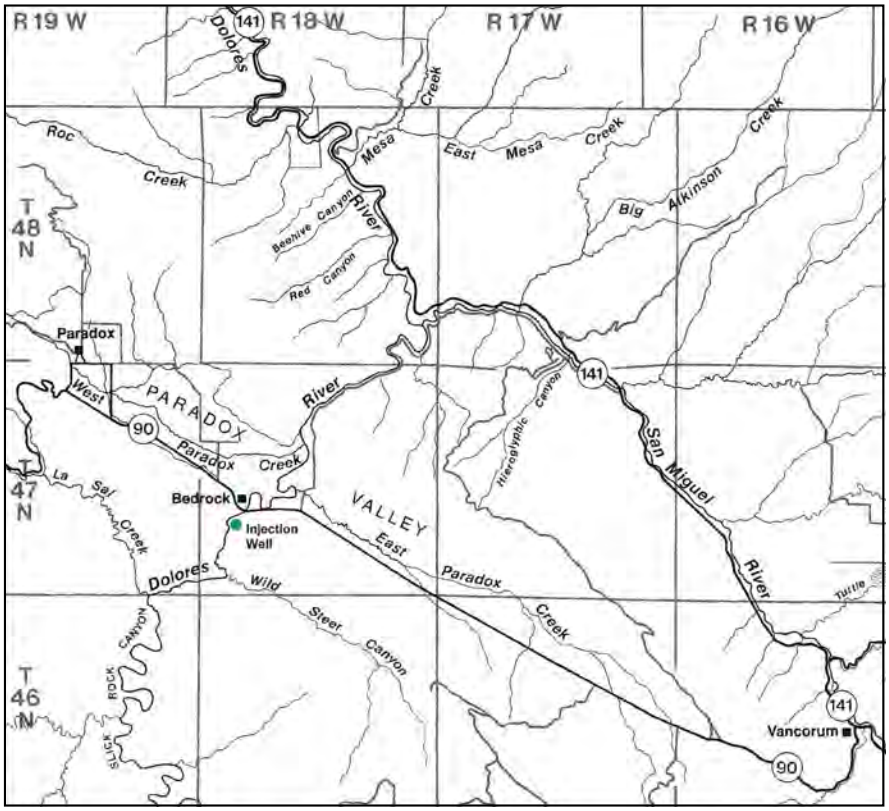

Figure 3-3 Paradox Valley Unit Injection Well and Local Geography. Figure is adapted from Parker (1992). Each square is approximately 10 km by 10 km

The Dolores River originates in the San Juan Mountains southwest of Paradox Valley in southwest Colorado and flows generally northwest for about 300 km to Paradox Valley and another 110 km to its confluence with the Colorado River northeast of Moab, Utah. Small tributaries in the unit area include La Sal Creek, which enters from the northwest about 8 km upstream from Paradox Valley, and West and East Paradox Creeks, which enter from the northwest and southeast within the valley. East Paradox Creek is intermittent, however, and has essentially no effect on the river flow. Over its path through Paradox Valley, the Dolores can pick up more than 180,000 metric tonnes (200,000 standard tons) of salts annually, primarily from brine-saturated ground water, PVB, percolating through seeps and springs in the salt and then through the Dolores' banks and beds. There are two general types of seeps and springs: brackish water with total dissolved solids (tds) varying from about 1,500 milligrams per liter (mg/l) to 4,000 mg/l and brine with ~260,000 mg/l. (For reference, fresh water is typically defined as < 400 mg/l tds.) Water pumped from the 9

extraction wells near the river has a salinity of ~260,000 mg/L (260,000 ppm which is about the maximum saturation for water). This brine, which is nearly eight times the salinity of sea water, consists mostly of sodium and chloride, with much smaller amounts of sulfate, potassium, magnesium, calcium, and bicarbonate. Heavy metals, particularly iron and lead, and non-radioactive strontium are also present in limited amounts. Noticeable amounts of hydrogen sulfide gas are released as the brine surfaces, creating a noxious odor.

3.1 PVU Salinity Control Well No. 1

The PVU Salinity Control Well No. 1 (**Figure 3-4)** was completed in 1987 at a total depth (t.d.)

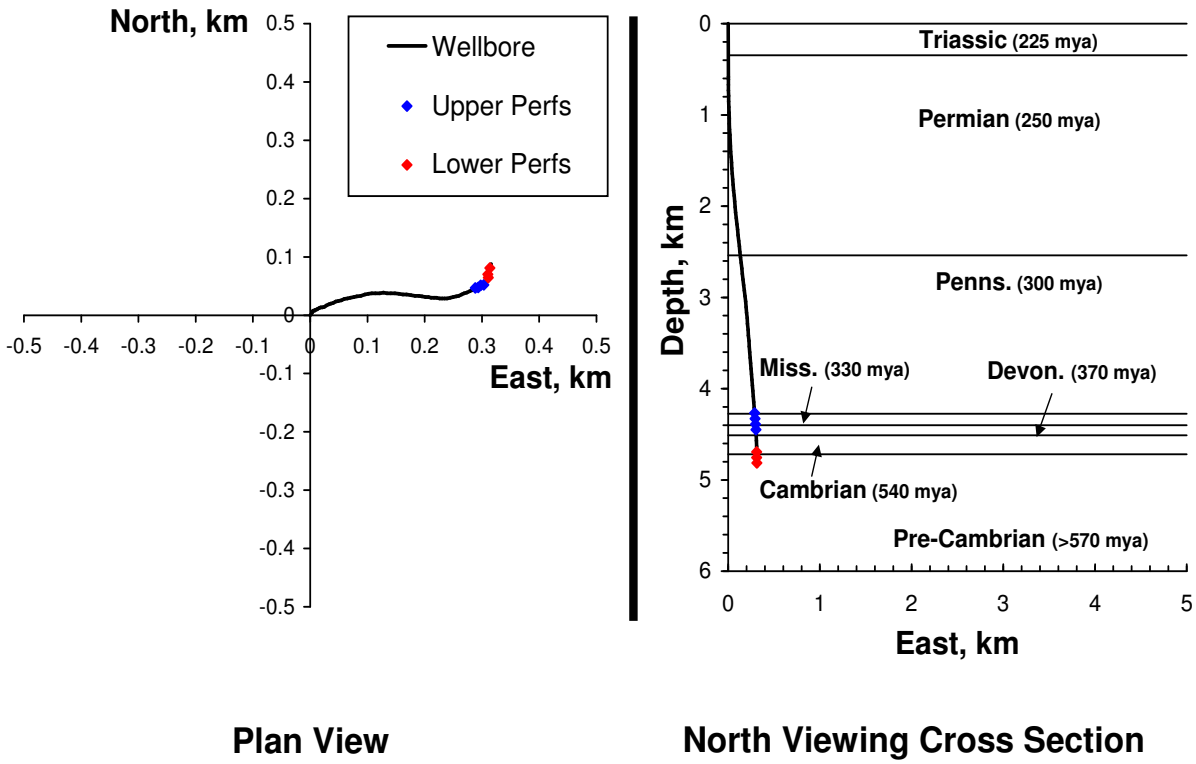

Figure 3-4 Plan view and north-viewing cross section of PVU Salinity Control Well No. 1, including the near-wellbore stratigraphic column based on well logging.

of 4.88 km (16,000 ft). The well was built to EPA Underground Injection Code (UIC) Class I standards, but was permitted in 1995 as a Class V disposal well. The well is located in SW SE section

30, township 47N, range 18 W Paradox Valley, Montrose County, CO. Its latitude and longitude are 38° 17' 43. 62" N and 108° 53' 43.32" W, respectively. The wellhead elevation (i.e. ground surface) is 1.523 km (4,996 ft) above mean sea level. The Kelly bushing of the well, a marker frequently used by drillers and well loggers, was 9.8 m (32 ft) above ground surface.

The well penetrates Triassic rock at the surface through Precambrian rock at t.d. and has a minor drift to the east and slightly to the north. Log-based, near-wellbore stratigraphy, the perforation intervals, and a plan view of the well are shown in **Figure 3-4**. Based on core and log data, the Mississippian Leadville carbonate was selected as the prime injection zone with the upper Precambrian as a secondary zone (Bremkamp and Harr, 1988). The well casing of PVU No. 1 was perforated at ~20 perforations/m in two major intervals between 4.3 km and 4.8 km.

3.2 Wray Mesa Fault and Fracture System

PVU Salinity Control Well No. 1 was sited to intersect the generally NW-SE trending Wray Mesa fault system. Movement on the Wray Mesa faults has created an extensive fracture field within the fault system. The main trend of the Wray Mesa fault system (N55^{o}W) is evident in **Figure 3-2**. In their 1988 report, Bremkamp and Harr predicted that the PVU injectate would move in the direction of least reservoir resistance and lowest hydrostatic pressure. This direction is to the northwest and up dip along the fracture permeability of the Wray Mesa system. Our findings, as discussed below and based on injection-induced, seismic source locations, support their prediction. **Figure 3-5** shows Bremkamp and Harr's (1988) original northeast-southwest cross section of Paradox Valley and bordering region. Note the Wray Mesa Fault system. The Bremkamp and Harr's (1988) cross section runs through the injection well and shows their original interpretation of the Wray Mesa faults. Note that the surface topography in **Figure 3-5** west of the salt anticline (i.e., Paradox Valley) is at the same level as the valley. However, the actual surface west of the valley shows a sharp elevation increase to plateaus (**Figure 3-1** and **Figure 3-2**). This discrepancy occurs because the survey used by Bremkamp and Harr did not follow the plateau topography, but instead ran through the incised canyons of the Dolores River before using the primary surface topography of the plateaus bordering Paradox Valley.

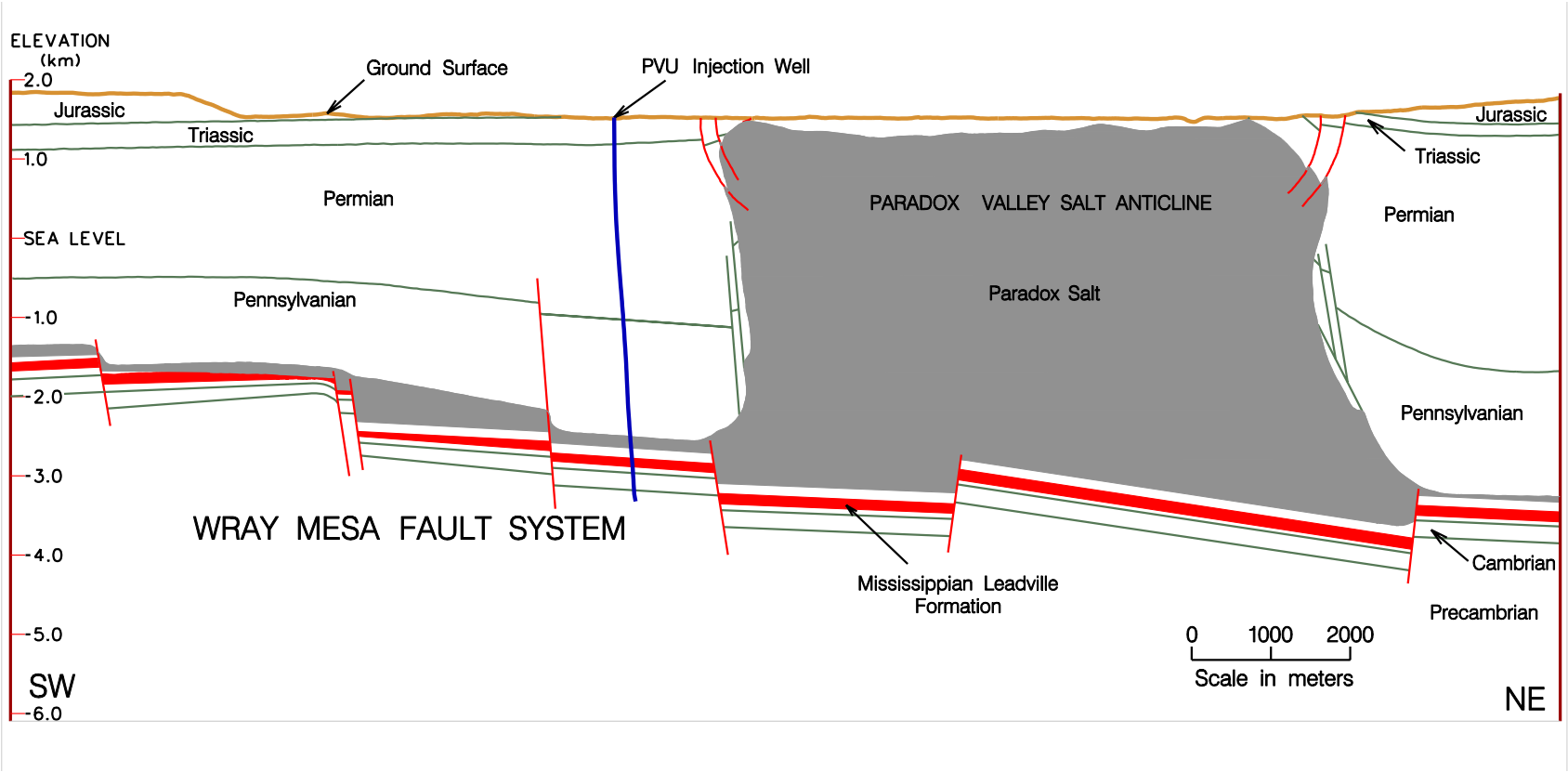

Figure 3-5 Bremkamp and Harr (1988) Original Northeast-Southwest Cross Section of Paradox Valley and Bordering Region. Cross Section runs through the injection well and surface topography reflection surface survey up canyons of the Dolores River.

4.0 PVSN INSTRUMENTATION

Paradox Valley Seismic Network (PVSN) provides seismograph coverage for roughly 5500 km^2 of the Colorado Plateau centered on the intersection of the Dolores River and the west side of Paradox Valley (**Figure 4-1**). PVSN was installed in late 1983 and has operated continuously since

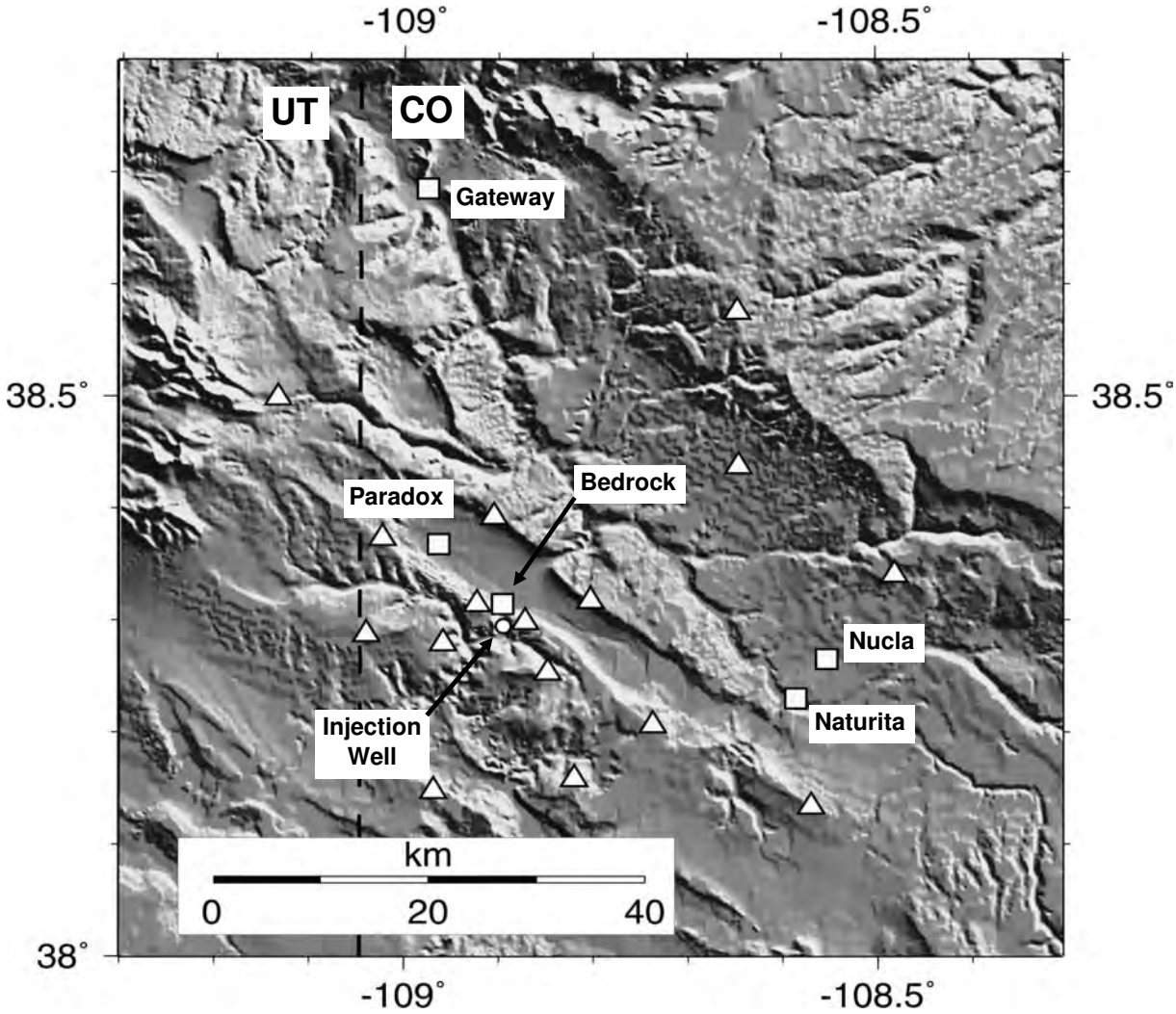

Figure 4-1 Regional Topography and Locations of Paradox Valley Seismic Network stations (triangles).

that time. For each station shown in **Figure 4-1**, **Table 4-1** gives station name, latitude, longitude, elevation, and operational parameters; and **Table 4-1** gives the legal description of the station locations. Within the limits of terrain accessibility and radio telemetry linkage, the network is loosely arranged in two concentric rings centered on the brine injection well. The outer ring diam-

eter is approximately 80 km.

Table 4-1 PVSN Station Locations and Characteristics

Station Designation	Station Name	Latitude deg., N	Longitude deg., W	Elevation m, msl	Date Installed	Gain, dB/ Filters, Hz
PV01	The Burn	38.13	108.57	2190	5/83	78 / 0.2-25
PV02	Monogram Mesa	38.21	108.74	2158	5/83	78 / 0.2-25
PV03	Wild Steer	38.25	108.85	1975	5/83	78 / 0.2-25
PV04	Carpenter Flats	38.39	108.91	2152	5/83	78 / 0.2-25
PV05	E. Island Mesa	38.15	108.97	2150	5/83	78 / 0.2-25
PV07	Long Mesa	38.44	108.65	2001	6/83	78 / 0.2-25
PV08	Uncompahgre Butte	38.58	108.65	2941	6/83	78 / 0.2-25
PV09	North LaSalle	38.50	109.13	2640	6/83	78 / 0.2-25
PV10	Wray Mesa	38.29	109.04	2300	6/83	78 / 0.2-25
PV11Z	Davis Mesa	38.30	108.87	1881	12/89	78 / 0.2-25
PV11N	Davis Mesa	38.30	108.87	1881	12/89	60 / 0.2-25
PV11E	Davis Mesa	38.30	108.87	1881	12/89	60 / 0.2-25
PV12	Saucer Basin	38.32	108.80	2091	12/89	78 / 0.2-25
PV13	Radium Mtn	38.16	108.82	2158	12/89	78 / 0.2-25
PV14	Lion Creek	38.37	109.02	2240	12/89	78 / 0.2-25
PV15	Pinto Mesa	38.34	108.48	2280	6/95	78 / 0.2-25
PV16Z	Nyswonger Mesa	38.32	108.92	2045	7/99	78 / 0.2-25
PV16N	Nyswonger Mesa	38.32	108.92	2045	7/99	60 / 0.2-25
PV16E	Nyswonger Mesa	38.32	108.92	2045	7/99	60 / 0.2-25
PV17	Wray Mesa East	38.28	108.96	1985	tbd	--

Notes: Elevations are relative to mean sea level (msl), the surface elevation of the injection well is 1540 m above msl. Stations designated with a, "Z", "N", or "E" suffix stand for instruments that sense motion in the vertical, north-south, or east-west directions, respectively. Stations without a suffix have vertical-only motion sensors.

Table 4-2 PVSN Sites - Legal Description

Station Desig.	Geographic Name	Legal Description
PV01	The Burn	T45N R15W S19 C,NM
PV02	Monogram Mesa	T46N R17W S27 C,NM
PV03	Wild Steer	T46N R18W S10 C,NM
PV04	Carpenter Flats	T48N R18W S30 C,NM
PV05	E. Island Mesa	T45N R19W S16 C,NM
PV07	Long Mesa	T48N R16W S9 C,NM
PV08	Uncompahgre Butte	T50N R16W S22 C,NM
PV09	North LaSalle	T26S R25E S35 U,SLC
PV10	Wray Mesa	T47N R20W S35 C,NM
PV11	Davis Mesa	T47N R18W S29 C,NM
PV12	Saucer Basin	T47N R18W S24 C,NM
PV13	Radium Mtn	T45N R18W S14 C,NM
PV14	Lion Creek	T48N R20W S36 C,NM
PV15	Pinto Mesa	T47N R15W S12 C,NM
PV16	Nyswonger Mesa	T47N R19W S24 C,NM
PV17	Wray Mesa East	T47N R19W S34 C,NM

Each PVSN station consists of a ground motion sensor or sensors (i.e., seismometer), amplifier, voltage control oscillator (VCO), low power telemetry radio, solar panel, and broadcast tower with antenna. All systems are powered by solar-recharged batteries. Most of the stations operate single, vertical-motion-only seismometers. The Davis Mesa and Nyswonger Mesa stations (PV11 and PV16, respectively), operate three-component seismometers, recording vertical, east-west, and north-south motion. When completed, PV17 will also be a three-component site.

The seismometers at all existing sites are Teledyne Geotech Model S-13's, a high-quality, reliable, ground velocity measuring instrument with flat response between 1 and 20 Hz (**Figure 4-2**). At all sites, the amplifiers and VCO's are also Teledyne Geotech (model 4250). The pass band (i.e. filters) of each field amplifier is set to minimize long-period noise (**Table 4-1**).

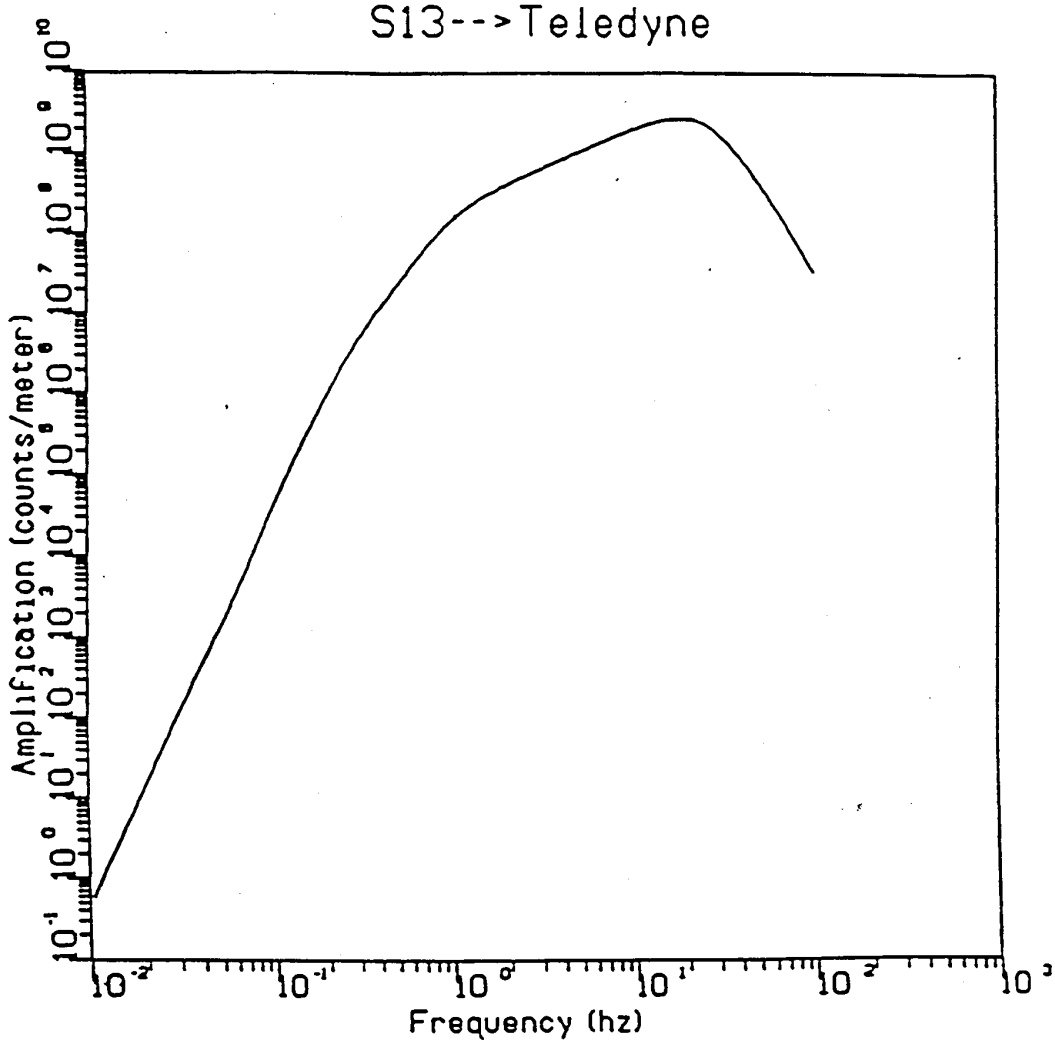

Figure 4-2 Typical response of a vertical-component Teledyne Geotech S13 seismometer, electronics, and digital recording system used at PVSN. Nominal gain is 48 dB for curve shown, Teledyne Geotech model 42.5 amplifier/VCO and model 4612 discriminator. Damping is 0.71 of critical.

4.1 Telemetry and Software

In October of 2000, Reclamation upgraded the data telemetry system and the detection, location and archiving software (Mahrer et al., 2001). Upgrading the software included adapting, refining, and implementing Earthworm, software developed by the US Geological Survey and used in its seismic arrays.

PVSN data telemetry begins with continuous analog signals broadcast from each seismometer site to a receiver in Nucla, CO. At Nucla, the signals are digitized and transmitted via a digital telephone link to the Bureau of Reclamation processing center at the Denver Federal Center (DFC) in Lakewood, Colorado. At the DFC, Earthworm detects events in the data stream, then classifies, locates, and archives the detected events. Subsequently, each event is re-evaluated by a Bureau of Reclamation seismologist.

In addition to the high-gain PVSN instruments/array noted in **Table 4-1** and **Table 4-2**, PVSN includes two strong motion, digital-recording instruments (Springnether Force Balance Accelerometers, FBA-23's recorded by Kinemetrics K2 digital data recorders). One is sited near the injection wellhead; the other is at PVU's pumping station (38.33^{o}N 108.85^{o}W). Both have telephone links to the DFC. The data from these instruments are not part of our normal analysis stream, but, if triggered, can be integrated into the analysis. In the past, the data from these instruments have been used separately to analyze large (i.e., strong) events that have overdriven the high-gain PVSN instruments.

4.2 PVSN Operational Efficiency

[*Operational Efficiency (OE) is the percentage of operating data channel days for the whole year. OE is calculated by summing the number of operating PVSN data channels for each day of the year and dividing that total by 6935 (i.e., 19 channels x 365 days), the number of possible data channel days for a year, if every channel operates every day of the year. If DFC witnesses a power failure resulting in the loss of data, this is included in the calculation as if all PVSN stations were down for the duration of the power failure*.] During 2003, the seismic network and telemetry system operated at 83% efficiency. Previous years averaged about 90% efficiency. **Figure 4-3** shows the individual data channel operational efficiencies and the efficiency of the whole network or cumulative for 2003. **Figure 4-4** shows the number of seismic data channels in operation at any time during 2003. Note that with the exception of 3 power failures or shut downs at DFC and one power supply problem at Nucla, on average, 15 or more stations of PVSN were operating.

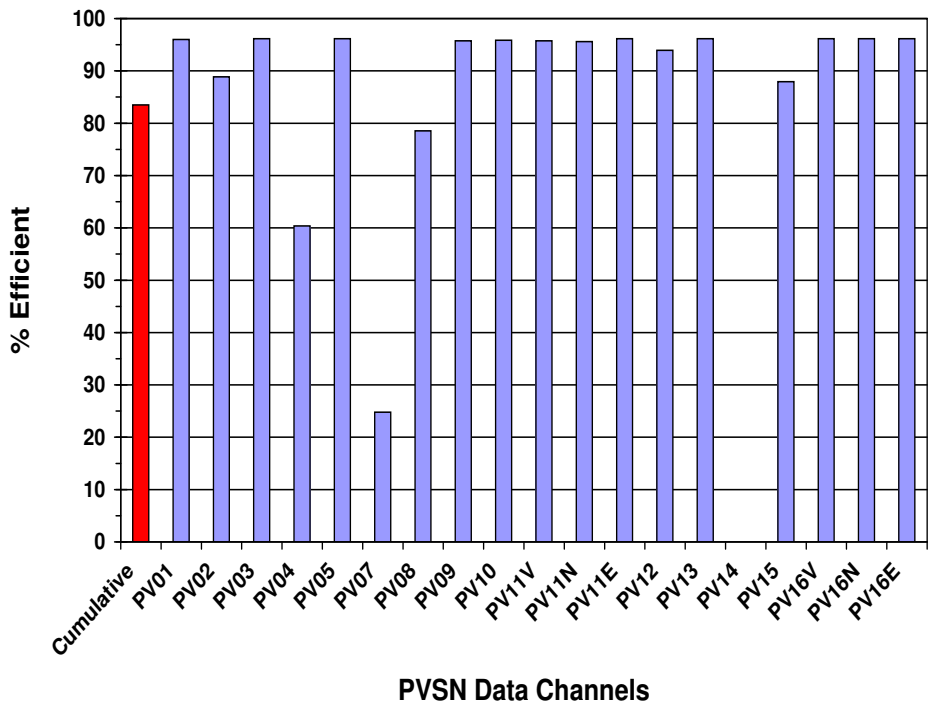

Figure 4-3 PVSN Operational Efficiency: Cumulative ("All") and By Individual Data Channel

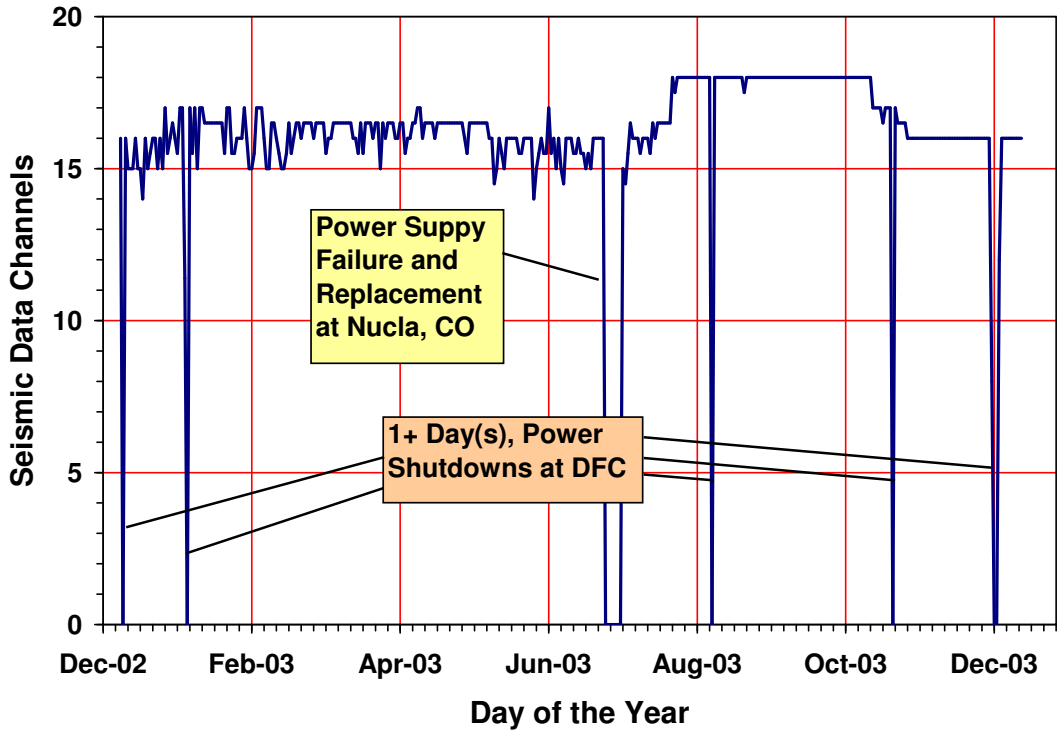

Figure 4-4 PVSN Cumulative Operations, Number of Seismic Data Channels in Operation versus Day of the Year

5.0 WELL OPERATIONS

The PVU Salinity Control Well No. 1 is located at 38.2995^{o} N and 108.8953^{o} W along the western boundary of Paradox Valley, approximately 1.5 km up a canyon formed by Dolores River (**Figure 3-1**, **Figure 3-2** & **Figure 3-3**). As shown in **Figure 3-4**, the well is essentially vertical, deviating only ~0.3 km to the east and slightly to the north over its 4.8+ km depth. **Figure 3-4** also shows the two major perforation intervals of the wellbore casing. The upper perforation interval is within the primary injection target, the Mississippian-aged Leadville Limestone formation. As noted throughout this report, from 1991 through 1995 PVU pumped a series of 7 injection tests. These tests were conducted to acquire an EPA permit for continuous waste disposal. Following these tests and the granting of an EPA Class V permit, in 1996 PVU began continuous pumping that has resulted in a sequence of four pumping schedules (i.e., *Phases*, as discussed in section 2.1). **Table 5-1** summarizes PVU Well No. 1's injection history. For expected reader convenience, the values in **Table 5-1** are in standard units, millions of gallons (Mgal) and thousands of tons (ktons).

Table 5-1 Annualized Summary of PVU Injection

Year	Phase	Injectate	Paradox Valley Brine	Salt
		Mgal	Mgal	ktons
1991	Tests	11.7	3.9	4.3
1992	Tests	9.8	7.8	8.4
1993	Tests	26.2	10.0	10.8
1994	Tests	81.7	58.7	63.7
1995	Tests	34.4	24.1	26.2
1996	*Phase I*	44.6	31.1	33.7
1997	*Phase I*	127.8	89.4	97.0
1998	*Phase I*	166.2	116.1	126.0
1999	*Phases I & II*	150.4	104.5	113.3
2000	*Phases II & III*	112.4	85.4	92.7
2001	*Phase III*	99.6	69.7	75.6

Table 5-1 Annualized Summary of PVU Injection

Year	Phase	Injectate	Paradox Valley Brine	Salt
		Mgal	**Mgal**	**ktons**
2002	*Phase IV*	103.0	103.0	111.8
2003	*Phase IV*	104.2	104.2	113.0
TOTAL		**1,072**	**807.9**	**876.7**

5.1 Operational Adjustments to Reduce Seismicity

As noted in section 2.1, PVU has instituted 3 major injection changes, resulting in 4 injection phases. Each of these changes was invoked either to help reduce unacceptable seismicity or to optimize brine emplacement.

5.1.1 Bi-Annual Shutdowns

During 2003, PVU witnessed all or parts of three, scheduled shutdowns: 12/19/02 to 1/6/03, 5/31/03 to 6/18/03, and 12/20/03 to 1/07/04. Scheduled shutdowns were implemented to mitigate seismicity following two **M** 3.5 events, one in early June 1999 and one in early July 1999. Prior to the June event, we had noted that the rate of seismicity in the near-wellbore region (i.e., about 2 km from the wellbore) reduced during and following unscheduled, maintenance shutdowns and during the shut down following the injection tests of 1991 through 1995. Based on these observations and following the July 1999 event, PVU began scheduling two, 20-day shutdowns each year, one in December-January and one in May-June.

5.1.2 Reduced Injection Rate

Prior to May 27, 2000, PVU pumped injectate at a maximum rate of ~ 1100 lpm (lpm=liters per minute; 345 gal/min (gpm)). Operationally this meant 3 constant-rate pumps, each operating at ~115 gpm, resulting in an average wellhead pressure of ~4,800 psi.

During 3-pump operations, the surface pressure on occasion approached the wellhead pressure safety limit of 5,000 psi; at these times PVU would shut down one injection pump, reducing injection rate, and letting pressure drop a few hundred psi before returning to 3-pump operations; this resulted in an overall average injection rate of ~300 gpm. These shutdowns normally lasted hours.

Immediately following the May 27, 2000 **M** 4.3 event, PVU shutdown for 28 days. During this shutdown period, PVU evaluated operations and its effect on seismicity and decided to change pumping strategy to reduce the seismic threat. The new strategy reduced injection from 3 pumps to 2 pumps. On June 23, 2000 pumping resumed using 2 pumps, giving an injection rate of ~230 gpm. At this reduced rate, surface pressure normalized between ~4,400 and 4,500 psi. It was believed that reducing the injection rate combined with previously-instituted, bi-annual 20-day shutdowns would reduce the potential for large events.

As demonstrated by the May 27th event, 20-day shutdowns alone were not sufficient for stemming large event production. However, the combination of shutdowns and reduced injection rates have, to date, reduced seismic production, as discussed throughout this report. As noted earlier, shut downs and reduced injection rate is not the full picture. The excess energy model, discussed above shows that event production will, most likely, increase as the injection excess energy increase.

Another word of caution needs to be extended. No matter what method of event control or mitigation is invoked, mitigation is not equivalent to elimination. Larger (i.e., **M** 3 or greater) events are still probable, but careful monitoring and the methods discussed above have and probably will continue to minimize the rate of event production.

5.2 Injectate: 70/30 PVB/Fresh Versus 100% PVB

Beginning with continuous operations in 1996, PVU diluted the injectate to 70% PVB and 30% Dolores River fresh water. This dilution was based on a geochemical study that predicted when 100% PVB interacted with connate fluids and the dolomitized Leadville Limestone at downhole (initial) temperatures and pressures, it would precipitate calcium sulfate that would restrict perme-

ability (Kharaka, 1997). During October 2001 at a meeting at the Denver Federal Center, the injectate concentration question was reconsidered. Temperature logging in the injection well recorded substantial near-wellbore cooling in the injection interval, indicating that if precipitation occurred, it would not be near, and possibly clog, the wellbore perforation. Further discussions at the meeting indicated that, if precipitation occurs, its maximum expected rate is ~8 tons of calcium sulfate per day. To put this amount into perspective, injection at ~230 gpm, assuming a density of 8.33 lbs/gal, gives a daily injection tonnage of ~1380 tons/day. The maximum expected precipitate is ~0.6% of the daily injection mass. At the completion of the meeting, it was decided that after the December-January-2001 20-day shutdown, the injectate would be changed to 100% PVB. Injecting 100% PVB began on January 8, 2002 and has been maintained through the end of 2003.

We have been and continue to be interested in how this injectate change affects the induced seismicity. Possibilities include: (1) reduced seismicity, since flow paths become clogged and more injectate is forced into the native porosity away from activatable faults; (2) increased seismicity, since clogging established flow paths will cause injectate diversion into untouched reservoir regions inducing additional seismicity and expansion of the seismicity zone, or (3) no noticeable change. To date, no positive or negative effects on the seismicity have been found to be directly associated with the change to 100% PVB.

6.0 SEISMIC ANALYSIS

6.1 Local Seismic Magnitude Scale

Typically, seismologists calculate the size of an earthquake using one or more methods. In most cases, seismologists calculate magnitude for local events following a procedure calibrated for local conditions. For PVSN, we compute magnitudes from the duration of the recorded signal. This scale, called the duration or coda magnitude, is denoted **M**. (For a more complete discussion of the magnitude scale for PVSN see Mahrer et al., 2001)

6.2 Preliminary Event Location Method

Accurately locating earthquakes requires (1) identifying arrival times of specific phases in the recorded signals, (2) appropriate array geometry, and (3) an accurate velocity model of the region through which the signals travel. As noted above, seismologists manually pick the phase arrival times for all local earthquakes recorded by PVSN. We do this to minimize uncertainty frequently found in automated (i.e., software-based) phase identification and arrival time picking. We require a minimum of four arrival times from at least three stations to locate an event. In the PVSN analysis, we pick the primary or P-wave arrival times from all stations with acceptable signal-to-noise ratios. We then pick secondary or S-wave arrival times from only the three-component stations PV11 (Davis Mesa) and PV16 (Nyswonger Mesa) and from the closest single-component station to the injection well, PV03 (Wild Steer). Although S-wave arrival times are very important to the analysis, we use only 3 stations because the closeness of the sources to these stations. For the other stations of PVSN, the complexity of local geology facilitates mis-identifying S-phases which causes mis-locating events.

We currently determine preliminary earthquake locations using a flat, one-dimensional, layered earth velocity model and the computer program SPONG (Malone and Weaver, 1986). The velocity-depth profile of the one-dimensional model is summarized in **Table 6-1**. The P-wave velocity depth profile began with Wong and Simon (1981), to which we added results from seismic refraction surveying and sonic logging. The refraction data were obtained using local mining explosions and the sonic logs were obtained immediately following the drilling of the injection well. We

computed the S-wave velocities from P-wave velocities by assuming Poisson's ratio = 0.25 (i.e., P-wave to S-wave velocity ratio = 1.732). To augment our preliminary analysis, we refined the velocity model and increased event location accuracy using seismic tomography; these are described later.

Table 6-1 PVSN 1-D Velocity Model

Depth below Surface (km)	P-Wave Velocity (km/sec)	S-Wave Velocity (km/sec)
0.00	3.595	2.076
0.20	3.950	2.281
0.60	4.330	2.500
1.00	4.650	2.685
1.40	5.050	2.916
2.20	5.100	2.945
2.80	5.340	3.083
4.00	5.420	3.129
4.20	5.700	3.291
4.60	5.850	3.378
5.80	5.872	3.390
11.0	5.897	3.404
18.0	6.000	3.464
40.0	7.200	4.157

Notes: Depth indicated is relative to a datum of +1850 m above mean sea level (msl). The wellhead is 1540 m above msl

In addition to the earthquakes, PVSN records non-seismic signals. These signals are caused by thunder, lighting strikes, landslides, low-flying aircraft, oil and gas exploration blasts, and mine and quarry blasts. We know the locations of established mining facilities, which helps differentiate local earthquakes from blasts. Blast signals arrive from a number of Colorado, Utah, and New Mexico sites. The most prevalent in Colorado that affect PVSN include a distributed area around Uravan, Paonia (e.g., West Elk Coal Mine), Rifle (e.g., Rifle Quarry), and open-pit coal mining

west of Nucla (e.g., Western Fuels Coal Mine End). Since local explosions generate distinct waveforms (e.g., impulsive or very abrupt P-waves, unusually weak S-waves, and enhanced surface waves for small magnitude events) we can discriminate between the blasts, regional earthquakes, and the PVU induced microseismicity. We know of no explosive sources within 10 km of the PVU injection well that produce signals we could be misidentified as injection-induced microseismicity. Occasionally oil and gas exploration blasting is done in Paradox Valley or on the mesa bordering Paradox Valley to the east. The source location of these signals and their unique waveform allow us to easily discriminate them from possible earthquakes or induced seismicity.

6.3 Advanced Event Location - Seismic Modeling

To evaluate the potential relationship of seismicity to reservoir and fluid transport characteristics, we made a significant effort to obtain accurate earthquake locations. First, we developed a three-dimensional velocity model for the Paradox Valley area using a progressive, three-dimensional velocity-hypocenter inversion (Block, 1991). In this inversion, we used a data set consisting of 682 earthquakes with **M** greater than 0.7 and good signal-to-noise ratios. Second, we performed a relative relocation of as many earthquakes as possible (i.e., clean waveforms with strong signal-to-noise ratios) using the three-dimensional velocity model developed in the first step (Waldhauser and others, 1999). Approximately 95% of the events recorded between 1991 and 2003 had sufficient signal-to-noise ratios to be included in the relative relocation. For the remaining events we used the original one-dimensional model locations.

The immediate goal of this modeling is reducing the arrival-time root-mean-square (rms) residuals (i.e., the difference between the observed and the theoretical travel times). Compared to the one-dimensional model residuals, the three-dimensional velocity model reduced the rms residuals by ~14%. The relative relocation procedure resulted in more than a 90% reduction in rms residuals relative to the three-dimensional results. The final, most-accurate earthquake epicenters for the 1991 through 2003 seismic data are shown in **Figure 6-1**, **Figure 6-2** and **Figure 6-3**. **Figure 6-2** and **Figure 6-3** show close-ups of the two regions, one region around the injection well and the second to the northwest, respectively. The linear groupings of seismic events is quite evident in these figures.

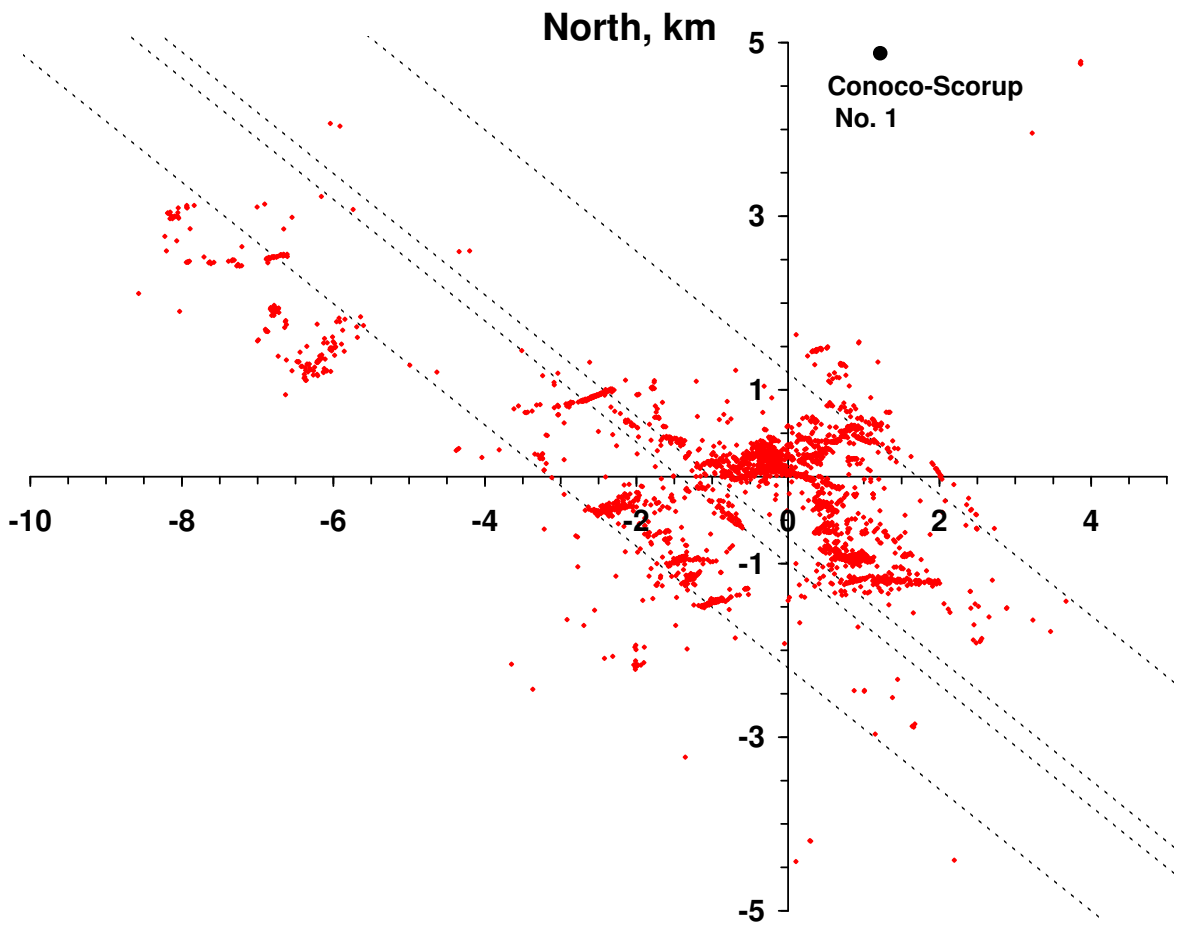

Figure 6-1 Relocated PVU Induced Seismic Epicenters from 1991 through 2003. Axes are centered on injection wellhead and are in units of km.

As discussed in previous annual reports (e.g., Ake et al., 2000; Mahrer et al., 2001), the loci of relocated earthquakes are consistent with our interpretation that most of the tectonic stress release takes place along (existing) linear features with orientations consistent with either the two sets of focal mechanisms (set 1: N81W and N9E; set 2: N21W and N69E) or the two sets of fractures observed in the oriented core samples (primary: N69W and N74W; secondary: N38W and N42W; Ake and Mahrer, 1999). Very little seismicity appears to be occurring along planes (i.e., strike) consistent with the Wray Mesa fault system as defined by Bremkamp and Harr (1988). Bremkamp and Harr (1988) estimated the strike of the Wray Mesa fault system to be ~N55°W. It is likely that these features are the most through-going structures in the area. The locations of the linear fea-

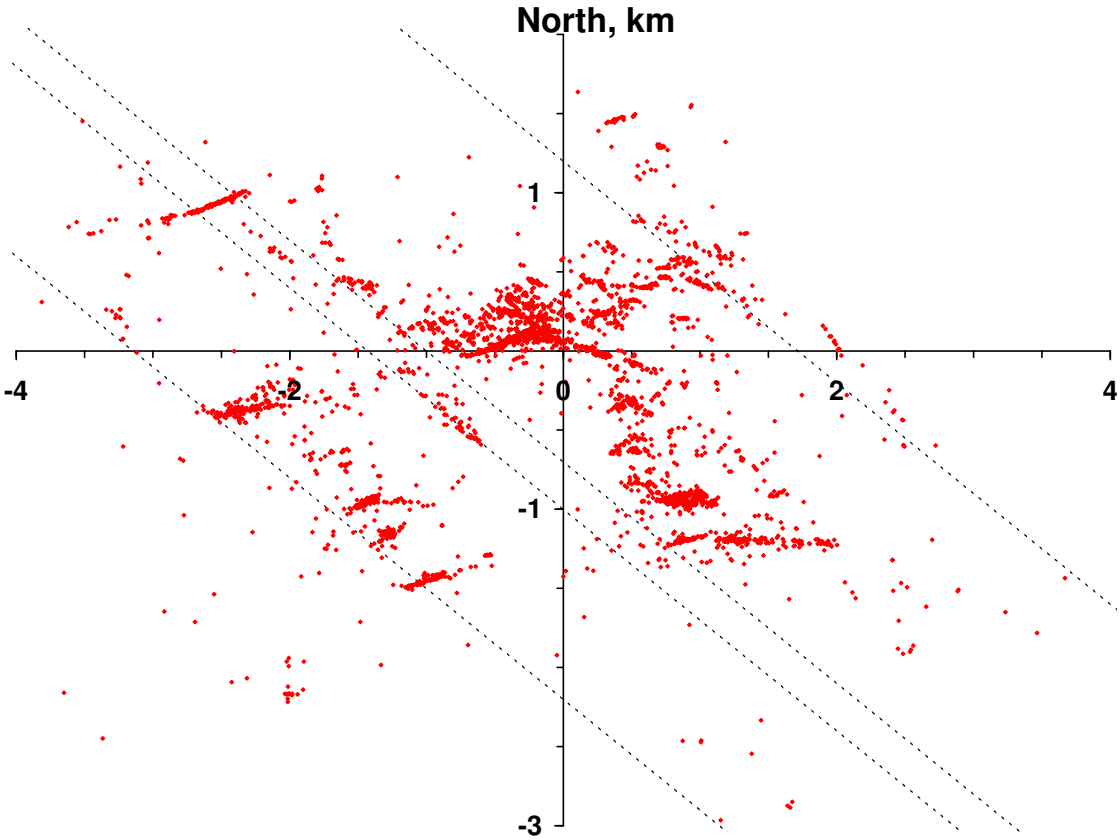

Figure 6-2 Close-up of Relocated Event Epicenters in Primary Seismogenic Region Surrounding Wellbore. Axes are centered on injection wellhead.

tures in **Figure 6-1**, **Figure 6-2** and **Figure 6-3** suggest communication through "conduits" in a ~N55°W direction. (See Microsoft Excel animation file on attached compact disk for an interpretation of conduits superimposed on the seismic linear features.) We believe this behavior suggests fluid is being preferentially carried along these steep planes with a northwest strike (i.e., the through-going elements of the Wray Mesa system). Opening of these planes will require the least energy and are less likely to induce surface-measurable events, since these planes are oriented normal to the least principal stress direction.

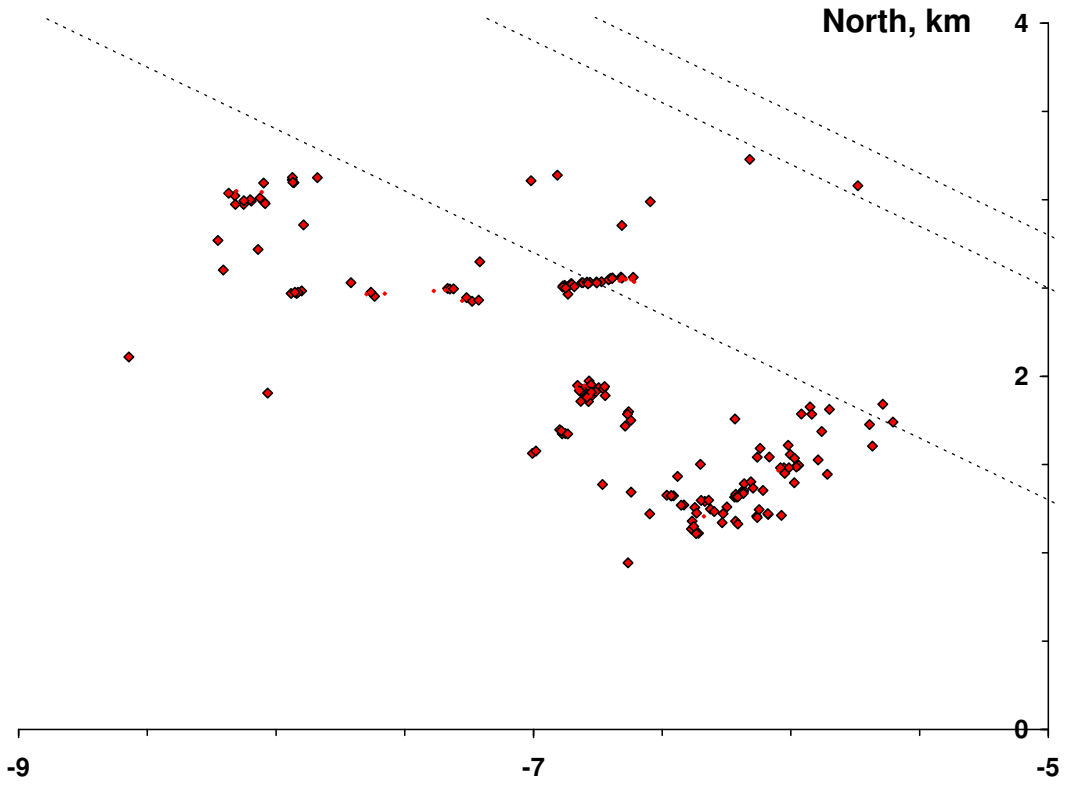

Figure 6-3 Close Up of Relocated Event Epicenters in Secondary Seismogenic Region ~8.5 km Northwest of Injection well. Axes are relative to injection wellhead

7.0 OBSERVATIONS

7.1 Local, Pre-Injection Seismicity

In the 1960's, the US Army high-pressure injected waste fluids ~3,000 m deep at the Denver Arsenal, north east of Denver, CO. As a result hundreds of seismic events were induced (Healy, 1968). Recognizing that the proposed injection at Paradox Valley would, most likely, induce seismicity, BOR decided to record pre-injection, background seismicity in the region surrounding the proposed injection. In 1983 the US Geological Survey began installing the first 10 stations of PVSN, PV01 through PV10 (PV06 eventually became PV15); recording seismic data began in 1986, 5 years prior to the PVU injection tests. **Figure 7-1** shows the epicenters of the pre-injection data. The data consists of a few tiny, natural earthquakes and a number of local explosions. None of the earthquakes were within 15 km of the future injection well. Most of the local explosions are associated with known mining and quarrying operations.

From the injection tests in 1991 through 2003, PVSN recorded and located more than 4,000 events within 10 km of the injection well. Based on the lack of pre-injection seismicity, we can safely infer that PVU injection induced these events.

7.2 Seismic Events and Well Testing (1991-1995)

As noted in **Figure 7-1**, prior to injection at PVU, the Paradox Valley region witnessed few seismic events (EnviroCorp, 1995; Ake and others, 1996) and none close to the injection well site. Between July 1991 and April 1995, PVU ran 7 injection tests. Each test consisted of a continuous pumping period followed by a wellhead shut-in to monitor downhole pressure fall off with time. The tests were implemented to qualify the well for an EPA Class V disposal well permit. (PVU Injection Well No. 1 is permitted as a Class I well run under Class V guidelines.) **Table 7-1** summarizes the injection tests including injected volume, pumping duration, and number of local (i.e., induced) seismic events recorded. In conjunction with **Table 7-1**, **Figure 7-2** shows the injection rate and seismic events per days. The boxed numbers at the top of the figure identify the tests; the boxed numbers at the bottom of the figure are the number of seismic events recorded during and immediately following the specific tests. Also noted in the figure is the 1993 acid stimulation. The

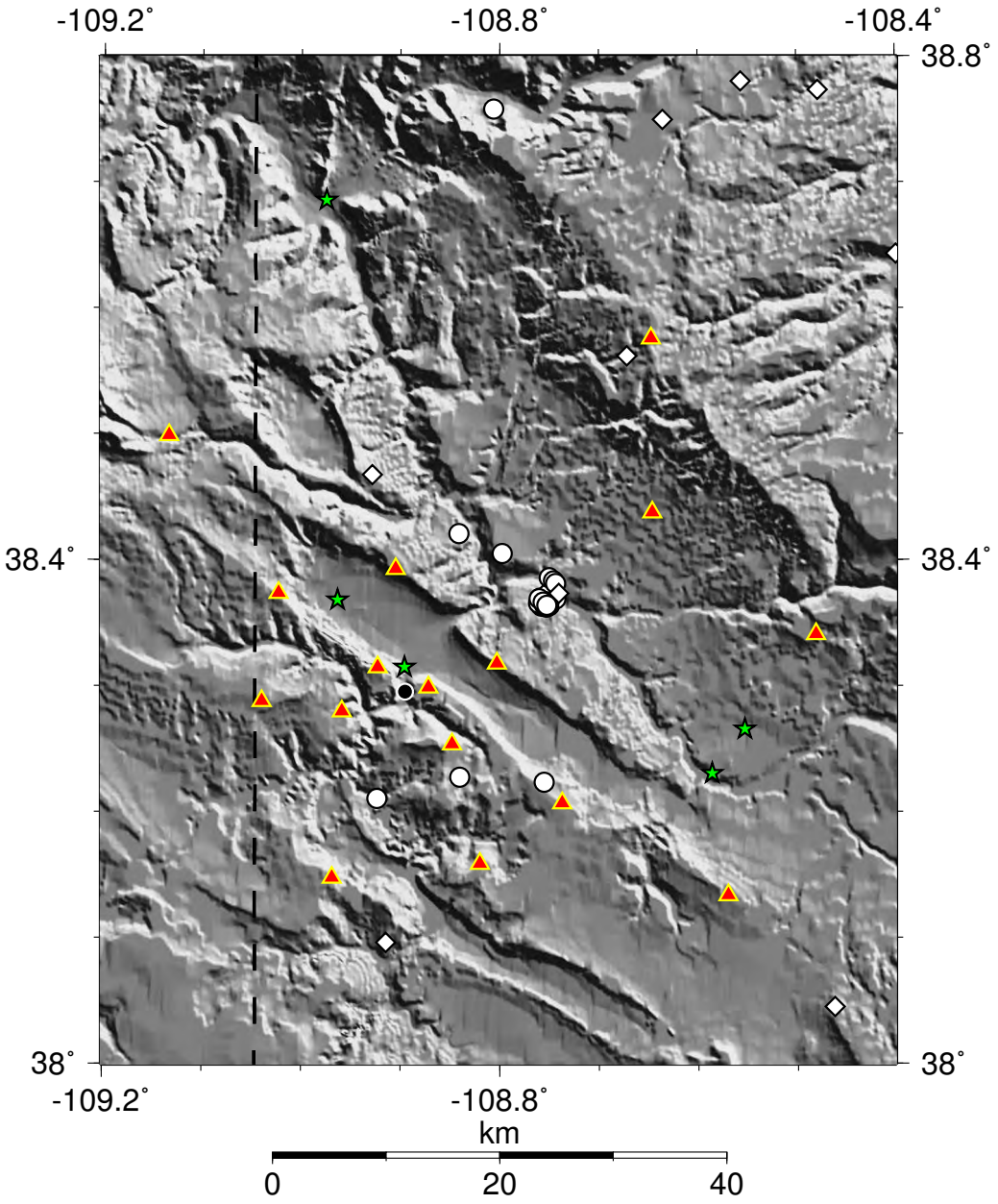

Figure 7-1 Paradox Region Seismicity, 1985-1991. Triangles show PVSN seismometer sites, the white outlined black circle is the injection well, the black outlined white circles are explosions, the black outline white diamonds are natural seismic events, and stars are the local municipalities (see Figure 3-1 & Figure 3-2).

stimulation was performed to increase the imbibition of the well (Envirocorp, 1995). **Figure 7-3**

Table 7-1 Injection Tests 1991-1995

Test No.	Injected Volume	Initial Pumping Date and Duration	Injectate	Hydrostatic Pressure @ 4,300 m[a] depth	No. Induced Seismic Event
	m^3	***(init. day) days***	***%PVB[b]:%FreshWater***	**(MPa)**	
1	11,000	(11Jul91) 14	0%:100%	42	20
2	16,000	(15Aug91) 12	33%:67%	44	9
3	54,000	(5Nov91) 54	67%:33%	47	16
4	42,000	(6Jul93) 47	0%:100%	49	0
--	38	(20Sep93) 14	28% HCl acid injection	--	--
--	34		100% fresh water flush following acid injection[c]		
5	54,000	(3Oct94) 28	70%:30%	47.2	81
6	89,000	(18Jan94) 41	70%:30%	47.2	170
7	354,000	(14Aug94) 242	70%:30%	47.2	370
Total	620,000	438 days	---	--	666

[a]Depth = Top of the casing perforation interval; i.e., the top of the injection target horizon, the Leadville Limestone

[b]PVB = Paradox Valley Brine (260,000 mg/l total dissolved solids)

[c]Injection well surface pressure became negative (i.e., below hydrostatic) following water flush of acid injection;

shows the cumulative epicenters induced by the injection tests

.

7.3 Seismic Events and Continuous Injection (1996-Present)

*{Note: We have found that the Earthworm system, discussed above, is less sensitive for detecting very small events (i.e., events < **M** 0.0) than the system it replaced. Overall these events are not significant, having very small signal to noise ratios (i.e., poorly constrained locations) and representing only a few percent of the old data. Therefore, for consistency with the pre-Earthworm*

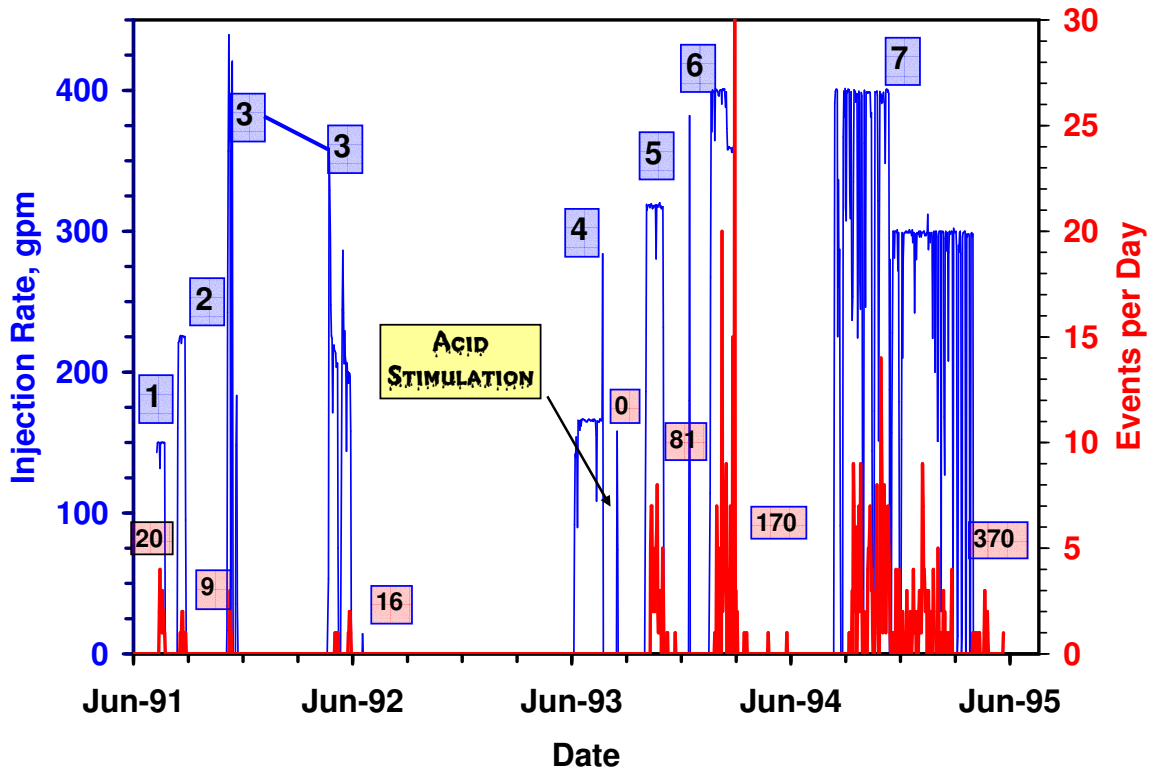

Figure 7-2 Injection Rate and Induced Events (red boxes) for Tests. Tests (blue boxes) were invoked to qualify injection well for an EPA Class V well disposal permit.

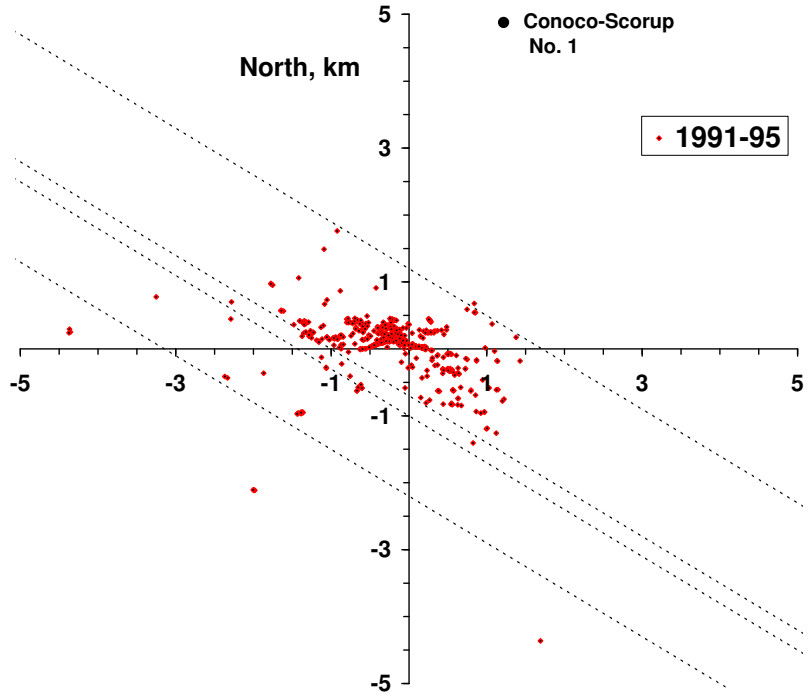

Figure 7-3 Epicenters of Seismic Events Induced by Injection Test, 1991-1995.

*data, all subsequent discussions and figures will only use **M** 0.0 or greater data.}*

During 2003 PVSN recorded and located 138 events with **M** 0.0 or greater. **Table 7-2** gives a year-by-year listing of event production. Note that the table does not include 1996 (it was only a partial year of pumping) and 1997 (we have some questions about the completeness of the data set due to computer problems). We have included **Table 7-2** for comparison of 2003 data with previous years' annual activity. However, we feel that much more insight is gain by examining the Paradox seismic data based on the injection phases described above. **Table 7-3** presents these data by PVU operational phase of which the 2003 data is included in *Phase IV*. Note the event count and number of days in *Phase I* in **Table 7-3** includes 1996 (111 days from pumping inception to first recorded event) and 1997 data and therefore the average events per day appear much

Table 7-2 Year Event Production

Year	Induced Events	Average Events Per Day
1998	1156	3.15
1999	1142	3.14
2000	306	0.85
2001	84	0.23
2002	59	0.15
2003	138	0.38

Table 7-3 Event Production by Injection Phase Through End of 2003

Phase	Induced Events	Duration	Avg. Events per Day	Injected Volume
--	--	Days	--	Ggal
I	2369	1100	2.15*	0.427
II	402	335	1.20	0.118
III	208	565	0.37	0.156
IV	195	723	0.27	0.207

lower than the values for 1998 and 1999. We feel that the real average events per day for *Phase I* should match the 1998 and 1999 values at about 3.15. Therefore in **Table 7-3** we have added an * to the *Phase I* average events per day. **Table 7-3** supports our assessment that shutdowns and reduced injection rate reduce event production. In support of **Table 7-2** and **Table 7-3**, **Figure 7-4** shows histograms of monthly injection volume and monthly event production since continuous pumping began in 1996. The figure shows the injection phases and emphasizes how dramatically event production has reduced since mid-2000 when PVU reduced the injection rate from ~345 gpm to ~230 gpm. **Figure 7-5** and **Figure 7-6** show events per day for PVU operation since

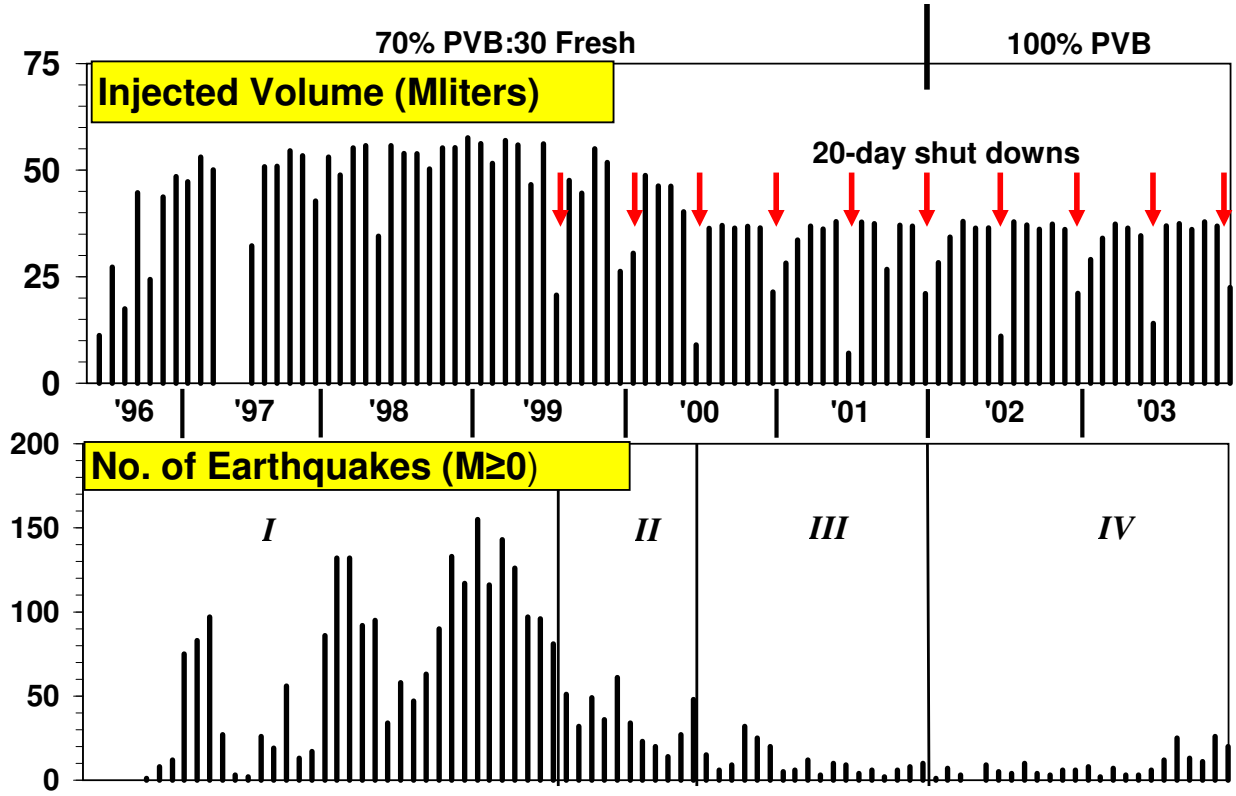

Figure 7-4 Injection volume (top) and earthquake production at PVU by month for each year since continuous injection began in 1996. Note the four injection phases, the bi-annual, 20-day shutdowns beginning in 1999, the reduced injection rate beginning in 2000, and the change in injectate beginning in 2002.

1996 (i.e., continuous pumping) plus average daily injection rate and average daily downhole pressure, respectively.

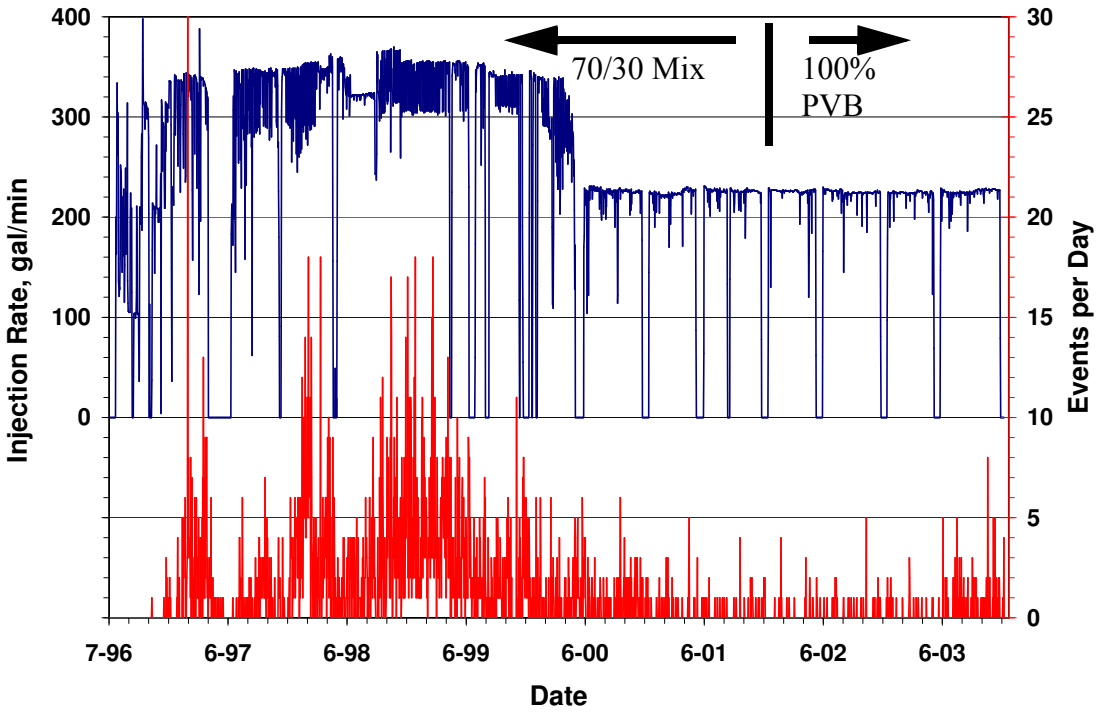

*Figure 7-5 Number of events per day (red) and average daily injection rate (blue) versus time. Event count only includes events with magnitudes **M** 0.0 and larger.*

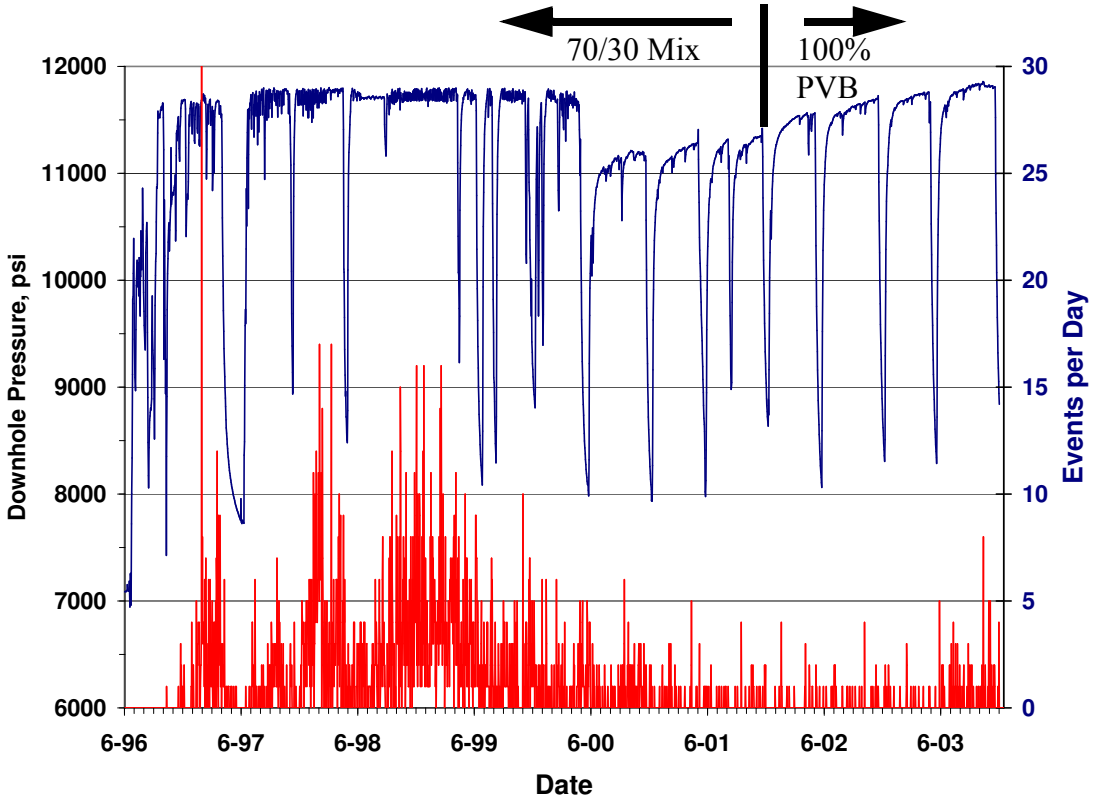

Figure 7-6 Number of events per day (red) and downhole injection pressure (blue) versus time. Downhole pressure is calculated at 4.3 km (14,080 ft).

7.4 Event Magnitudes

As shown in **Table 7-2**, in 2003, the daily seismic event rate was 0.38; this is an increase in production over 2002, which is the only other year of *Phase IV* injection. As discussed above, we feel this increase is a result of the increase in injection energy need to maintain constant rate injection.

Table 7-4 shows the event magnitude distribution by year for 0.5-magnitude wide bins. Examination of the data in **Table 7-4** shows that, although there was an increase in number of events during 2003 compared to 2002 (the only other *Phase IV* year) and to 2001 (*Phase III* pumping), there is only a slight increase in the number of events in the moderately large range (**M**2.0-**M**2.4) and no increase in events **M**2.5 and greater. A more complete discussion of magnitudes and recurrence statistics is given below.

Table 7-4 Distribution of Seismic Events by Year

Phase:	**1999**		**2000**		**2001**		**2002**		**2003**	
Range	**No.**	**%**	**No.**	**%**	**No.**	**%**	**No.**	**%**	**No.**	**%**
0.0-0.4	419	39	114	40	17	21	6	10	10	7
0.5-0.9	388	36	98	35	35	42	23	40	44	32
1.0-1.4	160	15	41	15	18	22	17	29	55	40
1.5-1.9	64	6	18	6	11	13	8	14	17	12
2.0-2.4	31	2.9	7	2.5	2	2.4	3	5	11	8
2.5-2.9	5	0.5	3	1.1	0	0	1	1.7	0	0
>2.9	2	0.2	1	0.4	0	0	0	0	0	0
Total	1070	100%	282	100%	83	100%	58	100%	137	100%

7.5 Felt Events

By the end of 2003, PVSU recorded more than 4,000 events attributed to PVU injection. Of these, more than 99% were imperceptible (i.e., < **M** 2.4) to people at the surface. From 1991 to 1996 no events were felt. Between August, 1997 (i.e., the first reported felt event) and the end of 2002

about 14 events were felt. During 2003, one felt-event was reported to PVU. It was a magnitude **M** 2.1, which is normally well below the detection threshold. It probably was felt because it was located due north of the injection well at the edge of the seismic swarm surrounding the well. This location is about the closest point to the community of Bedrock.

During 1996-2003, 18 events **M** 2.5 or greater were recorded, indicating not all larger events are felt. Of the larger events, 3 occurred in 1998, 7 in 1999, and 5 in 2000. In 2000 only 1 **M** 2.5-or-greater event occurred after the reduction in injection rate following May 27. In 2001 no events **M** 2.5 or greater occurred. In 2002, 1 event **M** 2.5 or greater occurred. In 2003, no events **M** 2.5 or greater occurred.

7.6 2003 Event Locations

Figure 7-7 shows a plan view (i.e., epicenters) of the 138 earthquakes induced by the PVU injection during 2003 and located using the preliminary one-dimensional model. The magnitudes of these events range from $\mathbf{M_D}$ 0.0 to **M** 2.5 (see **Table 7-4)**. With regard to magnitude, the error in locating events generally decreases with increasing magnitude. For smaller events, noise is proportionately larger, obscuring identification of the initial P and S-arrivals. As a result, most of our conclusions for this data set are based on events with **M** > 0.6.

Figure 7-7 shows that the epicenters recorded in 2003 are, as in previous years, contained within the two distinct region. The first and most populated region surrounds the injection well in an elongated envelope whose long axis runs approximately NW-SE and extends to a maximum of ~4 km west of the injection well and ~2km east of the well. The second region is centered about 8 km northwest of the injection well. The figure also shows the swarm events (discussed above) located to the north west and very near the injection well.

Figure 7-8 compares the epicenters for all events from 1991 through 2002, and the 2003 events. Because it uses data from the relative relocated procedure, this figure upgrades **Figure 7-7** so that all epicenters are relocated from the original one-dimensional model. The relocation method was discussed above and detailed in the PVSN 2000 annual report (Mahrer et al., 2001), given on the

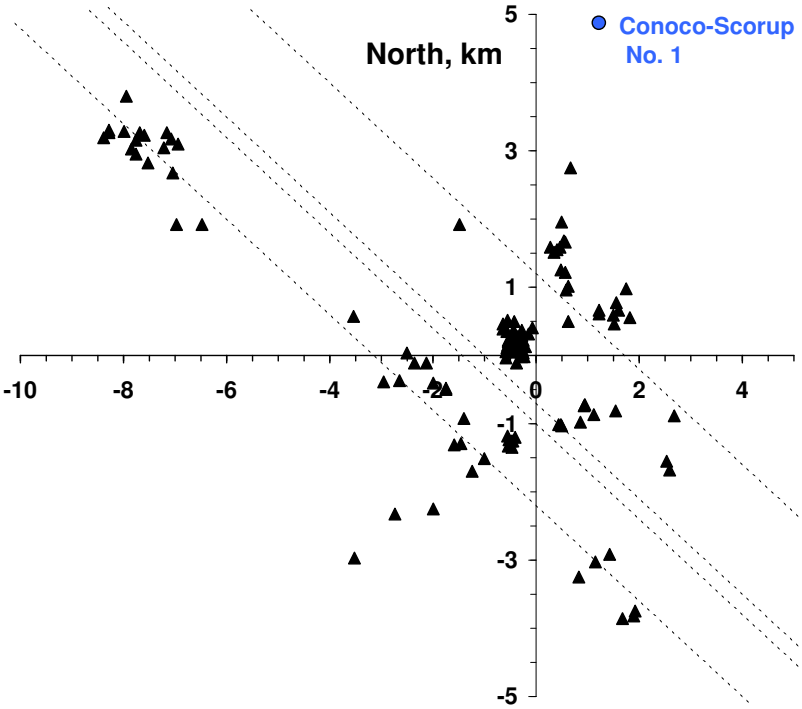

Figure 7-7 Epicenters located during 2003 by PVSN using one-dimensional velocity model; 138 events plotted (triangles). Injection wellhead is the origin of the axes; solid (blue) circle is the Conoco-Scorup well. The approximate strike and locations of Wray Mesa fault system (Bremkamp and Harr, 1988) are shown as dashed lines.

accompanying CD.

As noted earlier, **Figure 7-8** shows that the relocated 2003 events fall within the two groups defined by previous year events. The figure also shows dashed lines; these lines run N55^{o}W, the implied strike of the main faults of the Wray Mesa Fault System and are our interpretation of candidate locations for through-going faults of the Wray Mesa System. As discussed in previous annual reports (e.g. Mahrer et al., 2002), the relocated epicenters and the shapes of the seismic zones align well with the strike of the fault system.

The group 8 km northwest of the well first appeared in 1997. We believe that the paucity of events between the two groups, which has been maintained for almost 5 years, indicates the zones com-

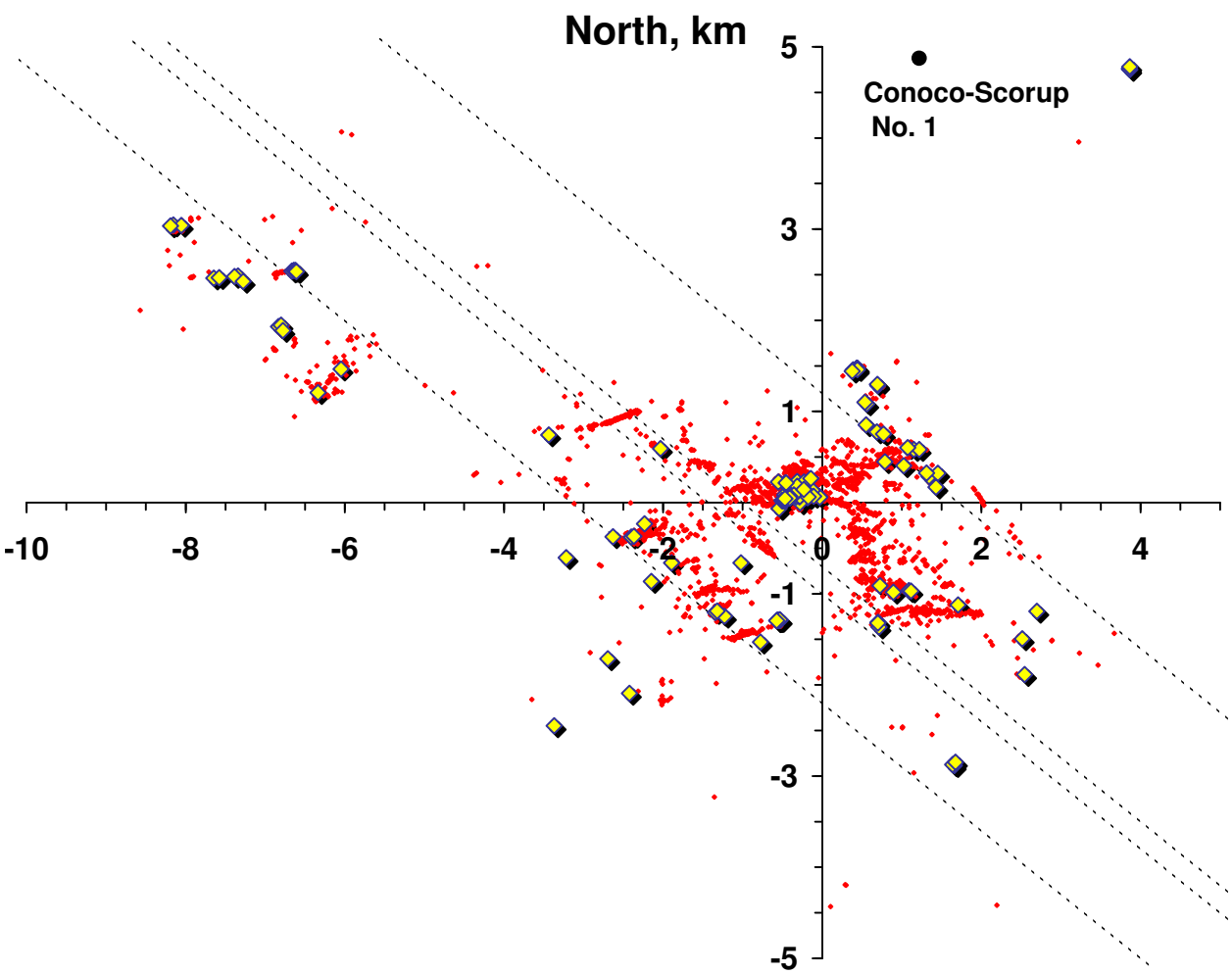

Figure 7-8 PVU-induced earthquake epicenters for 2003 (diamonds) and years 1991-2002 (red dots). All epicenters are relocated from one-dimensional model. Axes are centered on the PVU injection wellhead. Dash lines run N55^{o}W and are the interpreted main, through-going faults of Wray Mesa Fault system.

municate hydrologically by a conduit(s) of fluid, probably through one or more principal faults of the Wray Mesa system. The dashed lines in **Figure 7-8** show our interpretation of potential elements of the fault system based on our interpretation and on Bremkamp and Harr (1988) with the west-most dashed line aligning well with the spatial relation between the northwest epicenters and the wellbore-center epicenters.

Complementing **Figure 7-7**, **Figure 7-8**, and **Figure 7-9** shows a NE-SW geological cross section normal to the strike of the valley and passing through the injection well. The geology, fault structures, etc. are based on Bremkamp and Harr's (1988) original interpretation and speculation. Pro-

jected on the cross section are all events from 1991 through the end of 2002 and within 1.5 of the viewed plane.

Figure 7-9 shows a number of features. First it shows two vertical groupings of events: one in the Precambrian near the injection well and one starting in the Leadville and rising through the salt about 1.5 km southwest of well. Most likely the second grouping is the actual location of the fault Bremkamp and Harr (1988) speculated to lie about 1.5 km west of the well. **Figure 7-9** also shows that many events near the well occur at depths between the top of the Mississippi-aged Leadville Formation, the primary injection horizon (4.3 km below surface) and the bottom of the well. This seismicity shallows to the southwest in agreement with the inferred shallowing of the Leadville Formation (Bremkamp and Harr, 1988). The figure also shows that the actual shallowing may be steeper than originally interpreted by Bremkamp and Harr.

Figure 7-9 shows a significant number of earthquakes appear below the bottom of the well in the Precambrian basement rocks. In 1998 approximately 18% of the events had depths greater than 4.8 km relative to the wellhead, the depth to the top of the Precambrian at the well. During 1999, 24% were below this depth horizon. In 2000, before the May 27th event, 30% of the events were below this depth horizon. After pumping resumed in June, 16% were below this depth. In 2001, 35% were below 4.8. In 2002, about 34 of the 59 (relocated) events or 58% were 4.8 km or deeper. In 2003, 38 of the 138 (relocated) events or 28% were 4.8 km or deeper. Note that since the Precambrian shallows to the west, these numbers represent a minimum number of events in the Precambrian.

The earthquake locations for 2003, as with previous years (Ake et al., 1999; Ake et al., 2000; Mahrer et al., 2001), suggest that these events occur primarily over a depth interval of ~3.5 to ~6.0 km relative to the wellhead. Much of the activity is centered on the depth interval of the perforations of the injection well. It needs to be recognized that the range of depths computed using the initial, one-dimensional velocity model may be representative of the true range of depths or the results may be controlled by the uncertainty in depth determination arising from using a small number of vertical-component stations with a poorly constrained velocity model.

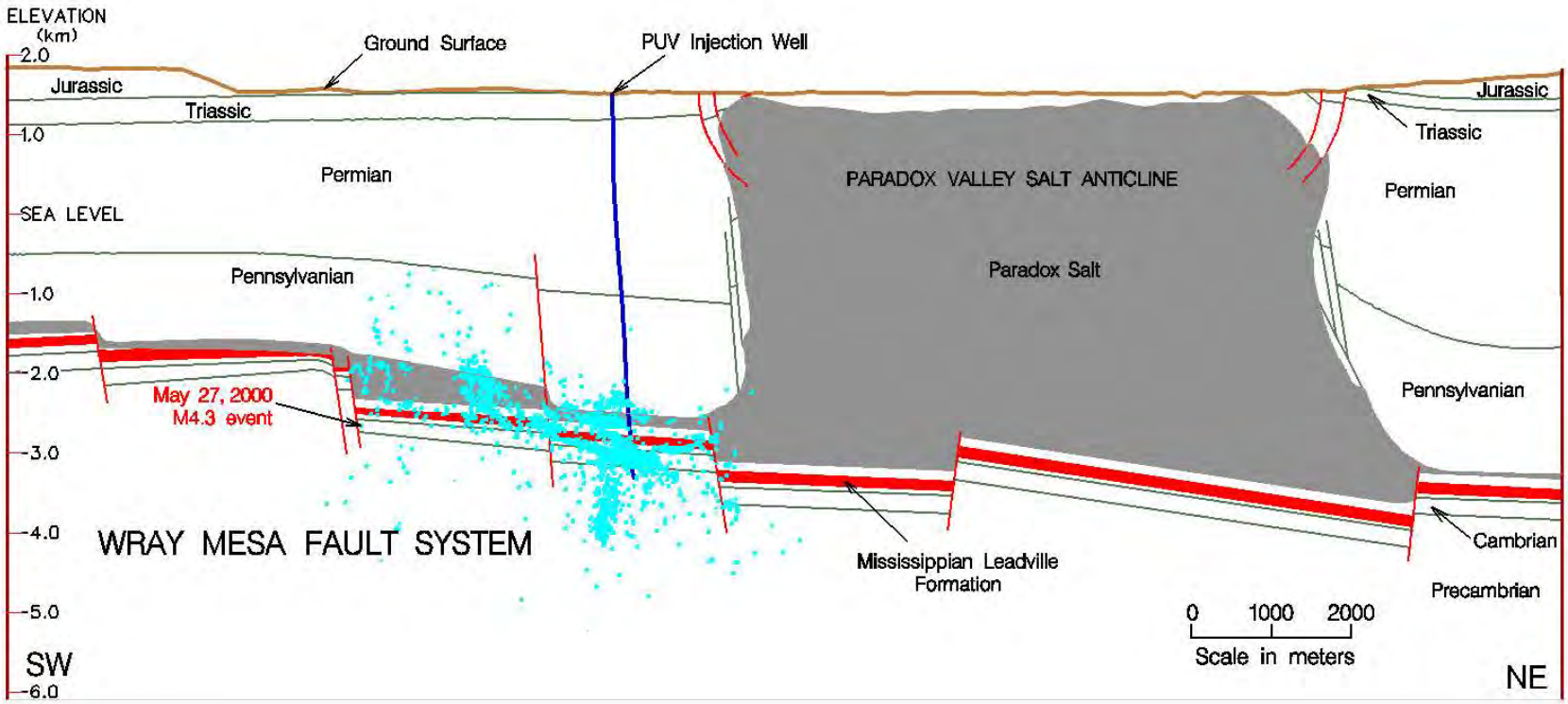

Figure 7-9 Bremkamp and Harr (1988) cross section interpretation of Paradox Valley and bordering region through PVU injection well and normal to strike of the valley. Projected on to cross section are seismic events (1991-2002) within 1.5 km of the viewed plane.

7.7 1991-2002 Near Wellbore Event Locations

For comparison with the event locations in 2003 (previous section), **Figure 7-10** through **Figure 7-17** show the near-wellbore seismic event locations by years from initial injection testing in 1991-1995 (**Figure 7-10**) through 2002 (**Figure 7-17**). This time sequence shows the growth of the near-wellbore seismic zone indicating that by the end of 1998, the expansion of the seismic zone surrounding the well had reached maturity and further expansion is very slow, if at all.

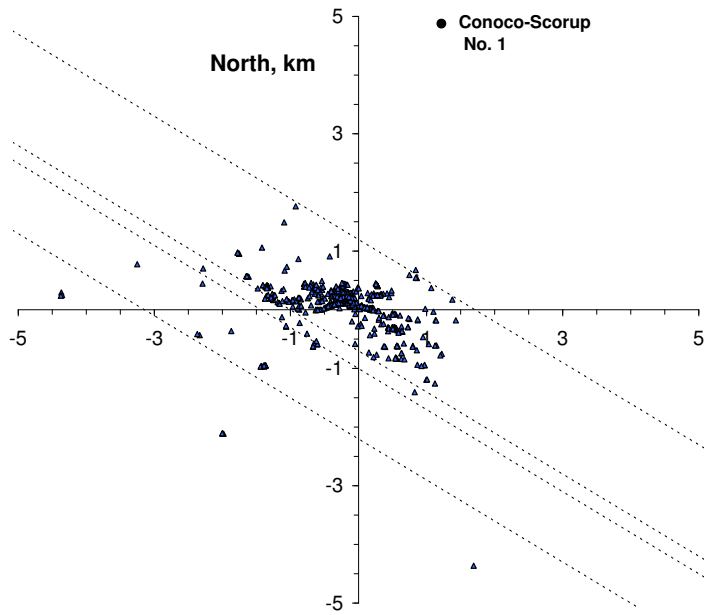

Figure 7-10 1991-1995 Near-Wellbore Epicenters. Axes are centered on injection wellhead; dashed lines are implied locations of through-going Wray Mesa normal faults.

7.8 Earthquake Recurrence

Table 7-5 shows the data and calculated *b*-values and **Figure 7-18** shows the calculated cumulative recurrence data, linear fits to the data (solid lines), and back projection of the linear fits (dashed lines) for small magnitude events, respectively for the **Table 7-5** data. As noted, the figure uses all the events recorded since continuous injection began through the end of 2003 and for each of the injection phases described above. These calculations assumed a maximum magnitude

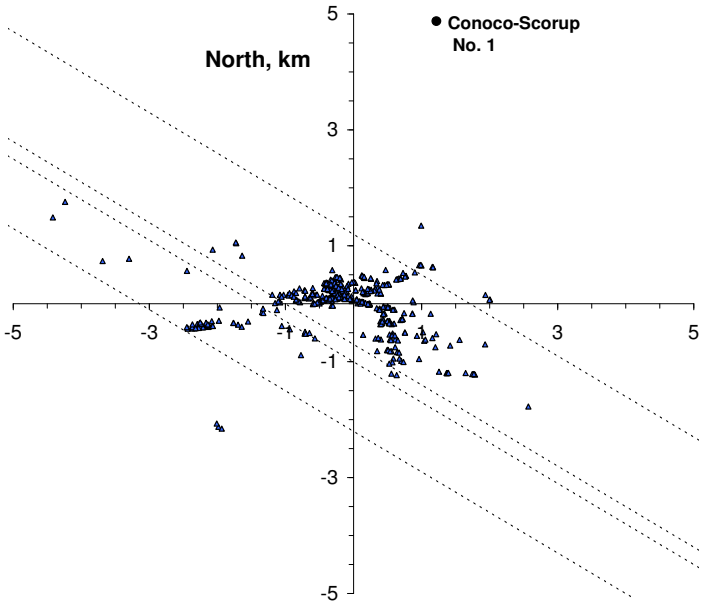

Figure 7-11 1996-1997 Near-Wellbore Epicenters. Axes are centered on injection wellhead; dashed lines are implied locations of through-going Wray Mesa normal faults.

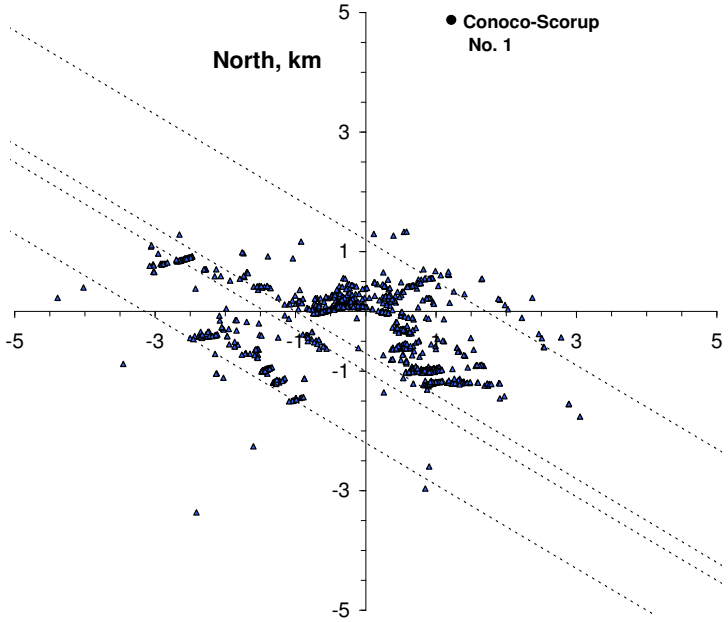

Figure 7-12 1998 Near-Wellbore Epicenters. Axes are centered on injection wellhead; dashed lines are implied locations of through-going Wray Mesa normal faults.

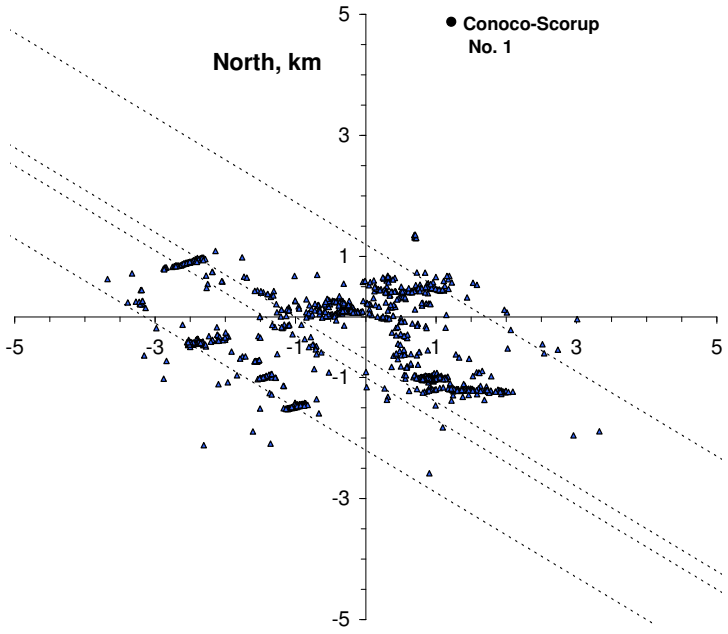

Figure 7-13 1999 Near-Wellbore Epicenters. Axes are centered on injection well-head; dashed lines are implied locations of through-going Wray Mesa normal faults.

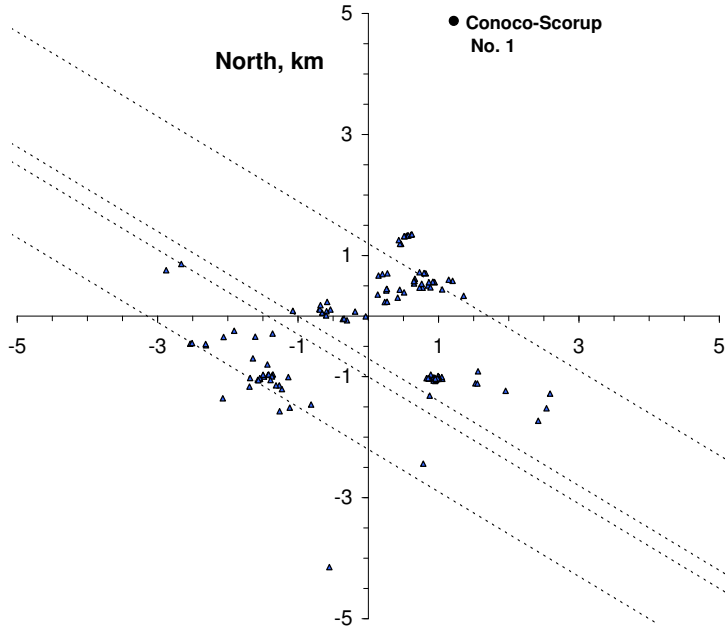

Figure 7-14 2000 January-May Near-Wellbore Epicenters. Axes are centered on injection wellhead; dashed lines are implied locations of through-going Wray Mesa normal faults.

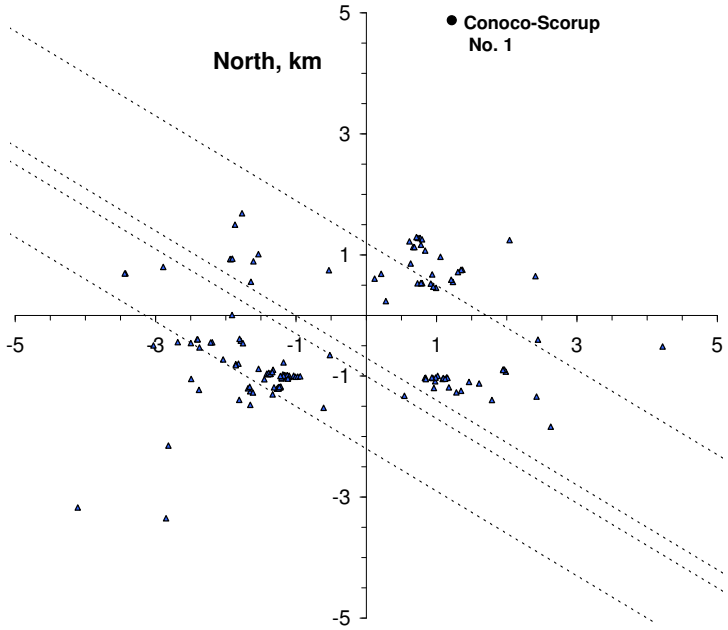

Figure 7-15 2000 June-December Near-Wellbore Epicenters. Axes are centered on injection well head; dashed lines are implied locations of through-going Wray Mesa normal faults.

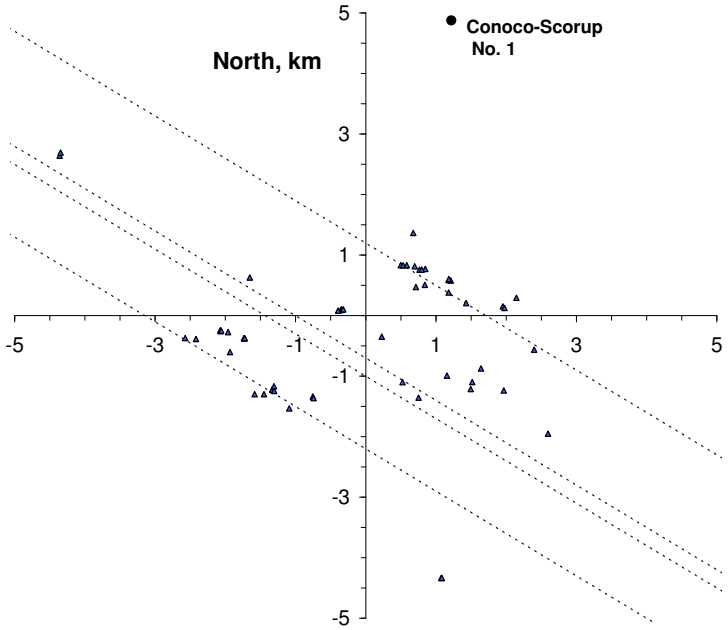

Figure 7-16 2001 Near-Wellbore Epicenters. Axes are centered on injection well head; dashed lines are implied locations of through-going Wray Mesa normal faults.

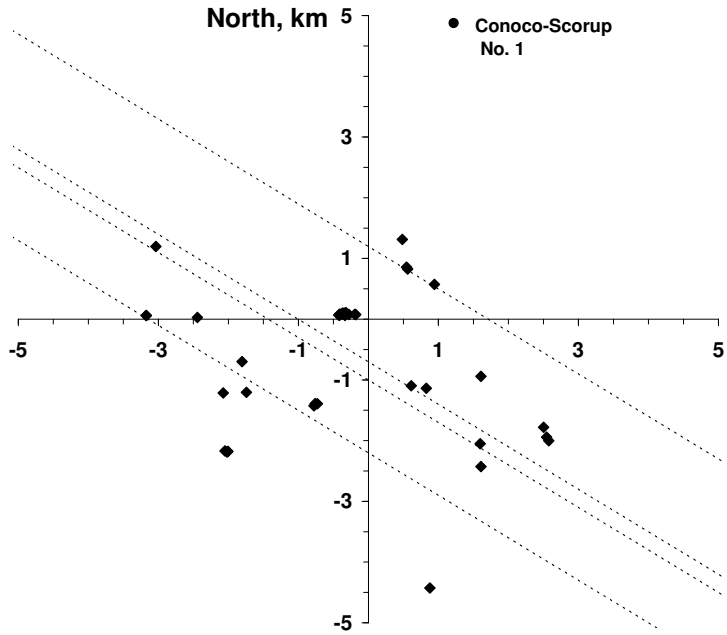

Figure 7-17 2002 Near-Wellbore Epicenters. Axes are centered on injection well head; dashed lines are implied locations of through-going Wray Mesa normal faults.

of 5. The flattening in the data at **M** 0.5 suggest that **M** 0.5 is the lower detection/location threshold at PVN (i.e., below ~**M** 0.5 ground motion is small and some events are detected, but detection is incomplete.) **Figure 7-18** also shows the *b*-values which relate the change in the number of earthquakes with a unit change in magnitude. In **Figure 7-18** we annualized the data so the *b*-values here relate the change in the number of earthquakes *per year* with a unit change in magnitude. In most tectonic settings, the *b*-value is typically about 1 which means each unit change in magnitude corresponds to a factor of 10 change in number of events. For a *b*-value of 0.8, the factor changes from 10 to 10 x 0.8 or 8.

The *b*-values for *Phases I*, *II*, and possibly, *III* in **Figure 7-18** are consistent with observations of earthquake recurrence within the seismically inactive Colorado Plateau (Wong and others, 1996; LaForge, 1996). This similarity of the Paradox *b*-values to other studies in the Colorado Plateau supports the concept that during *Phase I*, *II*, and *III*, many of the induced earthquakes at the Paradox site are due primarily to the release of tectonic shear-stress. This observation agrees with our source (i.e., focal mechanism) studies of the PVSN data discussed below. However, the *b*-value

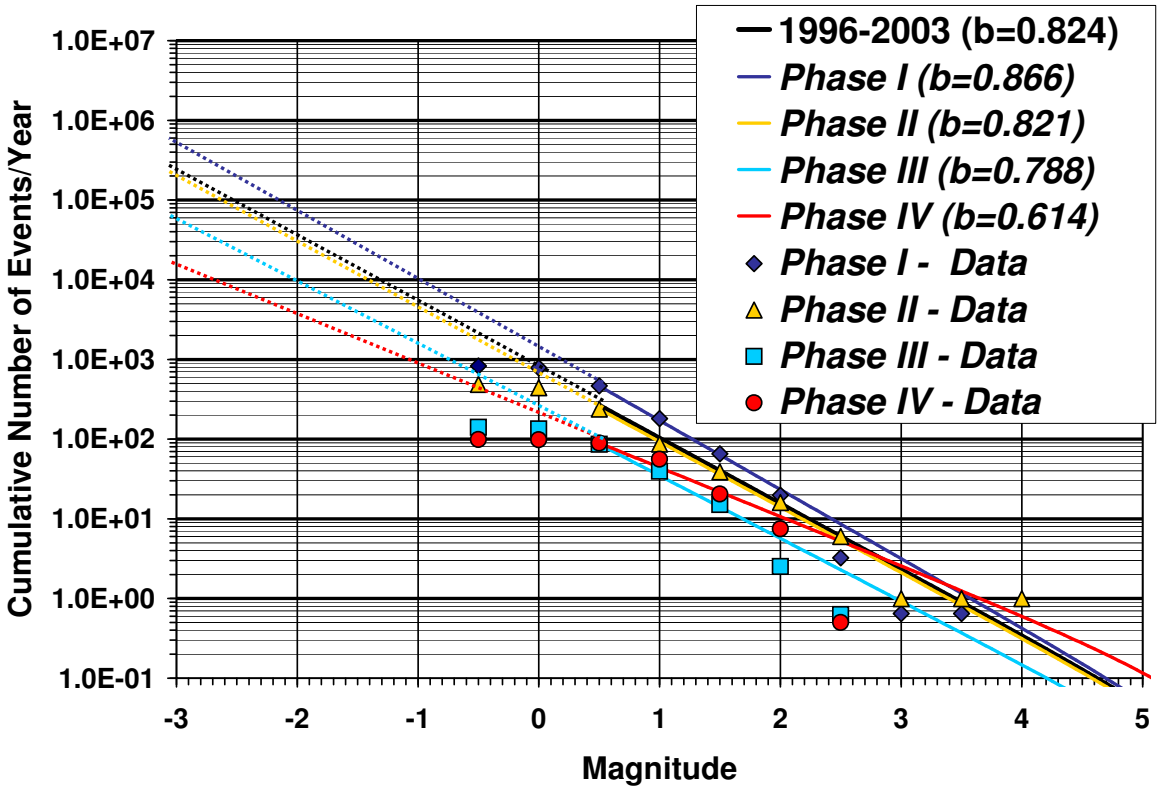

Figure 7-18 Cumulative recurrence curves for earthquakes located by PVSN near the brine injection well from 1996 through 2003 (All) and for each of the injection phases described in text. Colored symbols are data; solid lines are fits to the data; and dashed line are projection of the solid lines to smaller magnitude events.

for *Phase IV* is significantly lower than the earlier phases. This may mean a change in the nature of the induced seismicity; however, it is too early to make any definitive statements.

7.9 Focal Mechanisms - Preliminary Analysis

The waveforms of the 2003 data are consistent with previous years. Hence we did not feel a need to calculate new fault plane solutions. For completeness we repeat our statements from last year's report.

P-wave first motion observations are used to construct focal mechanisms for evaluating potential fault planes and characteristics of the *in situ* tectonic stress field. Using earthquakes with strong first motions and occurring over a range of locations, we constructed 75 focal mechanisms. As

Table 7-5 Number of Events by Magnitude Range and Pumping Phase Used in Calculating Earthquake Recurrence Curves (Figure 7-18)

Magnitude Ranges	**All** (7/96-12/03)	***Phase I*** (7/96-7/99)	***Phase II*** (7/99-7/00)	***Phase III*** (7/00-1/02)	***Phase IV*** (1/02/-12/03)
	no. events	no. events	no. events	no. events	no. events
0.5-0.9	1170	877	152	74	67
1.0-1.4	513	355	48	39	71
1.5-1.9	210	141	23	20	26
2.0-2.4	78	51	11	3	14
2.5-2.9	16	8	6	1	1
3.0-3.4	0	0	0	0	0
3.5-3.9	2	2	0	0	0
4.0-4.4	1	0	1	0	0
***b*-value**	0.824	0.866	0.821	0.788	0.614

with previous observations, the results are dominated by strike-slip faulting on west-northwest trending, steeply dipping (i.e., vertical to nearly vertical) fault planes. However, several events with oblique strike-slip-normal mechanisms were observed. **Figure 7-19** shows a Rose diagram of the fault plane angles of the 75 focal mechanisms. The Pressure (or P) axes and Tension (or T) axes for these events are shown as Rose diagrams in **Figure 7-20**. The T-axis direction is a consistent northeast direction and the P-axis is oriented northwest (~N 51°W). No difference in spatial distribution of focal mechanism types is evident throughout PVSN's entire data set.

7.10 Focal Mechanisms - Advanced

Focal mechanisms for the entire data set were calculated using *P*-wave first motion polarities and S_V/P amplitude ratios on vertical component seismograms (Kisslinger, 1980; Kisslinger and others, 1981). A simulated annealing downhill simplex algorithm (Press and others, 1992) was used to calculate double-couple focal mechanisms. First motions were weighted 10 times more than S_V/P ratio misfits and an L1 norm is used to calculate total misfits. The 20% of the S_V/P amplitude ratios with the worst misfit were ignored because S_V/P can become unrealistically large near nodal positions. The velocity seismograms were high-pass filtered with a one pole Butterworth

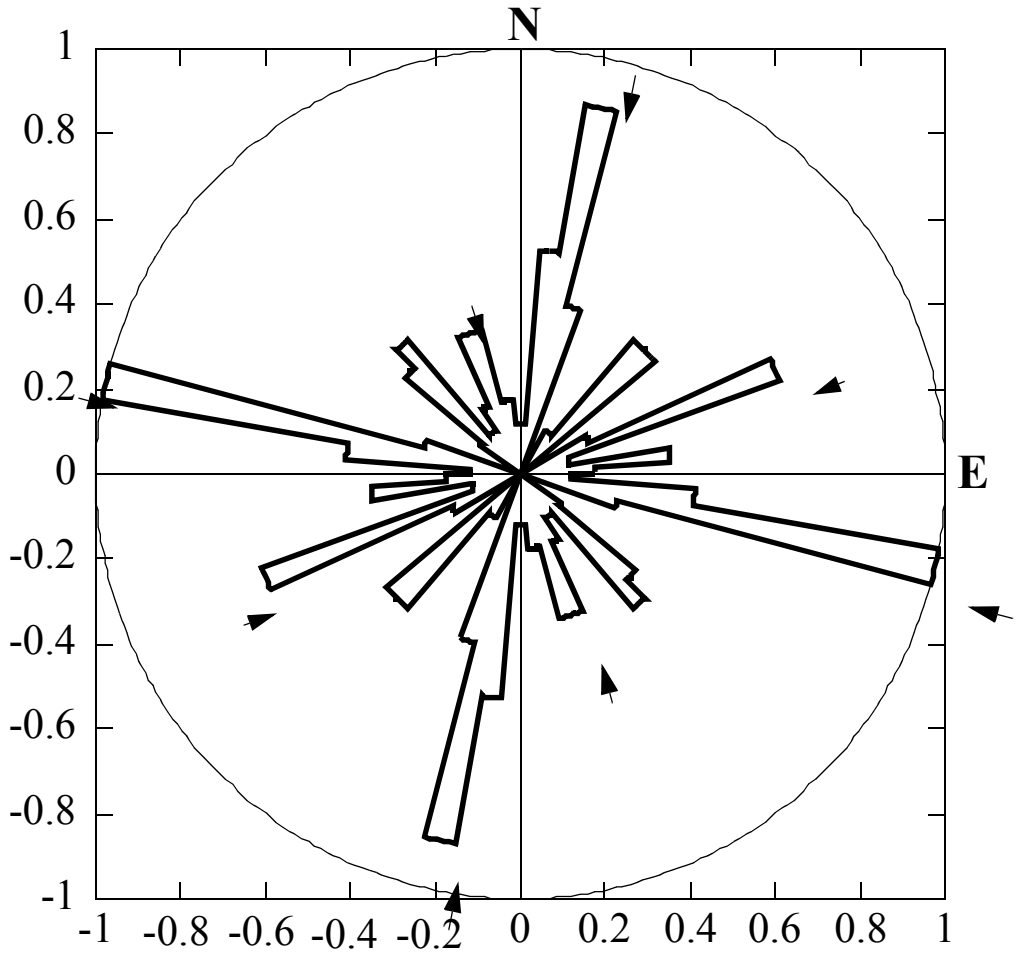

Figure 7-19 Rose diagram of fault plane directions from 75 focal mechanisms recorded in 2000. For comparison, paired arrows indicate directions from 1999 data analysis. The strike of the Paradox Valley is approximately N 55°W.

filter at one Hz and double integrated to estimate long-period displacement levels. One second P-wave windows and 5 second S-wave windows were used to calculate long-period displacement amplitudes. This method of calculating displacement integral amplitudes was compared to spectral fitting procedures to displacement spectra and found to be more stable than spectral approaches. A total of 28 levels were used in the simulated annealing inversions, with a maximum of 90 function evaluations at each level. The starting level was set to a value corresponding to 60 misfitting first motions and decreased using the schedule, $L = L_0(1-k/K)^a$, where L_0 is the initial level, K is the total number of function evaluations, k is the cumulative number of function evaluations so far, and a was set to two. At high levels, the process occasionally accepted models associated with increases in functional misfit to inhibit convergence to a local minima. As L tended

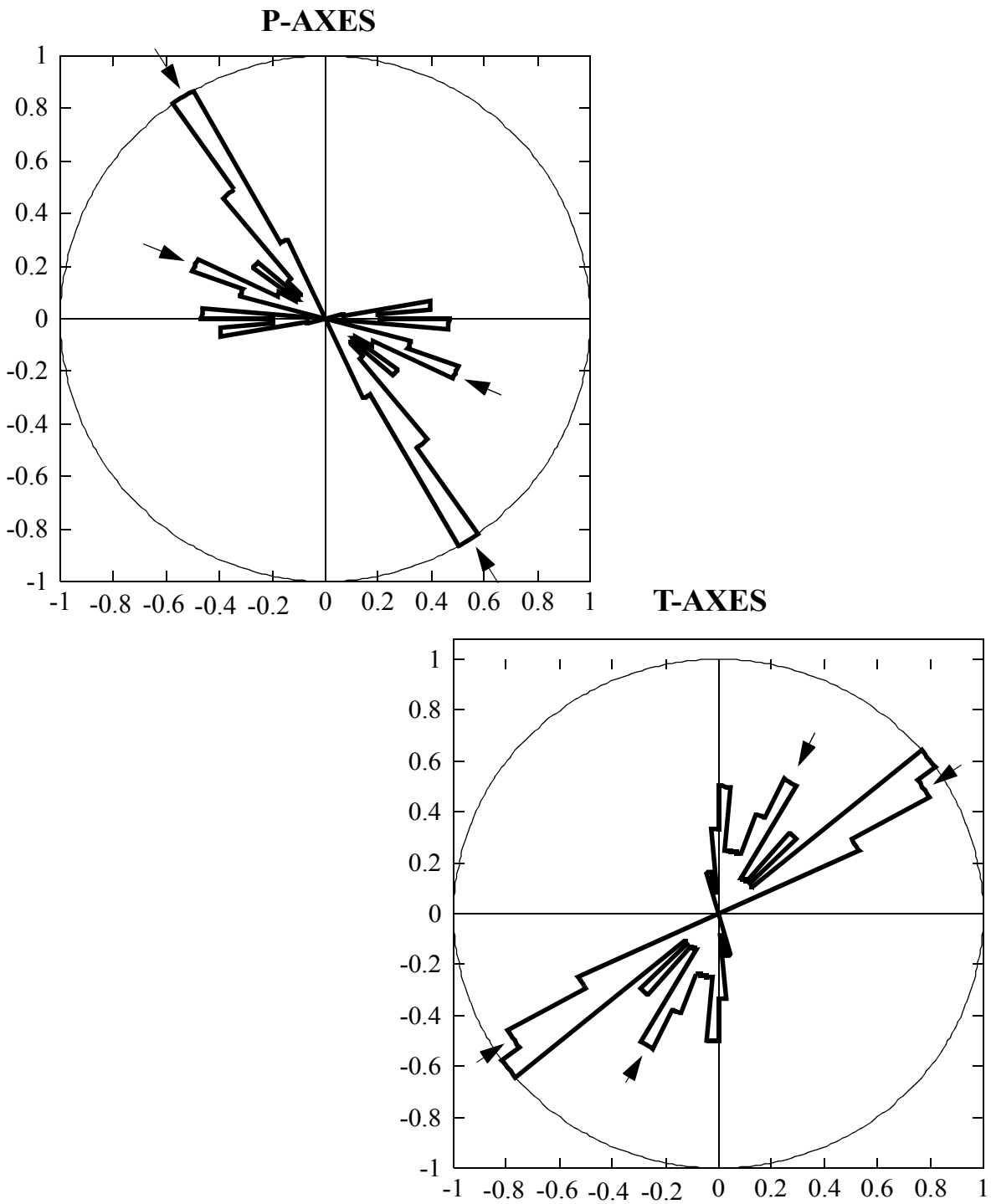

Figure 7-20 Rose diagram of P-axis directions and T-axis directions from 75 focal mechanisms obtained during 2000 from PVSN. Paired arrows show directions from 1999 data analysis. The strike of the Paradox Valley is approximately N 55°W. The x- and y-axes in each figure are east-west and north-south, respectively.

toward zero, the inversion reduced to a simple downhill simplex algorithm (Press and others, 1992). This approach effectively eliminates the local minima convergence problems Kisslinger and others (1981) experienced with an iterative least squares inversion approach. The azimuths and takeoff angles from the 3D P- and S-wave velocity models were used in the focal mechanism calculations.

Table 7-6 lists the starting simplex. Five solutions were obtained for each event, the solution obtained with the starting simplex, and four solutions obtained by inserting each trial solution in **Table 7-6** as the new starting solution at the end of the previous solution. Several criteria were used to determine the quality of estimated focal mechanisms. The first focal mechanism quality filter required a minimum of seven P-wave first motions, a total of 12 S_V/P amplitude ratios and P-wave first motions, and a first-motion misfit <= 0.5. First-motion misfit was defined as the sum of quality weight factors (**Table 7-7**) of first motions with incompatible polarities. Pick qualities of 0 and 1 correspond to impulsive (i.e., sharp) P-wave arrivals and pick qualities of 2 and 3 corresponding to increasingly emergent (i.e., gradual) P-wave arrivals. The first-motion misfit criteria rejected focal mechanisms with a single pick quality 0 or 1 first-motion misfits, two pick quality 2 first-motion misfits, three quality 3 first-motion misfits, or any combination of quality 2 and 3 first-motion misfits. The criteria of seven P-wave first motions establishes reasonable minimum seismogram signal-to-noise ratios. A total of 2145 events passed the first focal mechanism quality filter and are shown in **Figure 7-21**.

Table 7-6 Trial Starting Focal Mechanisms

Trial	Strike (degrees)	Dip (degrees)	Rake (degrees)	type
1	0	90	180	strike slip
2	270	45	-90	normal
3	180	45	90	reverse
4	300	65	135	oblique-reverse

Table 7-7 First-Motion Misfit Weights

Quality	Weight
0	1.0
1	0.75
2	0.5
3	0.25

A second quality factor ranked the independence of the focal mechanism solutions to varying starting solutions. The filtering criteria was that the maximum differences in P- and T-axes orientations between the subset of five focal mechanism solutions must be < 20 degrees. The maximum differences in P- and T-axes orientations were only calculated for event solutions with total L1 misfits no larger than 150% the minimum misfit. A total of 1345 well-constrained focal mechanisms were obtained. These were separated into strike-slip events by imposing the constraint that both the P- and T-axes must plunge < 25 degrees, yielding a total of 1196 strike-slip focal mechanisms shown in **Figure 7-21**. The nodal planes were separated into two sets by removing the left tail portion of the distribution in **Figure 7-22a** and placing those nodal planes into a secondary nodal plane set. Using the two nodal plane set distributions shown in **Figure 7-22b** and **Figure 7-22c** reduced estimated nodal plane distribution skew from -1.7 to -0.005 and kurtosis from 5.2 to -0.86 (**Table 7-8)**.

Table 7-8 Strike-Slip Nodal Plane Azimuth Statistics

Nodal Set	Median	Mean	Std. Dev.	Skew	Kurtosis	Events
Combined	262	257	30	-1.7	5.2	1196
Primary	266	266	19	-0.005	-0.86	1048
Secondary	311	311	3.5	0.11	-1.1	148

7.10.1 Strike-Slip Focal Mechanisms

If both nodal plane sets in **Figure 7-21** correspond to pre-existing faults, the P axis azimuth can vary about +/-10° about the position shown in **Figure 7-21**. If the 311° nodal set corresponds to the normal fault orientations, the P axis could be oriented at a relatively small angle to the 311°

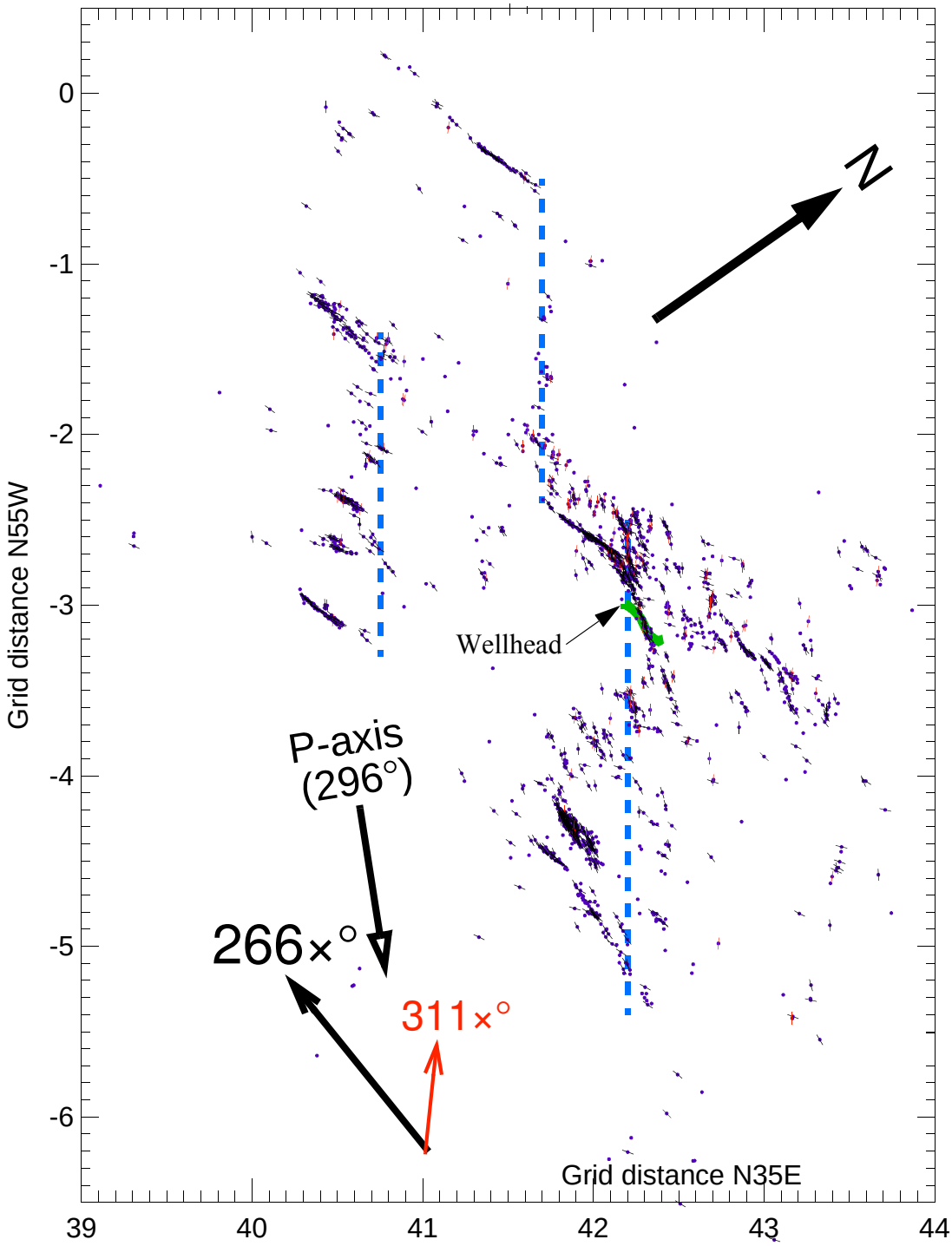

Figure 7-21 Purple dots are all epicenters. Black lines are 70 m strike-slip 227.5°-305°-azimuth nodal planes. Red 70 m line segments are 305°-355° azimuth nodal planes. Line segments > 70 m indicate nodal plane alignment for multiple adjacent events. The wellbore is shown in green (arrow at the top). Dashed blue lines show locations of normal faults at Leadville formation depths, as indicated by vertical changes in earthquake depths, well logs, and seismic reflection data. Intersecting arrows show median orientations of the two nodal plane sets labeled with azimuths. Open arrow is the inferred P-axis orientation.

nodal set. For instance a P axis azimuth of 296°, places the P axis 30° from the primary nodal set azimuth, consistent with internal friction angles for the Leadville limestone. A P axis azimuth of 296° is within 14° of the regional P axis azimuth over the past 5 Ma in Bird (2002) (see **Table 7-9)**. Alternatively, the primary nodal plane set could correspond to tear faults between the normal faults. Then both nodal plane sets correspond to relatively weak faults and the P axis azimuth is only constrained to be between the nodal plane azimuths. The 86% proportion of events in the primary set argues for the P axis making a smaller angle with the secondary set than the primary set, e.g., the P axis azimuth is probably ~295°.

Table 7-9 P-axis Azimuths for Colorado in the Past ~10 Ma from Bird (2002).

Feature, Location	Longitude	Latitude	Azimuth	Sigma	After	Before
dikes, Steamboat Springs, CO	-106.95	40.22	310	10.0	9.0	7.0
dikes, northern Routt Co., CO	-107.15	40.78	310	10.0	11.5	8.1
veins, W San Juan Mts., CO	-107.51	37.73	311	29.0	23.7	5.3

7.10.2 Oblique Focal Mechanisms

Oblique focal mechanisms were defined as focal mechanism where the plunge (i.e., angle between the vector and the surface) of the P (T) axis was >= 30° and the plunge of the corresponding T (P) axis was < 25°. There were a total of 55 normal-oblique events (**Figure 7-23**) and 43 reverse-oblique events (**Figure 7-24**).

7.11 Earthquake Slip Mode

The previous sections present data showing that the source mechanics of the PVU earthquakes is shear slip on existing faults and fractures. These faults are not sufficient to hold the volume of injectate emplaced at PVU. Hence, within the formations, the injection process creates additional "volume" (i.e., space) to accommodate the injectate. Therefore injection creates and opens tensile fractures (i.e., hydraulic fractures) into which the injectate squirts. The question then arises: Is any

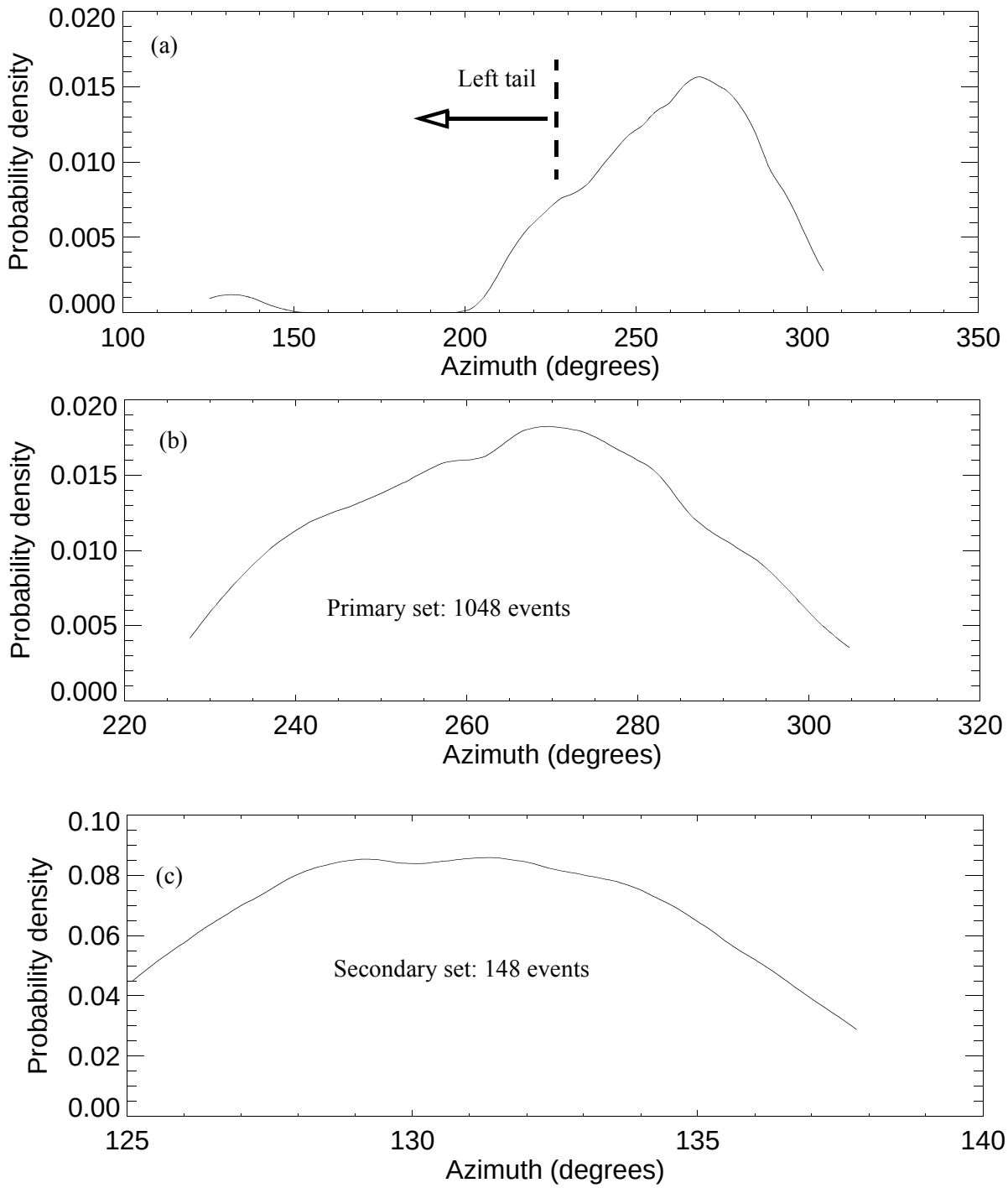

Figure 7-22 The complete strike-slip nodal plane inventory azimuth density function in (a) has a strong left skew. Separation of the nodal-plane azimuths into a primary set (b) and secondary set (c) by placing the left tail in (a) into a secondary set (c), produces a primary set with nearly zero skew and small-tailed distributions (negative kurtosis) for both nodal plane sets in (b) and (c) as indicated in Table 7-8.

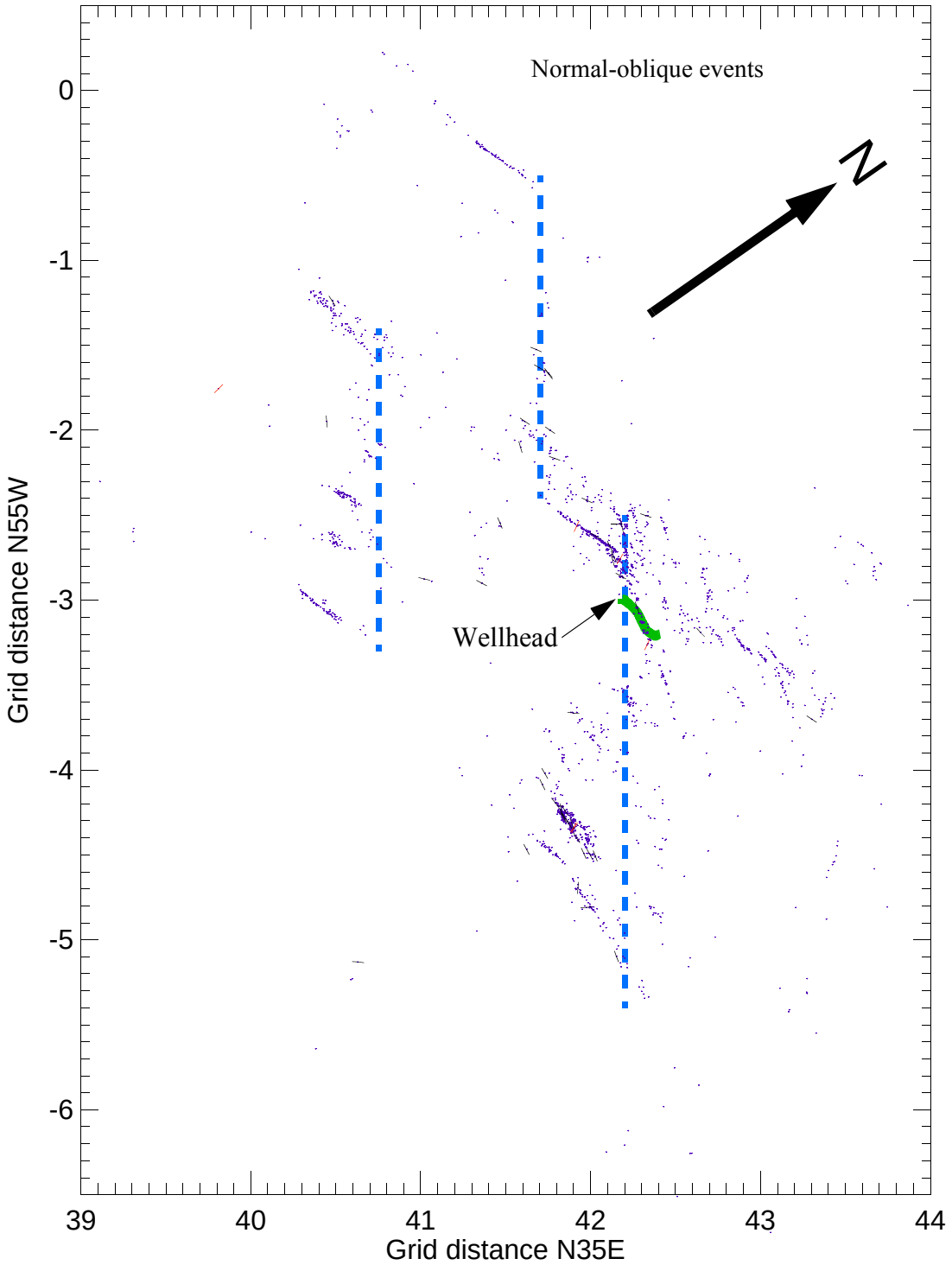

Figure 7-23 Purple dots are all epicenters. Black lines are 70 m normal-oblique-slip 227.5°-305°-azimuth nodal planes. Red 70 m line segments are 305°-355° azimuth nodal planes. Longer line segments indicate nodal plane alignment for multiple adjacent events. The wellbore is shown in green (arrow at the top). Dashed blue lines show approximate locations of normal-fault segments at Leadville formation depths, as indicated by vertical changes in earthquake depths, well logs, and seismic reflection data.

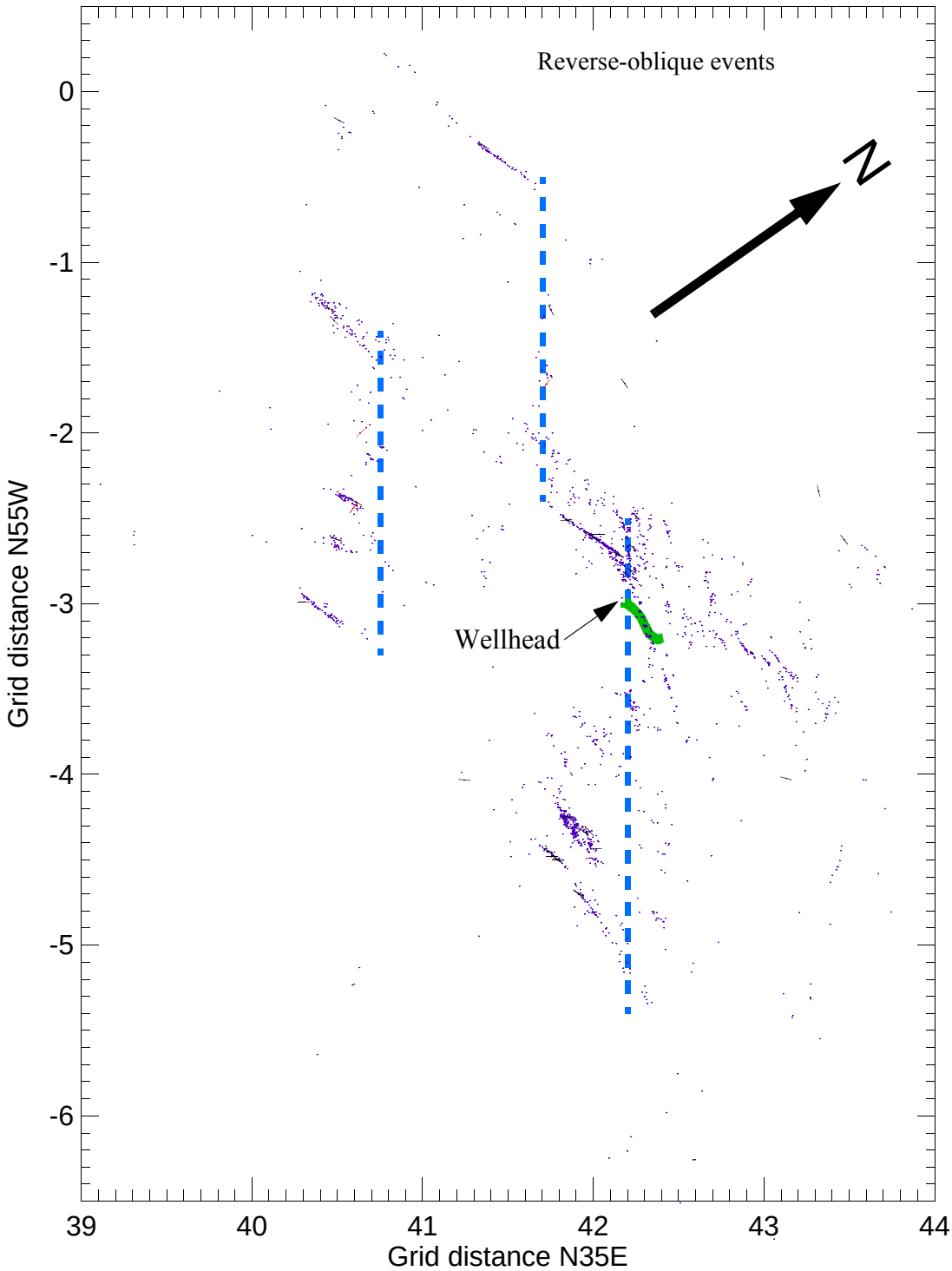

Figure 7-24 Purple dots are all epicenters. Black lines are 70 m reverse-oblique-slip 227.5°-305°-azimuth nodal planes. Red 70 m line segments are 305°-355° azimuth nodal planes. Longer line segments indicate nodal plane alignment for multiple adjacent events. The wellbore is shown in green (arrow at the top). Dashed blue lines show approximate locations of normal-fault segments at Leadville formation depths, as indicated by vertical changes in earthquake depths, well logs, and seismic reflection data.

portion of the seismicity recorded by PVSN due to these tensile events? Based on oil and gas field hydraulic fracture studies run at pressures comparable to PVU injection pressure, the hydraulic fracture opening or aperture is on the order of a few millimeters, at most. Therefore, with each squirt, the (new) surface area of a fracture is on the order of 10's of square centimeters, or less. Based on calculation of seismic moment (Wells and Coppersmith,1994), **Figure 7-25** shows the slippage on surfaces this size will generate tiny events (i.e., will radiate minimal seismic energy). At the surface, this radiation is well below the detection level of PVSN. In addition this radiation is in the frequency band of a few 100 hertz to a couple kilohertz. The seismometers at PVSN operate at frequencies below a few 10's of Hz and lower. Hence, based on the focal mechanics studies and the aforementioned arguments, the results of these fracture mechanics arguments are consistent with the findings that the ground motions recorded by PVSN are due to shear events, not tensile openings.

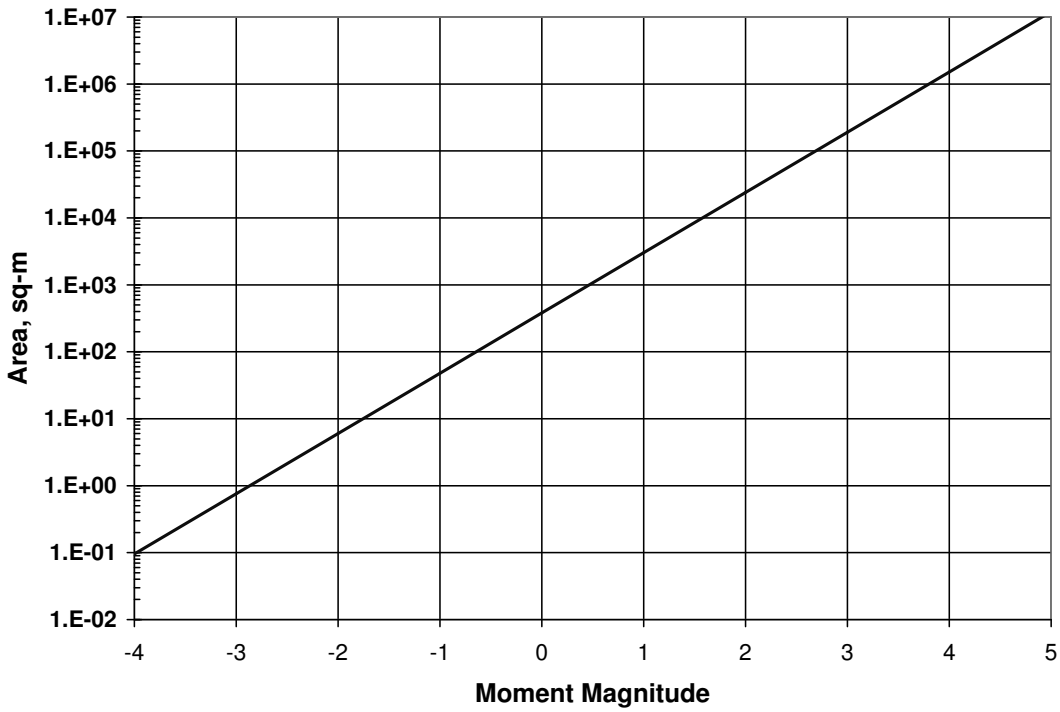

Figure 7-25 Earthquake Fault Area versus Size (i.e., Moment Magnitude). The curve is extrapolate from Wells and Coppersmith (1994)

7.12 Seismic Magnitude versus Location

One question that we have begun to examine is that with the highly accurate event location data how do the locations correlate with event magnitude? **Figure 7-26** and **Figure 7-27** show all events a magnitude **M** 1.7 and greater plotted against a background of all the events. **Figure 7-26** is a plan view and **Figure 7-27** is a depth cross section looking north. Note that all the linear features, which illustrate faults and fractures of the Wray Mesa system seismically activated by PVU injection, do not host larger events. Only a limited subclass of the fractures and faults have larger

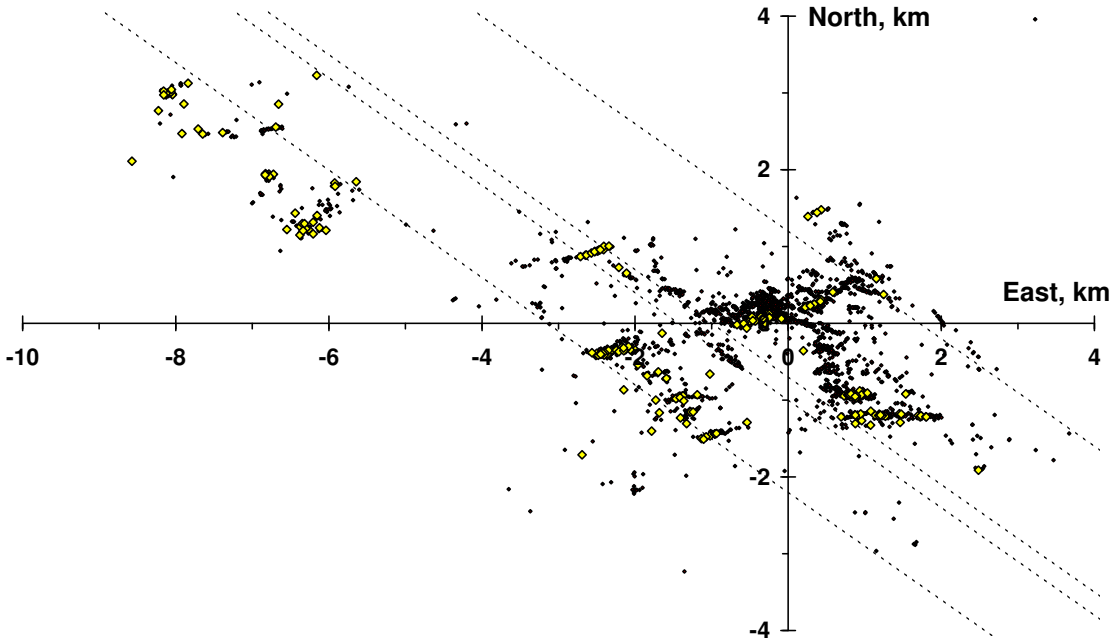

*Figure 7-26 PVU Epicenter Map of Events with Magnitude **M** 1.7 and Greater (yellow diamonds) Superimposed on All of the Seismicity. Origin is centered on wellhead. Note that the larger events only occur along a limited subset of the faults illuminated by the induced seismicity.*

events. Some of the fractures and faults have many larger events and some have only one or two. Initially we expected the larger events to be more uniformly distributed. Also note that a disproportionate number of larger events occur in the secondary seismogenic region, ~8 km to the northwest of the injection well. We are still evaluating the implications of these findings.

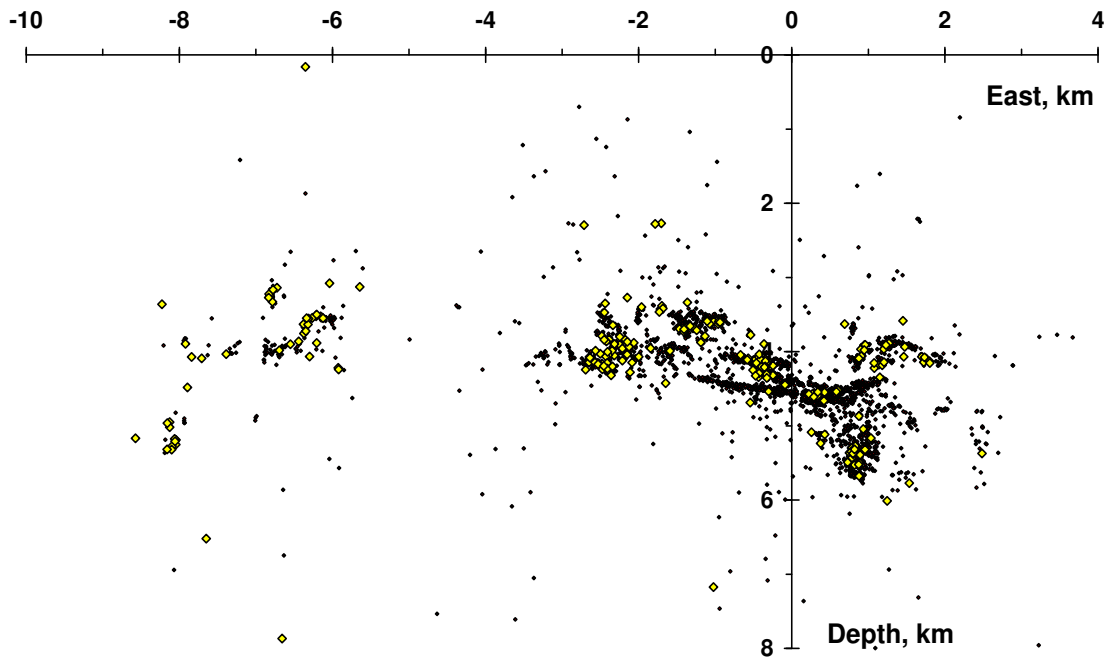

*Figure 7-27 Depth Cross Section Map Looking North Showing Events of Magnitude **M** 1.7 and Greater (yellow diamonds) Superimposed on All Seismicity. Origin is injection wellhead. Note that the larger events only occur along a subset of the faults illuminated by the induced seismicity.*

8.0 MODELING ROCK PROPERTIES

8.1 Injection Data and Fracture Modeling

As noted earlier, the 2003 seismicity generally locates within the zone defined by previous years' seismicity. From this we assume that the extent of the injectate envelope is expanding very slowly and much of the volume occupied by the 2003 injectate lies within this seismicity envelope. That is, the new volume (i.e., rock fracturing) caused by the injectate is probably occurring within the well-centered zone defined by the seismic envelope of previous years. The persistent spatial distribution of events suggests that the occurrence of induced earthquakes at this site (and hence fluid migration) is controlled by physical attributes, like stress, preexisting faults, planes or zones of weakness, etc., and is not a random process.

Supporting this are the results from BORFRAC, a computer code of Envirocorp (1995) that synthesized injection data based on formation parameters and fitted the synthetic data to real injection data from the 1991-1995 injection test sequence. BORFRAC synthesized the data by modeling the well and surrounding formations and their response to high-pressure fluid invasion. In the initial BORFRAC model, Envirocorp assumed that injection created traditional hydraulic fracturing: single vertical fracturing divided into two wings, each extending from opposite sides of the well at the depth of the casing perforations. This model assumes that the injectate fills the fracture wings and diffuses into the formation through the native permeability of the fracture walls. This type of model predicts seismic locations confined to a very narrow elliptical envelope centered on the well and whose semi-major axial plane overlays the wings of the fracture. From the seismic data which showed a diffused network of locations, Envirocorp interpreted a network of injectate flow paths in the Leadville Formation and recognized that the traditional, double-wing model was not correct. Envirocorp upgraded the BORFRAC model from a double-wing fracture to a network of fractures. Using the network model BORFRAC gave better agreement between the model data and wellbore injection data.

8.2 Seismicity, Fault Properties, and Injectate Volume

Between 1991 and the end of 2003, PVU injected ~4.1 billion liters (~1.08 billion gallons) of

injectate. In response to the greater than 11,000 psi pressure, at the injection depth the injectate is compressed to ~95% of its surface volume or about 3.9 million cubic meters. As noted earlier, this volume of fluid must occupy existing space or create new space within the rock matrix. The question then is where is the injected fluid being stored, in existing space (e.g., faults, old fractures and joints, or existing pores), in new space (e.g., new fractures), or a combination of both? It is not likely that at 4.8 km (16,000 ft) depth with ~100+ MPa (~14,500+ psi) of overburden stress, there is much open space. To evaluate the existing-space hypothesis, we considered existing faults and the possibility of opening these faults.

In previous sections we showed that many of the seismic events align in linear groups. We've interpreted these groups as delineating seismically-activatable faults and fractures of the Wray Mesa system. In addition, as an upper bound on available fracture and fault storage volume, we have interpreted these faults or fractures as having been reached by injectate. Noting, as discussed, the two major groupings, near the well and northwest of the well, we've stated that it is likely that a northwestern fault runs from the well group to the northwestern group. Based on our seismic map and the implied local faults of Bremkamp and Harr (1988), we tallied ~30 km of seismically-illuminated and implied fault length. We then assumed that the faults averaged about 0.5 km height, the height of the Leadville formation. To accommodate the full injectate volume would require opening these faults and fractures ~200 mm (~8 in). This opening is unrealistic in a rock mass at this depth and overburden stress with PVU's injectate and its pressures. Based on recovered cores from hydraulic fracture experiments in the oil and gas industry (per. comm., Mike Sorrells, Teledyne Geotech), we expect the fault openings to be a maximum of a few millimeters.

If we assume that the 30 km of faults and fractures have openings between 1 and 5 millimeters, then, at any time, only a few percent of the injectate volume can be stored in these faults and fractures. This means that the injectate either has created new fractures or its has diffused into the pore spaces of the rock mass. Considering the new fracture scenario, we calculated the length of new fracture needed, assuming 0.5 km high fractures. The amount of new fracture is on the order of several thousand kilometers. This is a prohibitively large amount of fracturing. To realistically accommodate this much fracturing requires a fractal distribution for the new fractures, which we discussed earlier. A second scenario is that the fluid temporarily occupies the seismically-defined

fractures and faults, and then slowly diffuses into the existing pore space of the rock. However, since we cannot quantify what percentage of fluid occupies new fractures and what percentage occupies pore space, we will assume all the injectate occupies fractures of a fractal distribution and show in the fractal model an upper bound on the amount of fracturing that is necessary to accommodate the injectate volume.

8.3 Seismicity and Effective Porosity

It is mostly likely that most of the injectate eventually migrates from the pressure-opened fractures and faults, through diffusion, into the rock mass. The seismicity has allowed us to study an aspect of diffusion, specifically the effective porosity of the rock mass.

As a first estimate for porosity we modeled the fluid volume as a vertical cylinder 2.0 km high and growing radially. We assumed a 2-km height since that is the vertical expanse of most of the seismicity. **Figure 8-1** shows the results of this modeling. The figure shows a number of features. First, the scatter data are the horizontal distance of the seismicity from the wellbore as a function of time. This shows the growth of the two seismic zones: the one surrounding the well and the one ~8.5 km to the northwest. For the model diffusion model discussed below we only consider the zone surrounding the well. Next we've plotted the radius of the growing cylinder based on the injected volume, again, as a function of time. Here we modeled five porosities; in decreasing porosities these are 0.05%, 0.01%, 0.005%, 0.0025%, and 0.001%. From smallest to largest, these porosities span a factor of 50.

Based in the pre-2000 seismic expansion rate in **Figure 8-1**, the porosity models suggest a porosity between 0.005% and 0.0025%. In 2000 with the inception of more shut downs and the reduced injection rate in late June, the growth of seismic zone is greatly curtailed and the model no longer fits the seismic zone expansion. This may mean that with overall reduced injection, the injectate is not being forced to move as quickly, but instead diffuses into the existing region defined by the extent of the seismicity. Using this scenario, a fixed region defined by the extent of seismicity, we assumed a seismogenic volume of about 30 cubic km. With an injected volume of about 0.004 cubic km (i.e., 4 million cubic meters), this gives a porosity of ~0.01%. This second value of

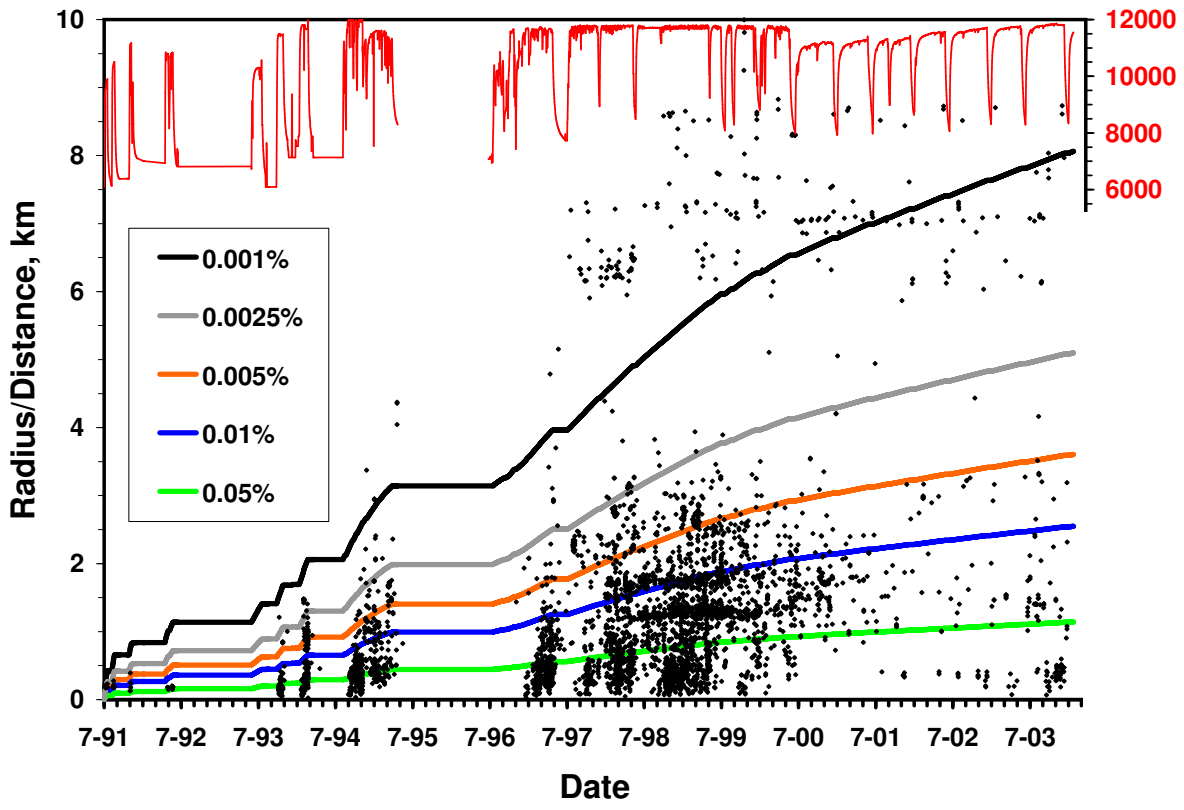

Figure 8-1 Horizontal distance of seismic events from the injection well (black dots) and downhole (injection) pressure (red) versus time. Also plotted are the (calculated) radii of theoretical models of an expanding cylinder model injectate for 5 rock porosities versus time. Injectate radius model uses the injected volume and assumed a fixed, 2-km height.

porosity is not the same as our first, but, given the impreciseness of these models, they are compatible. For comparison, when Envirocorp (1995) ran its BORFRAC reservoir model to simulate the performance of the injection well and the Leadville formation, it used 0.05% porosity.

9.0 CONCLUSIONS

9.1 Specific to 2003

The general objectives of recording, analyzing, and interpreting seismicity in the Paradox Valley region were successfully carried out during 2003. The seismic data showed that the adjustment to the PVU injection schedule in 2000 continued to maintain a low level of seismicity. Relevant observations from this reporting period include:

(1) The 138 microearthquakes of 2003 locate within the two seismogenic zones defined by previous years' microearthquake locations;

(2) As in previous years, the frequency of occurrence of observed earthquakes reduced following periods of cessation of brine injection and following a long-term reduction in injection rate;

(3) Induced earthquakes continued to occur ~8 km northwest of the injection well with a gap between those events and the event zone surrounding the injection well;

(4) The spatial patterns of observed seismic sources and observed seismic source mechanics seem to follow the Wray Mesa fault and fracture system and are consistent with relevant tectonic stress characteristics.

9.2 Since Inception of Continuous Pumping

Throughout the continuous pumping, beginning in 1996, the nominal injection pressure at PVU exceeds fracture pressure.

The initial induced seismicity was probably due to injectate or connate fluids reducing the friction across faults, liberating pre-existing, *in situ* tectonic stress across the faults. Later events may also include those resulting from changing the *in situ* stress due to pore and fault inflation from the injectate and displaced connate fluids.

The induced seismicity at Paradox illuminates an extensive, non-symmetric connected network of fractures, faults, joints, etc. and does not demonstrate the traditionally hydraulic fracture picture of two, vertical, symmetric fractures emanating from opposite sides of the injection well.

The surface-recorded seismic events radiate shear slippage on pre-existing faults, joints,

planes of weakness, not tensile or the openings of new fractures.

Injection has induced two, distinct seismic event zones: a primary zone, asymmetrically surrounding the well to a radial distance of ~3+ km and a secondary zone, displaced ~8 km to the northwest of the injection well along the trend of the known Wray Mesa fault system. The primary zone is within a reservoir covering between 20 and 30 cubic kilometers

More than 99.9% of the over 4,000 surface-recorded events induced at the Paradox Valley injection since 1991 have magnitudes less than **M**2.0. The human detection threshold at Paradox is ~**M**2.5; There have been ~15 induced events felt at the region.

Our best estimate indicates PVU has induced ~2 million events with magnitude **M**-3.0 and greater. Being a surface array, PVSN's recording sensitivity is ~0.1% of these events which includes those events with magnitude ~0.0 and greater.

The largest seismic event, an **M**4.3 in May 2000, occurred after ~4 years of continuous injecting.

The first seismic event induced by continuous pumping occurred 111days after pumping began.

The general rate of seismicity is not uniform nor following any discernible pattern; during periods of continuous injection, there are one-day, multi-day, and multi-week quiet periods and multi-hour to multi-day active periods.

Spatially, seismic events occur as isolated events and in swarms; swarms can occur over hours to days in a single location.

The seismic swarms at Paradox are like typical earthquake swarms that culminate in one large event and some smaller foreshocks and a few smaller aftershocks or have one large event followed by 5 to 15 aftershocks.

The seismicity continuously occurs within the interior and on the border of the existing seismic zones; since mid-1999, the expansion of the zones seem negligible, if at all.

By the end of 2003, PVU injected ~0.004 cubic kilometers of injectate. Because connate fluid has been displaced and this fluid can trigger seismic events, the volumetric extent of the injectate is probably less than the volumetric extent of the seismic zone

Seismic event depths are vertically contained between ~3.5 km and ~6.0 km below the injection wellhead.

Epicenters pattern of the secondary fracture and fault network seems to align with (e.g., termi-

nate along) the major, through-going faults of the Wray Mesa system and follows the predicted hydraulic gradient of target formation.

The major fault system aligns with the principal stress direction and acts as fluid conduits showing only minor, if any, surface-recordable seismicity.

The fault-planes defined by focal mechanism solutions (i.e., moment tensors) align with the strikes of the faults and fractures or with the predict shear planes.

Economically reasonable, 20-day shut downs has somewhat reduced the proclivity for large events by relaxing the local state of stress.

Percentage of brine (i.e.,% PVB) in injectate has not affected seismicity directly; however, it has increased the bottom-hole pressure due to the increase in specific gravity of injectate.

The storage of injectate is facilitated by the injection pressure exceeding the fracture pressure and creating new volume plus creating pathways to additional pore space; the seismically-illuminated faults and fractures can only accommodate a few percent of the injectate volume.

The *b*-value, a parameter related to the number of seismic events per size and indirectly related to repeatability of seismic events, seems to have been altered by the changes in injection phases.

10.0 MISCELLANEOUS

10.1 Appendices List

Following are the appendices of this report:

(1) Appendix A addresses our contributions to 2nd well considerations, including the memo we submitted and figures we used during tele-conference.

(2) Appendix B describes the manuscript we published and presented at the 39th Annual Rock Mechanics Symposium at Massachusetts Institute of Technology (MIT), Cambridge, MA, in June, 2003.

(3) Appendix C describes the paper presented and submitted for special publication at the 2nd International Symposium on Underground Injection Science and Technology at Lawrence Berkeley National Laboratory in October, 2003.

10.2 Accompanying CD File List

The accompanying CD contains 5 files:

(1) a Microsoft Excel file of the PVSN seismic data (i.e., time, date, and location of events) and contemporaneous (average) PVU injection data

(2-5) a .pdf files of this year's, the 2002, 2001, and 2000 PVSN annual reports

11.0 REFERENCES

Ake, J. P., D. R. H. O'Connell, L. Block, and U. Vetter, 1996. Summary report, Paradox Valley Seismic Network, Paradox Valley Project, southwestern Colorado (*draft*): Seismotectonic Report 96-9, U. S. Bureau of Reclamation, Seismotectonic and Geophysics Group, Denver, CO, 89 pp.

Ake, J., and K. Mahrer, 1999. 1998 Status report-Paradox Valley Seismic Network, Paradox Valley Project, southwestern Colorado: Technical Memorandum No. D8330-99-016, U. S. Bureau of Reclamation, Seismotectonics and Geophysics Group, Denver, CO, 18 pp.

Ake, J., K. Mahrer, and L. Block, 2000. 1999 Status report-Paradox Valley Seismic Network, Paradox Valley Project, southwestern Colorado: Technical Memorandum No. D8330-2000-012, U. S. Bureau of Reclamation, Seismotectonics and Geophysics Group, Denver, CO, 23 pp.

Bird, P., 2002. Stress direction history of the western United States and Mexico since 85 Ma: *Tectonics*, v. 21, 10.1029/2001TC001319.

Block, L., Ake, J. and Mahrer, K, 2001, The Association between Seismicity Induced by Deep-Well Injection, Injectate Migration, and Tectonic Stresses at Paradox Valley, Colorado, *Seismological Research Letters*, v72, n2, p. 286. (abstract)

Block, L. V., 1991. Joint hypocenter-velocity inversion of local earthquake arrival time data in two geothermal regions: Ph. D. Dissertation, Massachusetts Institute of Technology, 448 pp.

Bremkamp, W., and C. L. Harr, 1988. Area of least resistance to fluid movement and pressure rise, Paradox Valley Unit, Salt Brine Injection Project, Bedrock, Colorado: Final unpublished report to the U.S. Bureau of Reclamation, Denver, CO., 39 pp.

EnviroCorp, 1995. Report of evaluation of injection testing for Paradox Valley Injection Test No. 1: EnviroCorp Project Report No. 10Y673: Final report prepared for the U.S. Bureau of Rec-

lamation by EnviroCorp Services and Technology, Inc., Houston TX, 26 pp.

Hendron, A.J. Jr., 1968, **Mechanical Properties of Rock in Rock Mechanic in Engineering Practice**, ed by, K.G. Stagg and O. C. Zienkiewica, John Wiley & Sons, 442 pp.

Healy, J.H, W.W. Rubey, D.T. Griggs, and C.B. Raleigh, 1997. The Denver earthquakes, *Science*, **161**, p. 1301-1310.

Kharaka, Y. K. et al., 1997, Deep well injection of brine from Paradox Valley, Colorado: Potential major precipitation problems remediated by nanofiltrations, *Water Resour. Res*., v33(5), p. 1013-1020.

Kisslinger, C., 1980. Evaluation of S to P amplitude ratios for determining focal mechanisms from regional network observations, *Bull. Seis. Soc. Am*, v. 70, p. 999-1014.

Kisslinger, C., Bowman, J.R., and Koch, K., 1981. Procedures for computing focal mechanisms from local $(SV/P)_z$ data: *Bull. Seis. Soc. Am*, v. 71, p. 1719-1729.

LaForge, R. L., 1996. Seismic hazard assessment for Navajo Dam, Navajo Indian Irrigation Project, New Mexico: Seismotectonic Report No. 96-11, U. S. Bureau of Reclamation, Seismotectonics and Geophysics Group, Denver, CO, 34 pp.

Mahrer, K., 1999, "A Review and Perspective on Far-Field Hydraulic Fracture Geometry Studies," *J. Petroleum Science and Engineering,* 24, pp. 12-28, 1999.

Mahrer, K., L. Block, and J. Ake, 2001. 2000 Status Report-Paradox Valley Seismic Network, Paradox Valley Project, Southwestern Colorado: Technical Memorandum No. D8330-2001-007, U. S. Bureau of Reclamation, Seismotectonics and Geophysics Group, Denver, CO, 37 pp.

Mahrer, K., J. Ake, and L. Block, 2002. 2001 Status Report-Paradox Valley Seismic Network,

Paradox Valley Project, Southwestern Colorado: Technical Memorandum No. D8330-2002-003, U. S. Bureau of Reclamation, Seismotectonics and Geophysics Group, Denver, CO, 35 pp.

Mahrer, K., J. Ake, L. Block, and D. O'Connell, 2003. 12 Years of Injecting Brine and Inducing Seismicity near Paradox Valley, Southwest Colorado, USA, in **Soil and Rock America 2003**, 12th Panamerican Conference on Soil Mechanics and Geotechnical Engineering, 39th U.S. Rock Mechanics Symposium, June 22-26, 2003, Proceeding Vol II, ed by P.J. Culligan, H.H. Einstein, and A.J. Whittle, Eds, pp1443-1447.

Malone, S., and C. Weaver, 1986. Informal memorandum describing earthquake location program SPONG: University of Washington Geophysics Program, Seattle, WA, 10 pp.

Parker, B. H. Jr, 1992, **Gold Panning and Placering in Colorado How and Where,** Information Series 33, Colorado Geological Survey, Department of Natural Resources, Denver, CO, 83 pp.

Phillips, W.S., J.T. Rutledge, L.S. House, M.C. Fehler, 2002. Induced Microearthquake Pattern in Hydrocarbon & Geothermal Reservoirs: Six Case Studies, *Pure and Applied Geophysics*, v159, N1-3, p. 345-369/

Press, W.H., Teukolsky, S.A., Vetterling, W.T., Flannery, B.P., 1992. **Numerical recipes in FORTRAN: The art of scientific computing,** Cambridge University Press, New York, 963 p.

Turcotte, D. L., 1997. **Fractals and Chaos in Geology and Geophysics**, 2nd Edition, Cambridge University Press, 398 p.

Waldhauser, F., W. L. Ellsworth, and A. Cole, 1999. Slip-parallel seismic lineations on the northern Hayward Fault, California, *Geophysical Research Letters*, **26**, No. 23, p. 3525-3528.

Wells, D.L. and K.J. Coppersmith, 1994. New Empirical Relationships among Magnitude, Rup-

ture Length, Rupture Area, and Surface Displacement, *Bull. Seis. Soc. Am.*, **84**, No. 4, p 974-1002.

Wong, I. G., and R. B. Simon, 1981. Low-level historical and contemporary seismicity in the Paradox Basin, Utah and its tectonic implications: Rocky Mountain Association of Geologists-1981 Field Conference Guidebook, p. 169-185.

Wong, I. G., S. Olig, and J. D. J. Bott, 1996. Earthquake potential and seismic hazards in the Paradox Basin, southeastern Utah: *in* Geology and Resources of the Paradox Basin, 1996 Special Symposium, A. C. Huffman, W. R. Lund, and L. H. Godwin [*eds.*], Utah Geological Association and Four Corners Geological Society Guidebook No. 25, p 251-264.

12.0 APPENDIX A - 2ND WELL ACTIVITIES IN 2003

12.1 Memo Submitted October, 2003

Following is a copy of the memo which we submitted in Oct., 2003 to PVU regarding a proposed second injection well at the site.

Date: October 17, 2003

To: Andy Nicholas, Manager
Paradox Valley Unit (PVU)

From: Jon Ake and Ken Mahrer, Geophysicists,
Technical Service Center

Subject: Proposed Second Injection Well-PVU

After 12 years of operation and analysis we feel that both the economic and environmental success of PVU warrant considering the implications and ramifications of a second injection well. What further motivates considering a second well or other alternative is that the injection reservoir at PVU seems to be slowing in its ability to accept injectate. If this trend continues at the present rate, within the next 2 to 4 years, PVU injection will approach it maximum (safety) injection pressure and will be forced to perform unscheduled shutdowns. Given this window, now is the time for considering alternatives to keep PVU a viable, active, and economically rewarding project.

With regard to a second injection well, a full analysis will require a cost and benefits analysis that includes cost of drilling, completing, and bringing a new well into the existing infrastructure; cost of operation, incremental revenue, environmental benefits, etc. In this memo we present initial technical arguments for siting a second injection well based on what we have learned from Injection Well No. 1. Below we provide relevant background information, summarize observations that we feel are relevant to this discussion, and finally propose preliminary locations for a second well.

Background. By design, PVU Injection Well No. 1 was sited to intersect and utilize the extensive

Wray Mesa fault and fracture system both for injectate storage and as fluid conduits to smaller faults and fractures, joints, and pore spaces (i.e., the *in situ* porosity). Hypocenters located in the past 11 years indicate that this design criterion was met and that the Wray Mesa has functioned and continues to function in this capacity (see **Figure 1**, note the linear groupings of events and the alignment of the groupings with the inferred main faults of the Wray Mesa Fault System). Given this success, a second injection well should be sited with the same consideration: intersecting an existing, pervasive fault/fracture system.

From 1991 through the end of 2002 ~1.05×10^9 gal of injectate have been pumped into the reservoir beneath Paradox Valley. This corresponds to more than 750×10^3 tons of salt. Over that same 11 ½ years, the Dolores River, without PVU intervention, would have emplaced ~2300×10^3 tons of salt into the Colorado River system. If PVU had the ability to inject more brine, there is certainly more brine to be injected.

Prior to the inception of PVU we expected that deep well injection would induce earthquakes (e.g., deep well injection at the Rocky Mountain Arsenal in the 1960's produced events around Denver). Using the Paradox Valley Seismic Network (PVSN) we have been able to record induced events and use them as a diagnostic tool for (1) adjusting injection to mitigate feelable events, (2) mapping fluid migration, and (3) identifying major faults and fractures of the injection reservoir.

During the 11 ½ years of pumping, PVSN has recorded and mapped the source locations of more than 3960 seismic events. These source locations cumulatively envelop a volume of between 15 and 30 km^3. This volume has been quasi-stable for the last 3 to 4 years. Does this volume represent either the full extent of the injection reservoir (i.e., existing faults and major fracture system) or only the limit to which we induce detectable earthquakes, but not the full extent of the injection reservoir? At present we don't know the answer to this question.

Within the hypocenter envelope, we have identified approximately 30 km of faults (**Figure 1**). If we assume an average height of ~0.5 km and a maximum fault aperture of 5 mm, the identified faults give a maximum of ~7.5×10^4 m^3 of storage volume. Comparing this volume to the total injection volume, ~4.0×10^6 m^3, indicates that more than 98% of the injectate is presently stored in minor faults, fractures, joints, and pore spaces.

Over time, the final storage location for practically all of the injectate will be pore space. As long as the (injectate) fluid pressure in the faults and fractures exceeds the fluid pressure in the pore spaces, the injectate will push the pore fluids deeper into the formation and diffuse from the fractures and faults into the formation (i.e., the pore space). The available porosity (i.e., accessible pore volume minus connate fluid volume) of the injection reservoir gives the total available storage; this volume divided by its rate of filling gives an estimate of the (optimal) injection lifetime of the reservoir. We do know that we can shorten or extend the lifetime by shortening or extending the time the injectate has to displace the connate fluids. As discussed below we have extended that time using shutdown periods (a.k.a. "shut-ins") and reduced injection rate, but with adverse effects on economic and environmental benefits.

Our analysis of the observed seismicity shows it to result from shear slip, likely across existing planes of weakness (e.g., faults, old fractures and joints, etc.). The seismicity observed at the surface is not caused by opening new fractures. Even though new fractures are being created by the pumping, their opening radiates only minor seismicity which cannot be observed at the surface. The surface-observable seismicity is caused by slippage across the existing planes of weakness which are nominally locked by their frictional stress (i.e., effective normal stress). Prior to any injection (i.e., before 1991) occasionally a plane of weakness broke through its frictional stress and slipped causing the minor background seismicity in the Paradox region (i.e., approximately 6 small events between 1985 and 1991). With the introduction of injection, the fluid pressure across the planes of weakness increased, reducing friction (i.e., lowering effective normal stress), liberating the shear stress, and inducing the seismic events. As discussed below, we've implemented operational schemes (i.e., reduced injection rate) to keep the pressure across planes of weakness as low as possible by allowing the injectate to diffuse into the formation pores. Unfortunately, mitigating seismicity is counter to the economic and Colorado River salinity reduction benefits of PVU's mandate. Hence, the need for the second well: maintain the seismic mitigation methods while substantially increasing the injection economics and environmental benefits.

Observations. At PVU, continuous injection began the second half of 1996. Since then, we have noted four important injection characteristics germane to this discussion.

1. Operations have been punctuated with approximately a dozen shut-in periods (i.e., cessation of injection) that range from a few days to a maximum of ~70 days.

2. Beginning in mid-1999 (due to the occurrence of several felt earthquakes), we modified operations so that injection ceased for ~20 days twice each year.
3. Between 1996 and mid-2000, normal operations consisted of three pumps operating at a nominal injection rate of 345 gal/min and nominal surface pressure of ~4850 psi. In June, 2000 after a month-long shut-in, following an **M** 4.3 event (the biggest induced event to date), operations were resumed at a reduced injection rate, using only two pumps yielding a nominal injection rate of 230 gal/min and nominal surface pressure of ~4400 psi.
4. Since January, 2002 the injectate has been 100% PVB, compared to the previous injectate of 70% PVB and 30% fresh water. Despite the increase of ~300 psi in bottom-hole pressure, no adversity has been witnessed, especially regarding seismicity.

With regard to inducing seismicity, we correlate these characteristics with the following effects (see **Figure 2**):

1. Practically uninterrupted pumping at a rate of 345 gpm from mid-1998 to mid-1999 created the highest rate of seismic event production. (Data: Between mid-1997 and mid-1998 with one 71-day shut-in period, there were 711 record events; from mid-1998 through mid-1999 with one 6-day shut-in near the end of the period, there were 1112 events recorded; and for the same months in 1999 through 2000 with ~5 shut-ins, there were 586 events.)
2. Periodically shutting down appears to reduce the induced seismic activity. We feel these shutdown periods allow the injectate to diffuse into the pore spaces while pressures fall off within the faults and fractures. This keeps effective normal stresses on the planes of weakness higher and reduces the likelihood of seismic slip.
3. Allowing the injectate to diffuse by periodically shutting down has reduced the rate at which larger magnitude events are produced.
4. Pumping at the reduced injection rate (i.e., two pumps instead of three) has further mitigated the induced seismic activity. This observation suggests that the diffusion from the fractures into the formation is <u>highly dependent on the rate of injection</u>.

These observations suggest that a return to 345 gpm, continuous pumping of PVU Injection Well

No. 1 is not prudent. It would, most likely, create unacceptable levels of seismicity. In contrast, the level of seismicity observed under the current operating procedures is acceptable and we expect will continue to produce acceptable levels of seismicity in the long-term. Unfortunately, pumping at the reduced rate plus two, 20-day mandated shut-in periods each year has significantly reduced revenue and environmental benefit from the project. Further, the injection of a 70/30 mix from 1991 through 2001 had consumed ~30% of the storage for fresh water, removed fresh water from the Dolores River, and produced no economic benefit. As noted above, the change to 100% PVB injectate has shown no ill effects and has increased the economic viability of the project. However, this increase in economic benefit has not mitigated the need for a second well, i.e., the need for a second injection reservoir. Sooner or later Injection Well No. 1's ability to accept injectate will reduce and require unscheduled shutdowns, which will reduce the economic viability of the project. However, a second well will allow longer, scheduled shutdown periods for the first well, allowing stress relaxation (i.e., migration of the injectate into the pore structure) to re-invigorate the injection reservoir of Well No. 1.

Implications of a Second Well:

1. As discussed above, pumping at reduced injection rates and with schedule shut-ins has reduced benefits. (a mandated shut-down for 40 days per year @ 230 gpm injection means ~13.2 million gallons of lost injection which, in turn, means ~14,400 tons of salt @ 70/30 PVB/fresh or 20,500 tons @ 100% PVB entering the river system.) The revenue associated with this lost injection could conceivably be realized using a second well.
2. We plan to site the second well so that its injection reservoir would be isolated from Injection Well No. 1's reservoir. **At the simplest level, this would effectively double the total project life. However it is most likely that here, one plus one will be greater than two; giving a reservoir more than the 40 days per year shut down presently used, should extend its life.**
3. The possibility that each well may operate for ~6 months/year should significantly reduce the production of larger seismic events (if 20 days of shut-in time is good, 180 should be much better). Based on what we have observed in the most recent 20 day shut down, the down-hole, near well-bore pressures should be restored to near ambient conditions well

before 180 days. This may allow considerable flexibility in selecting operational schemes (e.g., operating both wells during times of increased ground water flow into the river etc.).

Preliminary Siting Considerations. At this time we suggest three possible locations for a second well. This is not to say these are the only possibilities. The first is the alternative site identified during the initial well-site selection process, twinning the Conoco-Scorup No. 1 well (**Figure 1**) near the center of the valley (across the Dolores from the extraction well field). This site was identified by Harr and Bremkamp as having good porosity and permeability in the Leadville Formation. The geologic cross-sections drawn through the valley (**Figure 3**) show a fault with significant throw near the site of the existing well. We hope this fault(s) would serve a similar function as the Wray Mesa fault system near Injection Well No. 1 (a major conduit to allow communication with a large number of smaller fractures). This site has the advantage of being spatially near the extraction field which should reduce infrastructure development costs. The fault system beneath the valley should be hydrologically isolated from the Wray Mesa system and we would expect no pressure interference between the two reservoirs. However, a disadvantage of this site would drilling nearly the entire well through the Paradox salt. This could add significant cost to drilling, certainly to completion costs, and risk costs.

The second site we tentatively identify is southeast of the existing well along the trend of the Wray Mesa fault system a distance of ~8 km east-southeast of the current well. As mentioned, we feel the Wray Mesa system has provided very effective transport of fluid away from the injection well to numerous smaller fractures, faults, etc. We choose a set-off distance of ~8 km as that appears to be the maximum distance we have produced earthquakes from the existing well. This site would have the advantage of being remote from the major population centers of the valley in an area used for low-density grazing. The disadvantages are the greater distance from the extraction well field and exploiting the Wray Mesa system (we can't guarantee complete reservoir isolation). However, we would likely not be drilling through salt for the entire depth of the well. Based on **Figure 4**, a fluid pressure map of the Leadville Formation, adapted from Harr and Bremkamp's investigations prior to any injection at PVU, this site is also up gradient from the existing injection well which will likely produce a spatial bias in pressures toward the northwest.

The third potential site is within Dry Creek Basin (approximately 30 air km) southeast of the existing well. The rationale for considering this site is the shallowing of the Leadville Limestone

injection horizon in this region. A shallower injection reservoir could profoundly reduce expenses for drilling, completion and tubing costs for the second well. This site is also far removed from significant population. The costs of constructing a pipeline of this length (with some pumping required), may be great enough to offset the potential financial gain from reduced drilling costs. The benefits and disadvantages of this site warrant further study.

Proposed Actions.

We have considered the next steps and have developed a list of actions that need to be completed (some are already in progress). The list represents only our ruminations. It is certainly not complete and is neither prioritized nor ordered by importance.

- Further refine the various realistic options and implications for a second injection well. Compare the financial implications of a second well with other potential concepts for enhancement of PVU operations (increasing allowable pressure for example).
- Reprocess existing seismic reflection data to better define major faults within the Leadville.
- Revaluate the original Harr and Bremkamp investigations of the 1980's and determine if an updated investigation is called for.
- Since a lot of geophysical explorations have been done in the region since the late 1980's, contact oil and gas companies who have done the investigations and open up a dialogue.
- Begin soliciting cost estimates for the various options.
- Begin a dialogue with EPA regarding the permitting process.

Proposed Upcoming Actions. We feel that a meeting of all concerned participants is needed. This meet would address further evaluate options, consider obstacles, etc.; formulate a plan, set up a schedule for the plan; and assign tasks is needed.

This summarizes our current thoughts on this issue. We would strongly urge the project to evaluate potential sites and associated costs for a second well at the PVU. We would appreciate any thoughts that you might have.

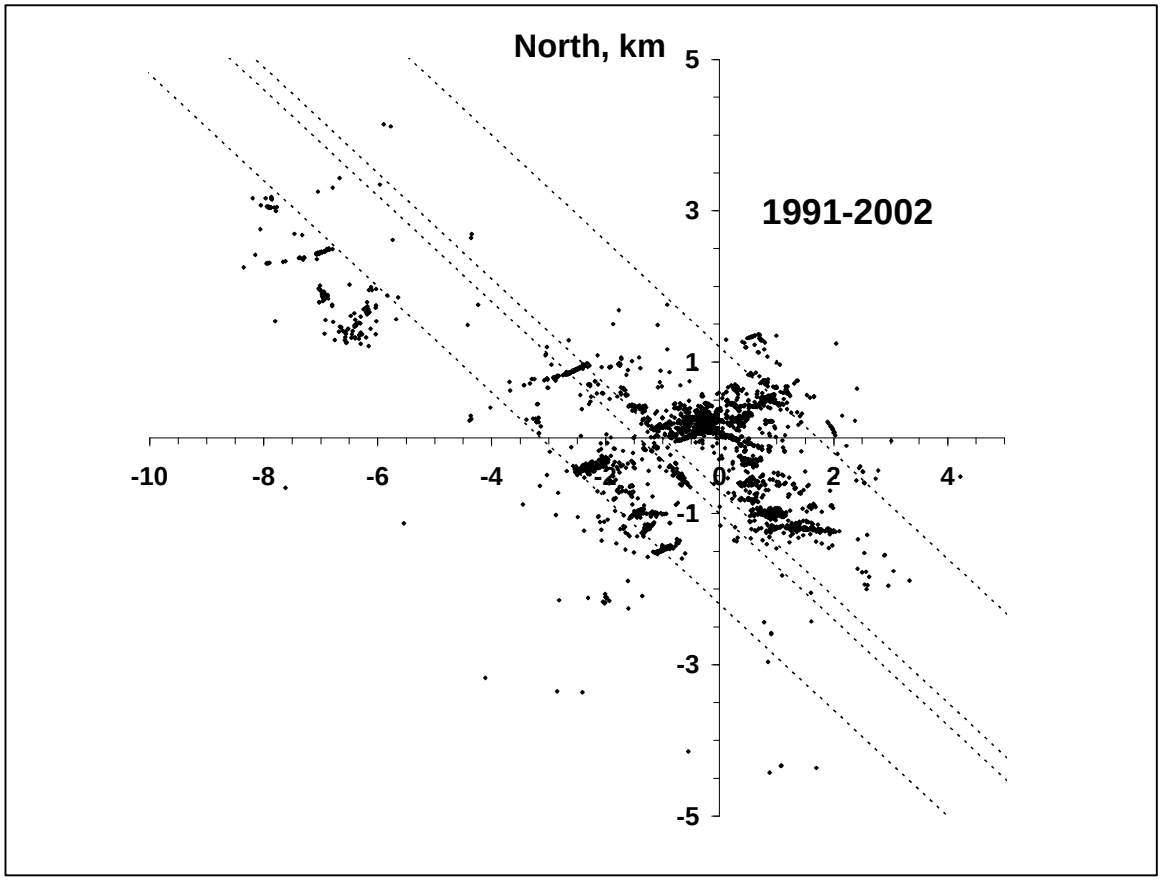

Figure 1. Map View of 1991-2002 Induced Events at PVU. Dashed lines show inferred main faults of Wray Mesa system. Axis is centered on PVU Injection Well No. 1.

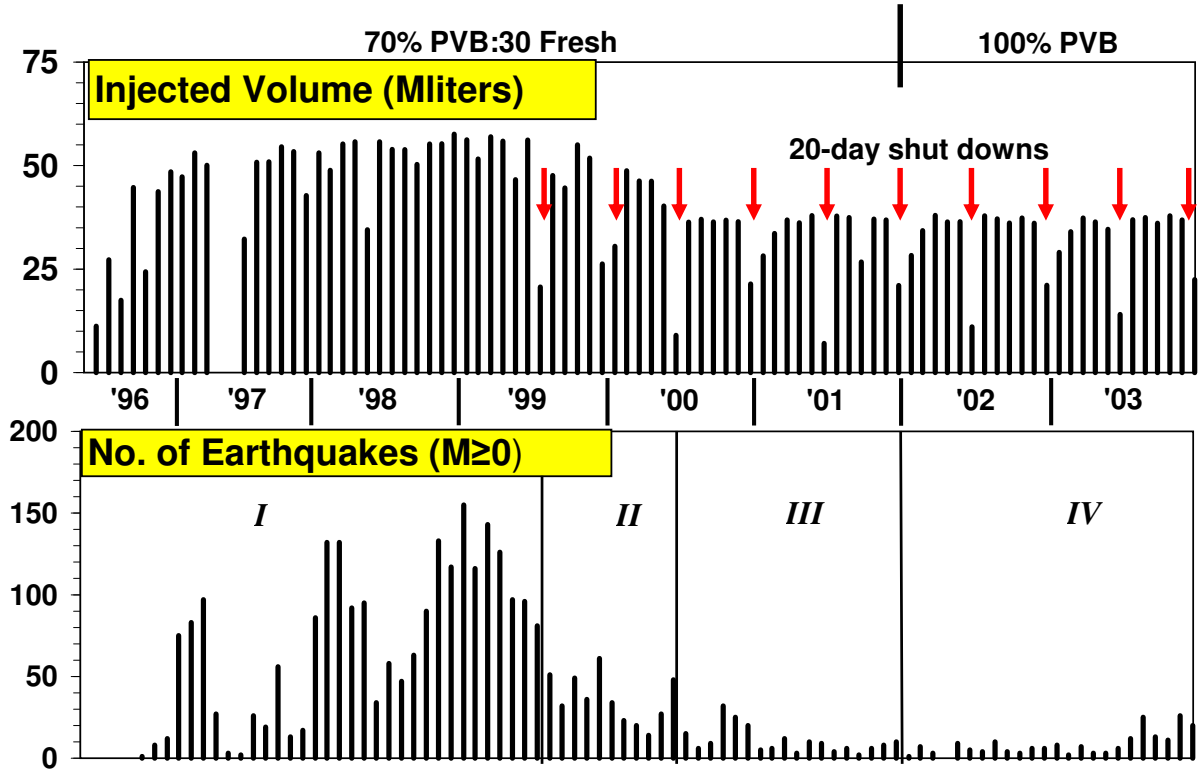

Figure 2. Comparison of Injection Volume per Month and Number of Induced Seismic Events per Month. Also shown are the two largest seismic events and changes in injection strategies: I - initial 3 injection pumps; II - institute biannual 20-day shutdown; III - biannual 20-day shutdown and reduce to 2 injection pumps; IV - maintain pumping strategy III, but increase injectate from 70:30 PVB:fresh water to 100% PVB.

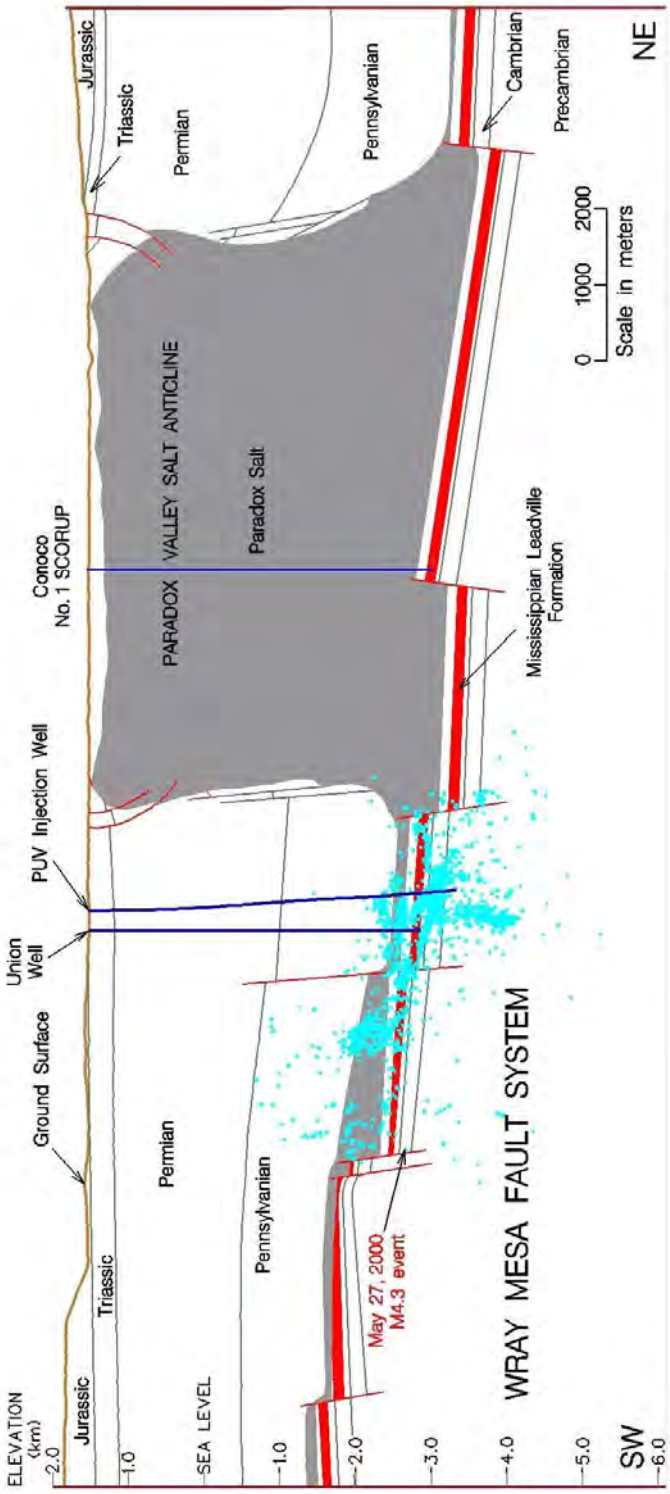

Figure 3. Geological Cross Section Perpendicular to Paradox Valley and Running through Injection Well No. 1. Induced seismicity near the injection well is shown as are the Union and Conoco wells.

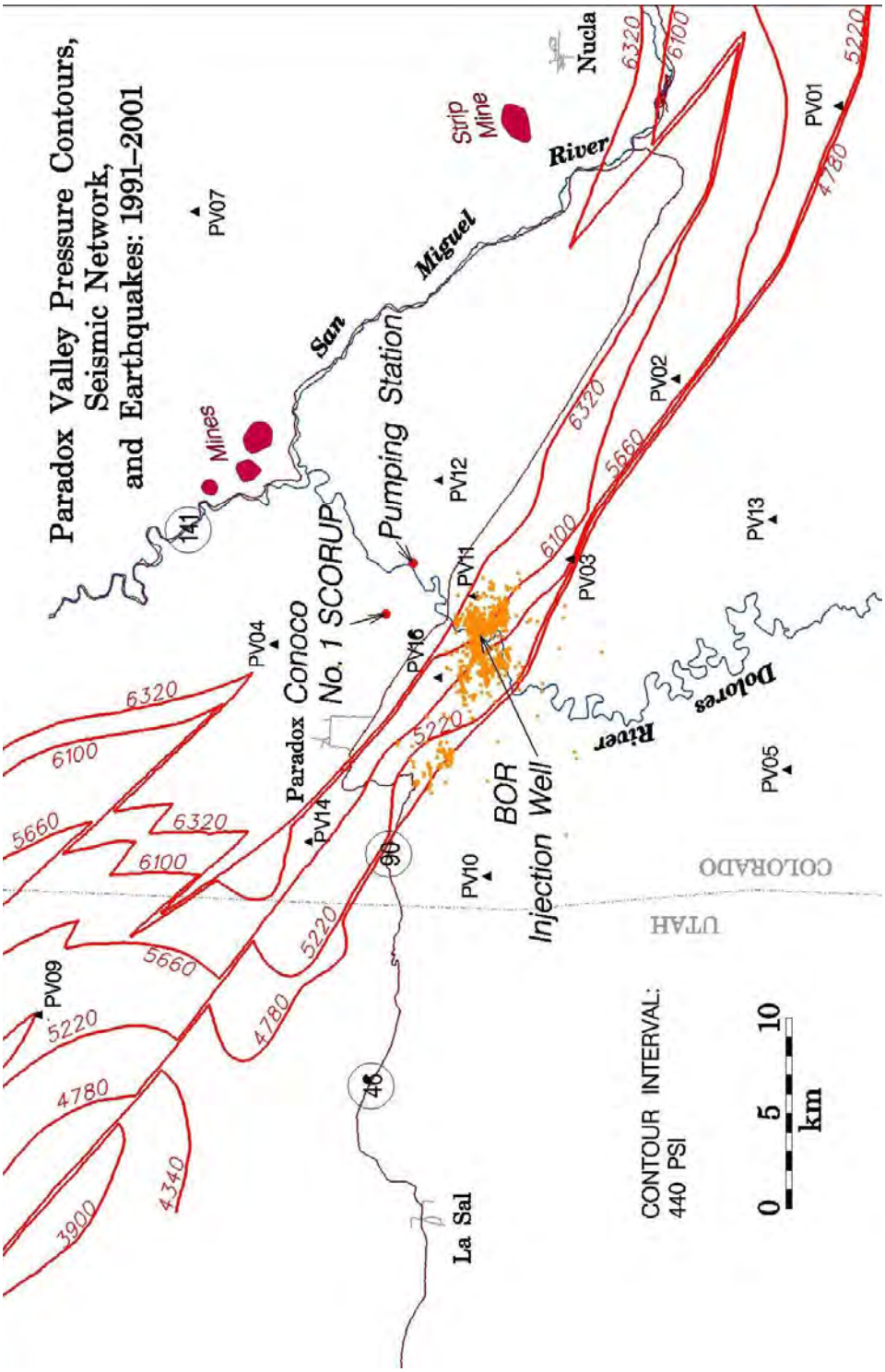

Figure 4. Map View of Paradox Region, Fluid Pressure Contours of the Leadville Formation Proposed by Harr and Bremkamp, and the Epicenters of the Local Seismicity Including the Seismicity Induced by PVU.

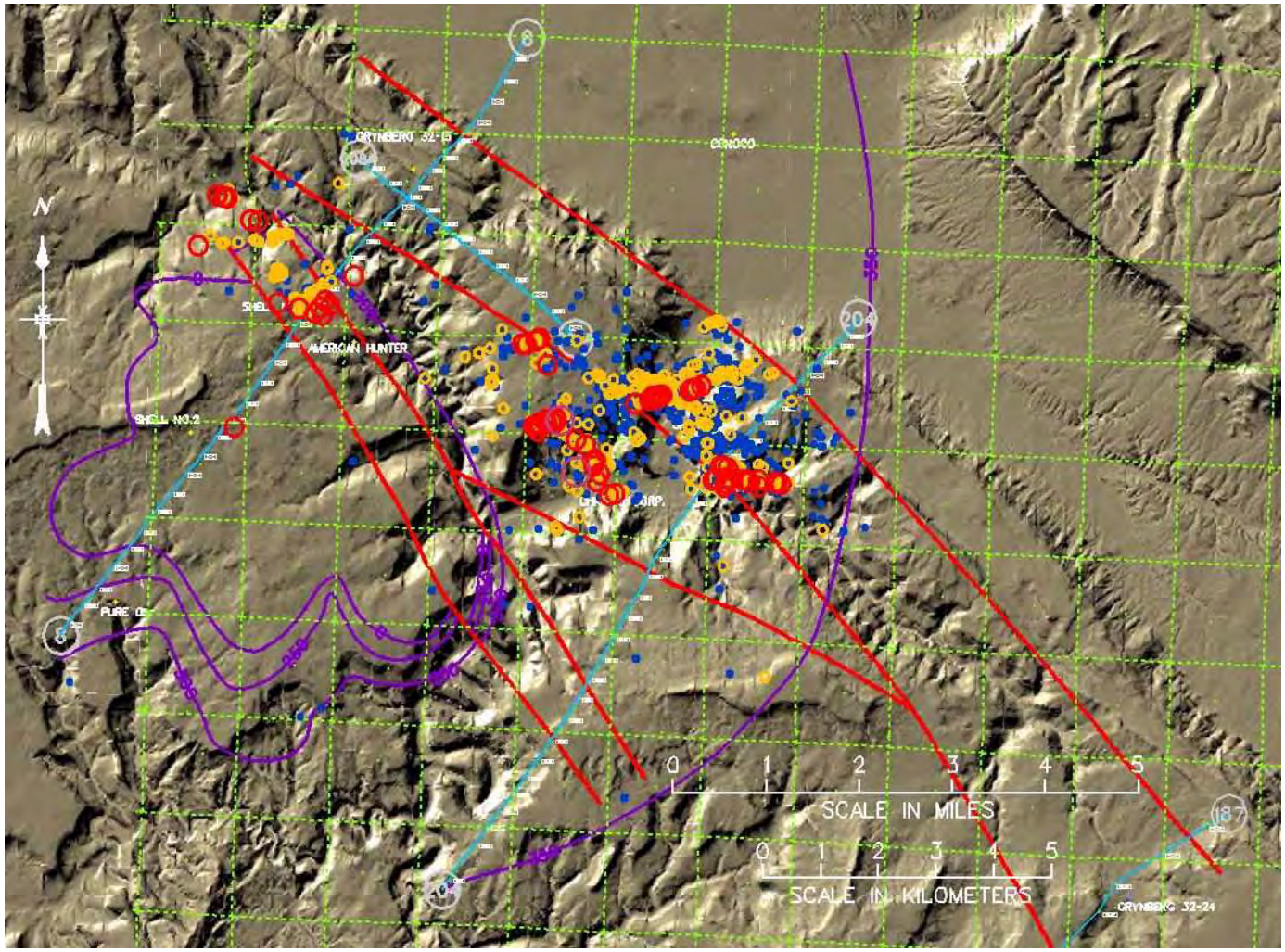

Digital elevation map of Paradox Valley region near injection well showing seismic reflection lines used in initial geological interpretation by Harr and Bremkamp (1988). Seismic lines are in cyan with line numbers indicated. Primary faults of the Wray Mesa as developed by Harr and Bremkamp for the Leadville elevation are shown in red. Thickness contours of the Leadville formation are shown in purple -- note the absence of Leadville in western portion of area. Seismicity associated with the injection are shown by small circles.

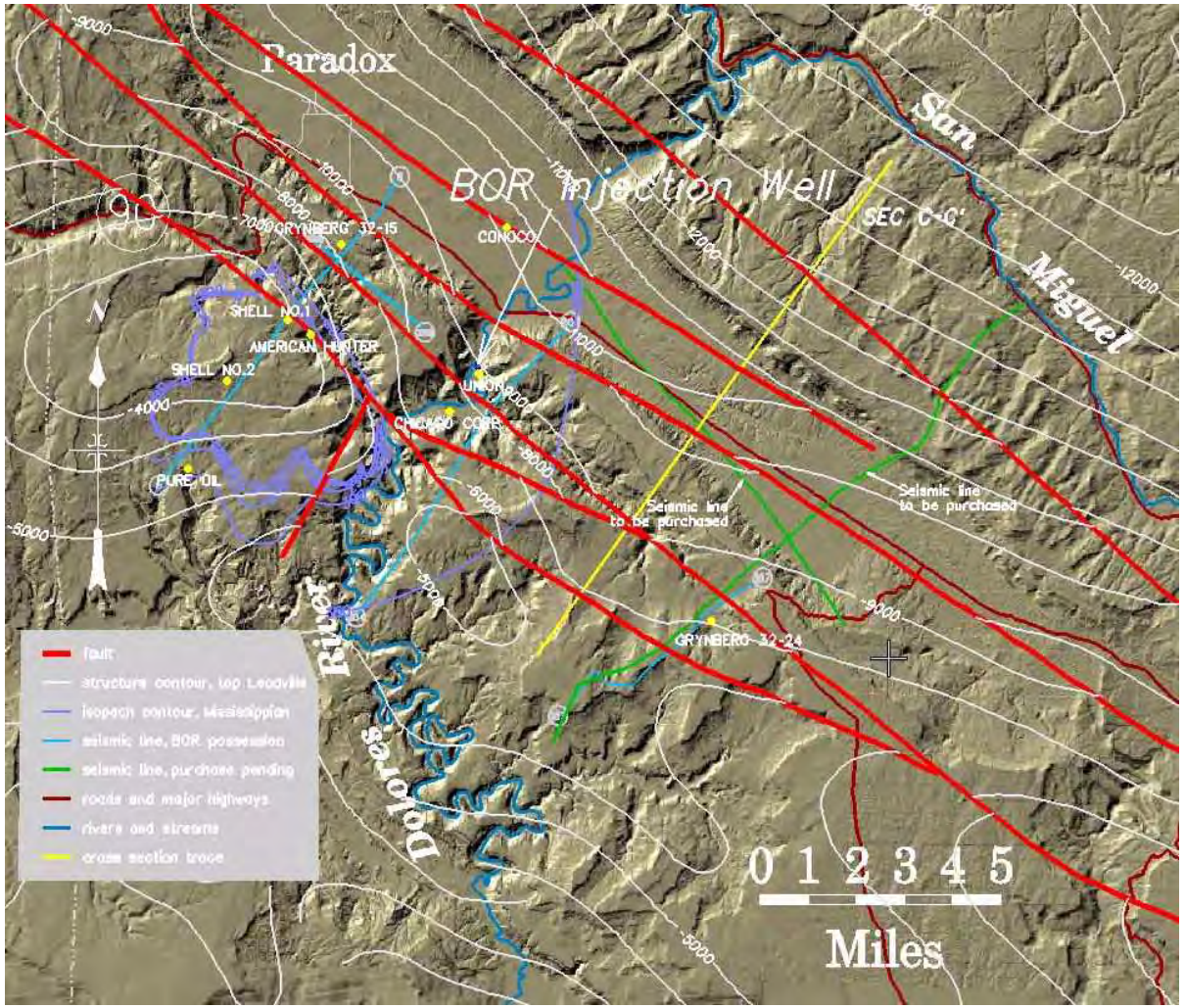

Digital elevation map of Paradox Valley region south of injection well and primary candidate region for second injection well. Shown in green are seismic lines to be purchased. Shown in yellow is surface expression of Harr and Bremkamp's C-C' section (next figure). Other features indicated are faults of the Way Mesa system in red, structure contours of the Leadville Formation in white, isopach contours of the Leadville Formation in purple, seismic lines used by Harr and Bremkamp to interpret local geology in cyan, and PVU injection well.

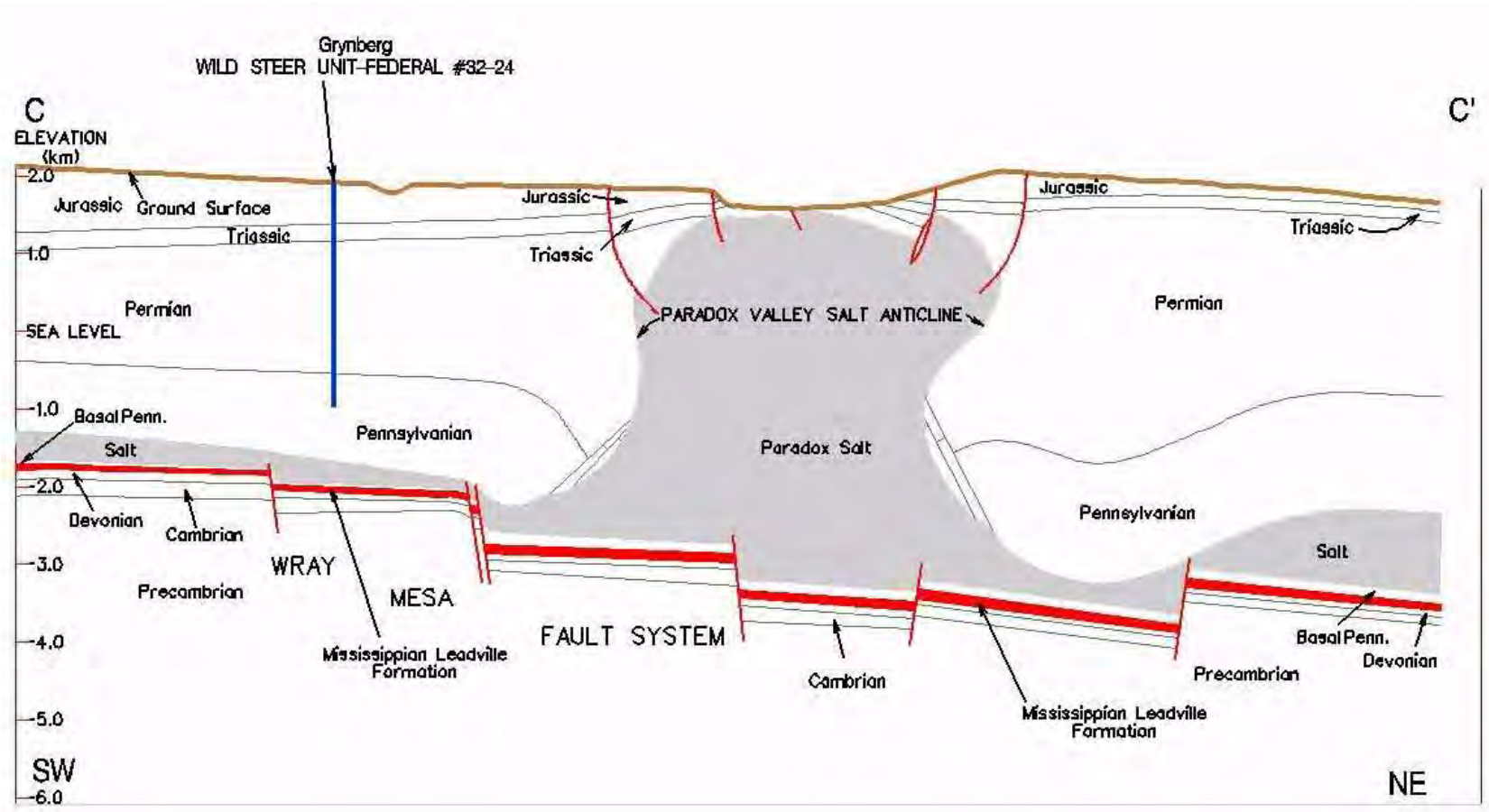

Cross-section C-C' (see preceding figure) from geological report of Harr and Bremkamp (1988). Section is normal to strike of Paradox Valley.

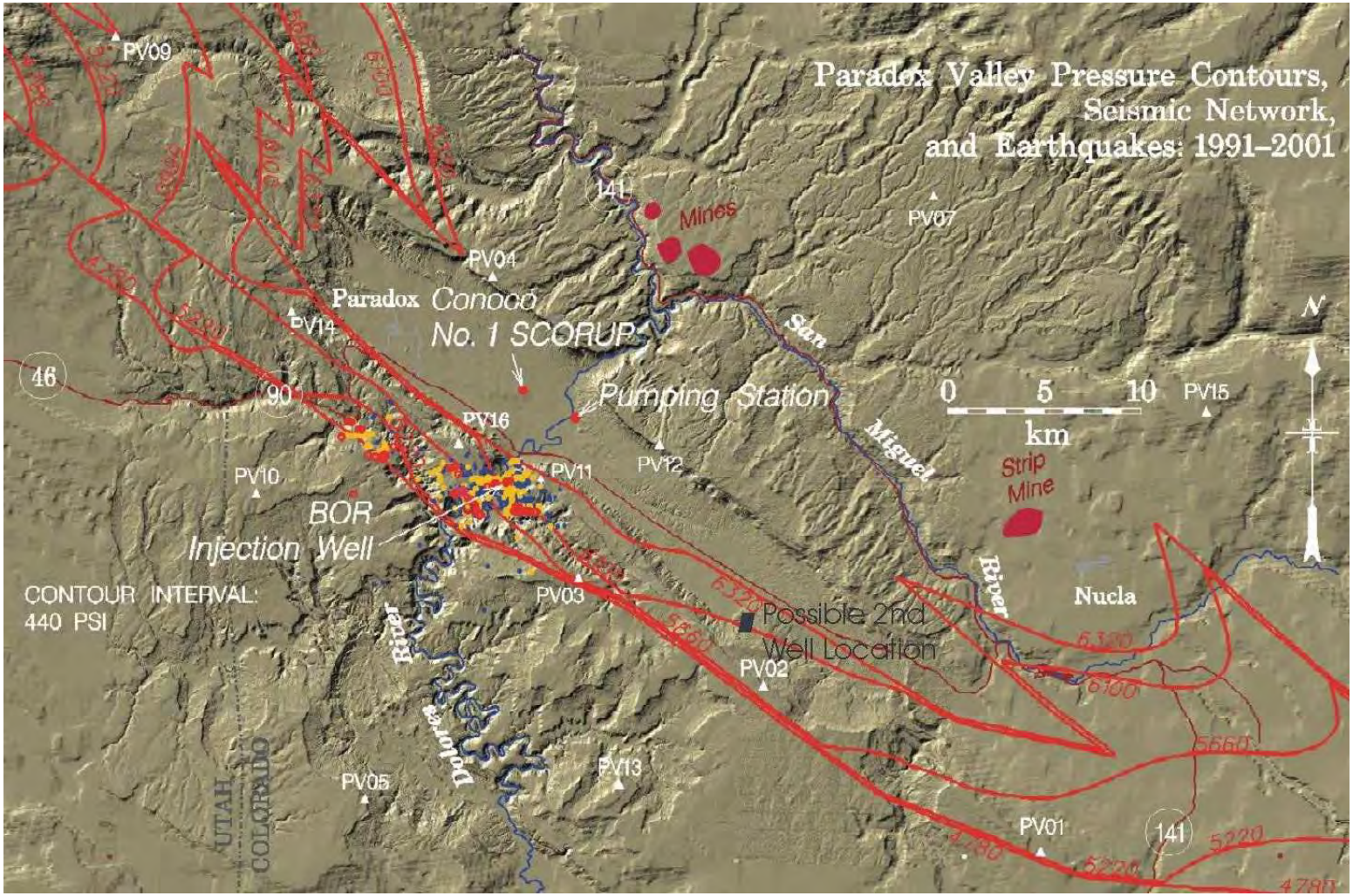

Digital elevation map showing potential second well location relative to Paradox Valley pressure contours (red) from Bremkamp and Harr (1988), existing injection well, and injection-induced seismicity (small circles). Subset of existing seismic network stations shown by white triangles.

13.0 APPENDIX B - 39TH ANNUAL ROCK SYMPOSIUM

A manuscript was published in the proceedings of the 39th Rock Mechanics Symposium: SOIL and ROCK AMERICA 2003, 12th Panamerican Conference on Soil Mechanics and Geotechnical Engineering, 39th U.S. Rock Mechanics Symposium, June 22-26, 2003, Cambridge, MA, USA, Proceeding Volume 2, edited by P.J. Culligan, H. H. Einstein, and A. J. Whittle (MIT) pp. 1443-1449.

14.0 APPENDIX C - INJECTION CONFERENCE

Between October 22 and 25, 2003, the U.S. Environmental Protection Agency (Office of Ground Water and Drinking Water) and the U.S. Department of Energy (Office of Fossil Energy, National Energy Technology Laboratory; and Office of Environmental Management, Office of Science and Technology) sponsor the Second International Symposium on Underground Injection Science and Technology at Lawrence Berkeley National Laboratory, Berkeley, CA. We presented and published in the proceeding of the symposium the paper, “Injecting Brine and Inducing Seismicity at the World’s Deepest Injection Well, Paradox Valley, Southwest, Colorado, USA”, by Jim Bundy, Kenneth Mahrer, Jon Ake, Lisa Block, and Daniel O’Connell. Based on the presentation, the conveners are putting together a special volume of the papers. We have submitted a modified version of the original manuscript.